



KTH Electrical Engineering

Look-ahead control for fuel-efficient and safe heavy-duty vehicle platooning

VALERIO TURRI

Doctoral Thesis
Stockholm, Sweden 2018

KTH Royal Institute of Technology
School of Electrical Engineering and Computer Science
Department of Automatic Control

TRITA-EECS-AVL-2018:33
ISBN: 978-91-7729-747-5

SE-100 44 Stockholm
SWEDEN

Akademisk avhandling som med tillstånd av Kungliga Tekniska högskolan framlägges till offentlig granskning för avläggande av teknologie doktorsexamen i Elektro och systemteknik den 4 maj 2018 klockan 14.00 i sal F3, Kungliga Tekniska högskolan, Lindstedtsvägen 26, Stockholm, Sweden.

© Valerio Turri, May 2018. All rights reserved.

Tryck: Universitetsservice US AB

Abstract

The operation of heavy-duty vehicles at small inter-vehicular distances, known as platoons, lowers the aerodynamic drag and, therefore, reduces fuel consumption and greenhouse gas emissions. Tests conducted on flat roads have shown the potential of platooning to reduce the fuel consumption of about 10%. However, platoons are expected to operate on public highways with varying topography alongside other vehicles. Due to the large mass and limited engine power of heavy-duty vehicles, road slopes have a significant impact on feasible and optimal speed profiles. For single vehicles, experiments have shown that optimizing the speed according to the road profile resulted in fuel saving of up to 3.5%. The use of such a look-ahead control framework is expected to lead to large benefits also for platooning.

This thesis presents the design of safe and fuel-efficient control of heavy-duty vehicle platoons driving on realistic road profiles. The scenario where the platooning vehicles cooperate to optimize their overall fuel-efficiency is studied together with the scenario where the vehicles do not explicitly cooperate.

First, we propose a control architecture that splits the cooperative platooning control problem into two layers. The top layer computes a reference speed profile that ensures fuel-efficient operation of the entire platoon based on dynamic programming. The bottom layer relies on model predictive control to safely track the reference speed. Simulations show the ability of the proposed controller to save up to 12% of fuel for following vehicles compared to existing platoon controllers and to safely react to emergency braking of the leading vehicle.

Second, we propose a gear management layer that fits in the cooperative platooning control architecture and explicitly takes the gear selection into account. The underlying optimal control problem aims at minimizing the vehicle fuel consumption and the reference tracking deviations. Simulations indicate how this formulation outperforms existing alternatives, both in terms of fuel-efficiency and tracking error.

Third, we address non-cooperative platooning by proposing a vehicle-following controller suitable for fuel-efficient control of heavy-duty vehicles. The proposed controller explores both the benefits given by the short inter-vehicular distance and those given by pulse-and-glide, i.e., alternating traction and coasting phases. A simulation study suggests fuel saving of up to 18% compared to the single vehicle case, and up to 7% compared to when a constant-distance vehicle-following controller is used.

Last, we propose a vehicle-following controller aimed at exploiting long preview of the preceding vehicle trajectory by directly manipulating the inputs of low-level vehicle controllers. This is achieved through a model predictive controller that uses a short prediction horizon and includes a terminal state set that incorporates preview information about the preceding vehicle. Experiments indicate the ability of the controller to avoid unnecessary braking, while simulations show behavior similar to the optimal control behavior.

Sammanfattning

Fordonståg där tunga lastbilar kör med korta avstånd mellan fordonen, även känt som kolonnkörning, sänker luftmotståndet och därigenom minskar även bränsleförbrukningen och utsläppen av växthusgaser. Utförda tester visar på en potentiell minskning av bränsleförbrukningen om 10 % på plana vägar. Dock förväntas fordonståg kunna köras på allmänna motorvägar med varierande topografi tillsammans med övrig trafik. På grund av den begränsade motoreffekten i förhållande till den stora massan har backar en stor inverkan på möjliga och optimala hastighetsprofiler för tunga fordon. För enskilda fordon har experiment visat att optimering av hastigheten med hänsyn till vägglutning kan resultera i upp till 3.5 % bränslebesparing. En reglerstrategi som tar hänsyn till vägglutning kan förväntas ge samma fördelar även för fordonståg.

I den här avhandlingen presenteras säkra och bränsleeffektiva reglerstrategier för fordonståg med tunga fordon som körs på vägar med verkliga vägglutningar. Både fallet där fordonen samarbetar för att minimera bränsleförbrukningen och fallet där fordonen inte uttryckligen samarbetar undersöks.

Först föreslår vi en reglerarkitektur där reglerproblemet för det samarbetande fordonståget delas upp i två laget. Ett centraliserat övre lager beräknar genom dynamisk programmering börvärden för fordonståget som ger bränsleeffektiv körning. Ett distribuerat undra lager använder modellprediktiv reglering för att på ett säkert sätt följa de beräknade börvärdena. Den föreslagna reglerstrategin visas i simulering kunna spara upp till 12 % bränsle för de efterföljande fordonen jämfört med tidigare reglerstrategier för fordonståg samtidigt som regulator på ett säkert sätt agerar på en nödbroms från ledarfordonet.

Vidare föreslår vi ett växelstyrningslager som kan användas i ovan nämnda reglerstrategi som explicit tar hänsyn till växelval. The underliggande optimala reglerproblemet är formulerat för att minimera fordonets bränsleförbrukning och avvikelser från börvärdet. Simuleringar indikerar att denna formulering överträffar tidigare alternativa reglerstrategier både vad gäller bränsleförbrukning och börvärdesföljning.

Vi studerar även det icke samarbetande fordonståget och föreslår en fordonsföljande regulator för bränsleeffektiv körning av tunga fordon. Den föreslagna regulatorn utnyttjar både fördelarna med korta avstånd mellan fordon och med att växla mellan aktiv framdrivning och frirullning. En simuleringsstudie visar på en möjlig bränslebesparing om 18 % jämfört med fallet med ett fordon och upp till 7 % jämfört med en regulator som håller konstant avstånd.

Slutligen föreslår vi en fordonsföljande regulator som utnyttjar förhandsinformation om det framförvarande fordonets körbeteende genom att direkt reglera lågnivåsignaler i det egna fordonet. Detta uppnås med en modellprediktiv regulator där en kort prediktionshorisont används tillsammans med bivillkor för tillstånden som tar hänsyn till förhandsinformation från framförvarande fordon. Experiment visar att regulatorn undviker onödiga inbromsningar. Vidare visar simuleringar regulatorbeteende som liknar det optimala.

To my parents and sister

Acknowledgements

The PhD has been a unique life journey from which I learned greatly, personally and professionally, and during which I had the opportunity to meet wonderful people that, in different ways, contributed to this thesis. I want to express my sincere appreciation to Karl H. Johansson that, as my PhD advisor, guided me through this journey. I will always be grateful for your continuous support and for your visionary and inspiring talks. I want to thank my co-advisor Jonas Mårtensson for the valuable discussions and for sharing his excitement in research. A heartfelt thanks goes to Bart Besselink for his wise guidance throughout the first part of my PhD and for strengthening my skills as a researcher. I'm also particularly grateful to Christian Larsson for all the interesting discussions, for helping out with the sammanfattning and for being a good friend.

A special thanks goes to Francesco Borrelli for giving me the opportunity to visit, in multiple occasions, his research group at UC Berkeley and for his invaluable inputs on my work. I'm thankful to all the great people that I have met there for our research collaborations and for the great time spent together outside the office. Thanks to Jacopo Guanetti, Ashwin Carvalho, Yeojun Kim, Ugo Rosolia, and Sarah Koehler.

I wish to thank Oscar Flårdh and Henrik Pettersson for giving me the opportunity to visit Scania and for their valuable inputs on my research. Thanks to Fredrik Roos, Mats Reimark, Assad Alam, Pär Degerman, Manne Held and Kuo-Yun Liang for all the fruitful discussions that helped to raise the quality of this thesis.

I want to thank all my past and present colleagues at the Department of Automatic Control for all the valuable and fun discussions and for making it a great place where to work. A special thanks goes to Demia Della Penda, Mohamed Rasheed, Arda Aytakin, Sadegh Shahi, Kaveh Paridari, Antonio Adaldo, Riccardo Risuleo and Sebastian van de Hoef for sharing this journey together through its joyful moments and the difficult ones. Thanks to Mikael Johansson and Pedro Lima for facing the adventure of creating a new course from scratch together. I'm also deeply grateful to Mohammad Pirani, Bart Besselink, Mohamed Rasheed, Christian Larsson and Claudia Rossini for proofreading part of this thesis and providing valuable comments. Thanks to Hanna Holmqvist, Anneli Ström, Gerd Franzon, Silvia Svensson and Felicia Gustafsson for taking care of all things that make the

department run smoothly and for creating such a nice working atmosphere.

I wish to gratefully acknowledge the School of Electrical Engineering through the Program of Excellence, the European Union through the project COMPANION, the Swedish Research Council, and the Knut and Alice Wallenberg Foundation for their financial support that made this thesis possible.

Lastly but no less importantly, I wish to thank my family and friends for always being there in the cheerful and the difficult moments, for sharing great adventures and, overall, for giving me a meaningful life outside work. A thanks full of love goes to my parents, Claudia and Corrado, and my sister Fulvia for their unconditional support and love throughout my life.

Valerio Turri
Stockholm, May 2018.

Contents

Contents	xi
1 Introduction	1
1.1 Motivation	1
1.2 Technology opportunities	3
1.3 Platooning for an improved fuel-efficiency and safety	4
1.4 Platooning challenges	6
1.5 Problem formulation	7
1.6 Thesis outline and contribution	10
2 Background	17
2.1 Technologies enabling platooning	17
2.2 Platooning control	21
2.3 Look-ahead control	25
2.4 Fuel-efficient road freight transportation	28
2.5 Optimal control	31
2.6 Summary	35
3 Modeling	37
3.1 Longitudinal vehicle dynamics	37
3.2 Powertrain model	41
3.3 Vehicle system architecture	45
3.4 Summary	48
4 Control architectures for platooning	49
4.1 Motivational experiment	49
4.2 Cooperative platooning	55
4.3 Non-cooperative platooning	58
4.4 Summary	61

I	Cooperative platooning	63
5	Cooperative fuel-efficient and safe platooning	65
5.1	Control architecture and problem statement	66
5.2	Platoon coordinator	69
5.3	Vehicle control layer	74
5.4	Evaluation of the platoon coordinator	83
5.5	Evaluation of the vehicle control layer	92
5.6	Evaluation of the integrated system	97
5.7	Summary	100
6	Gear management in cooperative platooning	101
6.1	Control architecture and problem statement	102
6.2	Gear management layer	103
6.3	Vehicle control layer	107
6.4	Performance evaluation	109
6.5	Summary	116
II	Non-cooperative platooning	117
7	Fuel-optimal vehicle-following control	119
7.1	Control architecture and problem statement	120
7.2	Modeling	120
7.3	Vehicle-following planner	124
7.4	Simulation study	126
7.5	Summary	133
8	Low complexity vehicle-following control	135
8.1	Control architecture and problem statement	136
8.2	Vehicle-following control	137
8.3	Experimental study	141
8.4	Simulation study	147
8.5	Summary	147
9	Conclusion and future work	151
9.1	Conclusion	151
9.2	Future work	153
	Acronyms	157
	Bibliography	159

Introduction

Hheavy-duty vehicles are responsible for a significant share of the global greenhouse gas emissions and energy consumption. Due to the strong link between freight transportation and the global economic growth, their environmental impact is expected to grow in the coming years, if no measures are taken.

Vehicle platooning is under investigation by governmental institutions, research communities, and private companies as a mean to reduce fuel consumption and emissions of heavy-duty vehicles. By letting vehicles drive at a short inter-vehicular distance, the overall aerodynamic drag can be lowered significantly and, as a result, the fuel consumption can be reduced. Tests conducted in controlled environments have shown that platooning has the potential of saving 10% of fuel with vehicles driving at an inter-vehicular distance of 20 meters. However, the general problem of control of heavy-duty vehicle platoons aimed at reaching a high level of fuel-efficiency while guaranteeing safety on public roads is still open. Platoons are expected to drive on existing highways, where altitude variations and traffic can have large impact. In this thesis we address this platoon control problem with a particular attention to the influence of slopes and external traffic.

The outline of this chapter is as follows. Section 1.1 introduces the challenges that the road transportation sector is facing, while Section 1.2 highlights some of the technologies under research to address them. Section 1.3 presents the concept of platooning as one of these technologies, and Section 1.4 underlines the main challenges faced in designing a fuel-efficient and safe platooning control system. Section 1.5 introduces the formulation of the problems addressed in the thesis. Lastly, Section 1.6 provides the thesis outline and contributions.

1.1 Motivation

Human activities over the last century are believed to be largely affecting our planet. The increasing trend in greenhouse gas emissions is exhibiting a strong correlation

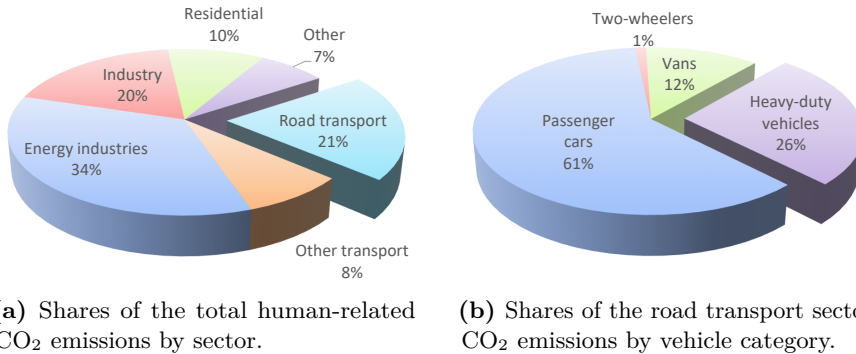


Figure 1.1: Overview of the CO₂ emissions in European Union in 2015 (European Commission, 2017b).

with the rise of the global surface temperature. Temperatures, on average, have increased 0.6 Celsius degrees from the pre-industrial era and are expected to increase by another 3.7 degrees by 2100 if no action is taken (IPCC, 2014). This rise in temperature is causing the melting of glaciers, the rise of sea levels and the increase of the number of extreme atmospheric events (NASEM, 2016). If a radical change of course does not take place, climate change will have a strong impact on the life of our future generations and other species (WHO, 2009). This acquired awareness is leading humanity to reconsider the way we live, and the way we transport.

A study commissioned by the European Commission has estimated that, in 2015, road transportation accounted for the 21% of the total human-related CO₂ emissions, see Figure 1.1 (European Commission, 2017b; Hill et al., 2011). In particular, 26% of these emissions are directly attributable to freight transportation. This is in line with statistics on the US transport sector, where heavy-duty vehicles account for 5.4% of the total CO₂ emissions (Frey and Kuo, 2007). While the emissions from other sectors have dropped in the last 30 years, those imputable to the road transport, and, in particular, to freight are still on the rise (European Commission, 2017b), due to the strong link between freight transportation and economic growth. Following the predicted growth of the world's GDP at an average annual rate of 3.3%, the freight transport sector is expected to continue to expand. Projections from the International Transport Forum predict a doubling of the global CO₂ emissions linked to the surface (road and rail) freight transport sector relative to the level of 2015 if no measures are taken (ITF, 2017). To contrast this evolution, governments all over the world agreed in introducing new policies aimed at strongly reducing human-related greenhouse gas emissions (European Commission, 2011; EPA, 2011; UNFCCC, 2015).

At the same time, the transport sector is responsible for a large share of the global energy consumption. At present, energy is a scarce resource and is therefore

associated to a high cost. The fuel cost for a transportation company accounts for almost one third of the total cost of owning and operating a vehicle (ICCT, 2018). Given an average of 130,000 km driven every year by a heavy-duty vehicle (Hill et al., 2011), the projected fuel cost of 1.4 €/l and an efficiency of 3 km/l, the fuel cost for a single vehicle amounts to approximately 60,000 €/year. Considering that transportation companies typically own several vehicles, fuel has a large impact on their economy. Being able to reduce the fuel consumption by a few percents can therefore translate into significant savings.

The road transport sector is also responsible for the loss of a significant number of human lives. Although fatalities due to road accidents decreased in the last years, they are still one of the leading causes of death. In particular, road traffic crashes are the main cause of death among those aged between 15 and 29 years (WHO, 2015). Road accidents involving heavy-duty vehicles tend to be more severe than other accidents because of their large mass. In the European Union in 2015, 17% of the total road traffic fatalities happened in accidents involving heavy-duty vehicles (ERSO, 2016) and heavy-duty vehicles are more likely to be involved in a fatal accident than passenger cars (SAFE, 2017). For this reason, further improving the safety of the road transport sector and, in particular, of heavy-duty vehicles is still a priority.

1.2 Technology opportunities

In order to address the demand for a a more sustainable, energy-efficient, and safer transportation system, research communities and private companies are investigating the technologies that will shape the future of mobility.

One part of the research is focusing on developing hardware technologies. These include, among others, hybrid and electric propulsion systems, tires with reduced rolling resistance and improved vehicle aerodynamics. Another part is focusing on developing software technologies. Developments in the latter can be classified in one or more of the three general categories displayed in Figure 1.2: vehicle automation, vehicle connectivity, and intelligent transportation. Vehicle automation aims at improving vehicle performance and driver convenience by controlling the longitudinal and lateral vehicle dynamics. Vehicle connectivity allows vehicles to share information between each other and the world. Intelligent transportation provides the framework for higher level functionalities aimed at supervising and intelligently routing vehicles. As shown in Figure 1.2, these frameworks enable a large variety of software technologies. For an in-depth discussion of these technologies we refer the reader to Spulber (2016) and Guanetti et al. (2018).

In this thesis we focus in the control of platoons of heavy-duty vehicles. A platoon consists of a group of vehicles driving at a short inter-vehicular distance. In particular, we discuss control strategies for what we denote as non-cooperative

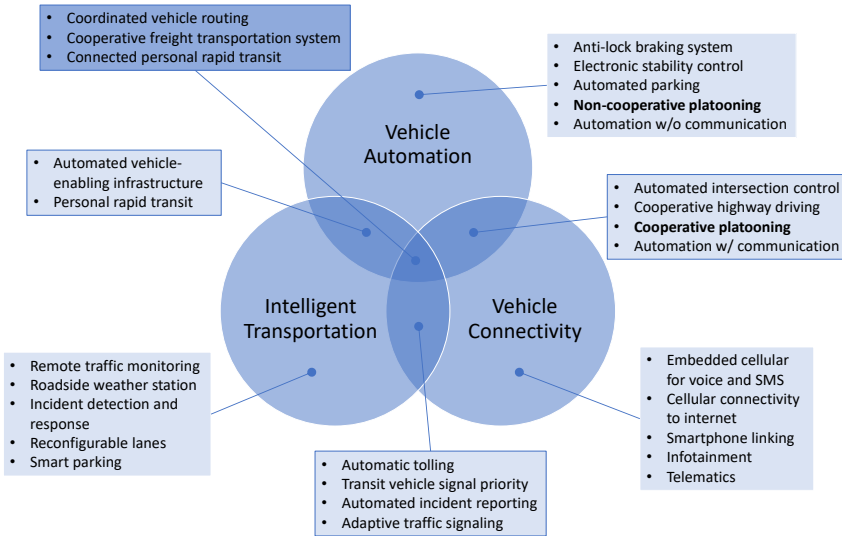


Figure 1.2: Overview on the software technologies for a more sustainable, energy-efficient, and safer transportation system. Adaptation from Spulber (2016).

and cooperative platooning. The first one implies that no cooperation between vehicles exists and can therefore be classified as a vehicle automation functionality. The latter relies on communication between vehicles and aims at cooperatively controlling the vehicles to reach a high level of fuel-efficiency. It is therefore both vehicle automation and connectivity, see Figure 1.2. Platooning research also studies higher-level functionalities that partially belong to the intelligent transportation framework, e.g., cooperative freight transportation systems aimed at coordinating heavy-duty vehicles for promoting platoon creation. Although these functionalities are not the focus of the thesis, they illustrate the future potentials of platooning and are briefly discussed in Section 2.4.

1.3 Platooning for an improved fuel-efficiency and safety

An example of a platoon is displayed in Figure 1.3. Vehicle platooning is an effective method to reduce fuel consumption and, consequently, greenhouse gas emissions. By operating groups of vehicles at a small inter-vehicular distance, the aerodynamic drag experienced by vehicles is reduced. This phenomenon is known as the slipstream effect and consists in the creation of a tunnel of air that moves at a lower relative speed with respect to the platooning vehicles. This translates in reduced air pressure acting on the front of the vehicles and in reduced air vortices on the back of the vehicles. It ultimately results in aerodynamic drag reductions for all following vehicles and, of smaller entity, for the leading vehicle.



Figure 1.3: Four-vehicle platoon driving over an uphill stretch. Photo provided by courtesy of Scania AB.

Figure 1.4 shows a diagram of the air pressure experienced by two vehicles driving at various inter-vehicular distances obtained by means of CFD simulations. Figure 1.5 displays an estimation of the reduction of the aerodynamic drag as function of the inter-vehicular distance on a three-vehicle platoon based on the experimental data reported in Hucho (1987). A distance of 10 m in a platoon of two vehicles driving at 80 km/h, for example, produces a reduction of the aerodynamic drag of 40 % for the second vehicle and of 4 % for the first one. As about a quarter of the heavy-duty vehicle fuel consumption is related to the aerodynamic drag (Hellström et al., 2010), platooning can have a large effect on the fuel consumption. Indeed, independent studies have shown that truck platooning has the potential to save approximately 10 % of fuel for following vehicles while driving at an inter-vehicular distance of 20 m (Bonnet and Fritz, 2000; Alam et al., 2010; Roeth, 2013; Lammert et al., 2014).

As human drivers cannot safely maintain the short inter-vehicular distances needed for the slipstream creation, automation of the platoon longitudinal dynamics is required. Such automation is expected to significantly increase highway safety (Roland B., 2016). In Europe, rear-end collisions represent 15 % of the serious or fatal road accidents where a heavy-duty vehicle is involved (Almqvist and Heinig, 2013). The automatic control of the longitudinal dynamics can largely reduce this percentage. Furthermore, vehicle platooning is typically seen as the first step toward fully-automated vehicles, which are expected to further decrease the overall number of fatalities on our roads.

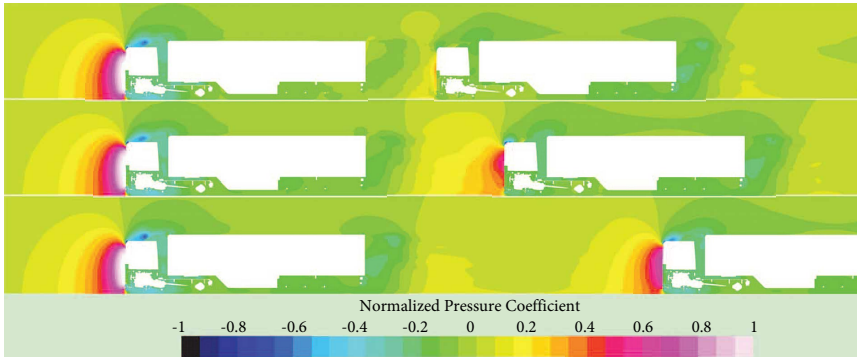


Figure 1.4: Illustration of the air pressure experienced by two vehicles driving at various inter-vehicular distances obtained by means of CFD simulations. Small distances affect the pressure experienced by the following vehicle and the air flow behind the leading vehicle. Image courtesy of Norrby (2014).

1.4 Platooning challenges

Although heavy-duty vehicle platoons are expected to commercially reach our roads in the next few years (e.g., Peloton (2018), Scania (2018), Ahola (2018)), there are still open challenges that need to be addressed to achieve a high level of fuel-efficiency, while guaranteeing safety. The majority of the experimental tests have been performed in controlled environments where altitude variations and the interference of external vehicles have not been included, e.g. Bonnet and Fritz (2000), Browand et al. (2004), Alam et al. (2010) and Lammert et al. (2014). Researcher who tested platooning on public roads reported how altitude variations can neutralize the benefits from the slipstream effect and external traffic can endanger safety, e.g. Alam et al. (2015) and Lank et al. (2010).

Figure 1.6 depicts a three-vehicle platoon facing a downhill segment. Because of the large mass and the limited engine power of heavy-duty vehicles, relatively small slopes can produce large longitudinal forces that cause vehicles to decelerate along uphill segments (because of the limited engine power) and accelerate along downhill segments. As these accelerations and decelerations highly depend on the vehicle characteristics (e.g., vehicle mass and tire rolling coefficient), altitude variation can lead the platoon to separate or require braking action of some of the vehicles in order to avoid collision. This behavior can easily result in the neutralization of the slipstream benefits. Look-ahead control for single trucks driving along hilly roads have shown the potential to reduce vehicle fuel consumption up to 3.5%, see Hellström et al. (2009). Look-ahead control for platooning is consequently expected to lead to much larger fuel savings.

The surrounding traffic can interfere with the nominal behavior of the platoon, see Figure 1.6. It is therefore important to ensure the safety of platoon operations,

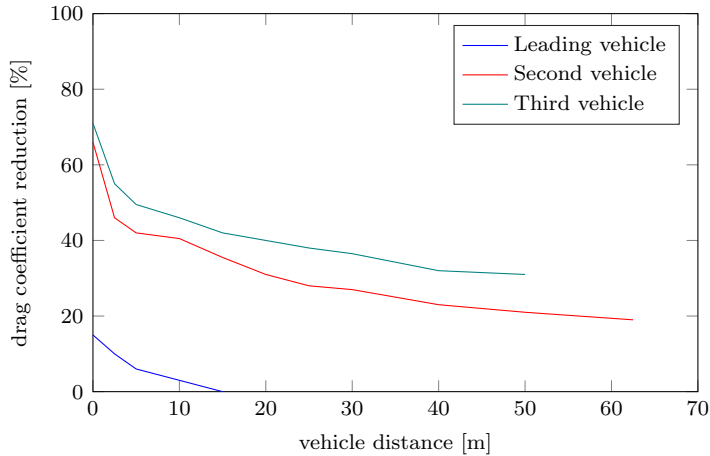


Figure 1.5: Estimation of the reduction of the drag coefficient for three heavy-duty vehicles driving in platoon formation at a speed of 80 km/h for varying inter-vehicular distance. Since the aerodynamic drag is linearly proportional to the drag coefficient a reduction in the drag coefficient reflects a reduction of the aerodynamic drag. The data are adapted from Hucho (1987). Similar results have been reported in Bonnet and Fritz (2000).

while aiming at the fuel-efficient control of the platoon. Due to the potential heterogeneity of the platooning vehicles, which can significantly differ in mass and braking capability, this is not an easy task. Additionally, the slipstream effect produced by platooning generates a reduced aerodynamic force on the following vehicles, which affects the maximum braking deceleration of the vehicles.

These challenges motivate the development of the platoon controllers discussed in the thesis that explicitly takes topography information into account.

1.5 Problem formulation

The overall problem studied in this thesis is the control of the longitudinal dynamics of a vehicle platoon driving along a road with varying topography with the aim of maximizing the fuel-efficiency while guaranteeing safety. A short inter-vehicular distance leads to a reduced overall aerodynamic drag and therefore a reduced platoon fuel consumption. However, to maintain such short distances while avoiding braking and guaranteeing safety requires advanced automatic controllers. In this thesis, we address two related platooning scenarios:

- Cooperative platooning: Platooning vehicles cooperate in order to reach an overall reduced fuel-consumption.



Figure 1.6: Illustration of a heavy-duty vehicle platoon driving on a public highway. Because of vehicle heterogeneity, altitude variations can significantly affect the platoon fuel consumption. Furthermore, external traffic can interfere with platoon operations.

- Non-cooperative platooning: Each vehicle greedily minimizes its own fuel consumption. We focus on two-vehicle platoons where the first vehicle acts as it was alone, while the second vehicle exploits prediction of the preceding vehicle to minimize its own fuel consumption.

In the remainder of this section, we first present the components common to the two problems and, second, we give details on their differences.

Figure 1.7 shows a heterogeneous platoon of $N_v > 1$ vehicles driving along a road with varying topography. The state of each vehicle i is represented by its longitudinal position s_i , speed v_i , and engaged gear g_i . Contiguous vehicles are separated by a distance d_i defined as

$$d_i = s_{i-1} - s_i - l_{i-1}, \quad (1.1)$$

where l_i denotes the length of vehicle i . The road is characterized by its road gradient $\alpha(\cdot)$ defined as a function of the longitudinal position. The longitudinal dynamics of each vehicle can be modeled as

$$\begin{aligned} \dot{v}_i &= \varphi_i(v_i, g_i, \alpha(s_i), d_2, \dots, d_N, \psi_i, F_{b,i}), \\ \dot{s}_i &= v_i, \\ g_i^+ &= \xi_i(g_i, g_{r,i}), \end{aligned} \quad (1.2)$$

where ψ_i , $F_{b,i}$, and $g_{r,i}$ represent the inputs of vehicle i and denote the fuel flow, the braking force, and the requested gear, respectively. Each vehicle is characterized

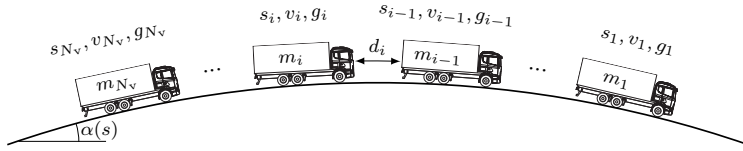


Figure 1.7: Sketch of a platoon of heterogeneous vehicles driving over a road with varying topography.

by parameters such as mass, roll friction, engine efficiency, etc., included in function φ_i . The coupling between the vehicles is defined by the aerodynamic drag, which, in general, is a function of the distance between all the vehicles. The function $\xi_i(\cdot, \cdot, \cdot)$ represents the discrete gear shift dynamics and g_i^+ the engaged gear at the following time step. Furthermore, each vehicle is constrained by input and state bounds, i.e.,

$$\begin{aligned} (v_i, s_i, g_i) &\in \mathcal{X}_i, \\ (\psi_i, F_{b,i}, g_{r,i}) &\in \mathcal{U}_i(v_i, g_i), \end{aligned} \quad (1.3)$$

representing speed limits and bounds on engine torque and speed, braking capability, and admissible gears. The fuel consumption of vehicle i can be defined as

$$\Psi_{\text{vehicle},i} = \int_t^{t+H} \psi_i(\tau) d\tau, \quad (1.4)$$

where t and H denote the current time and the prediction horizon, respectively, while the fuel consumption of the platoon is given as

$$\Psi_{\text{platoon}} = \sum_{i=1}^{N_v} \Psi_{\text{vehicle},i}. \quad (1.5)$$

Finally, the safety requirement can be formulated by demanding the platoon state to lie in a properly defined set, i.e.,

$$(s_1, v_1, \dots, s_{N_v}, v_{N_v}) \in \mathcal{X}_{\text{safe}}. \quad (1.6)$$

In this work, with ensuring safety we mean that the platoon can manage the emergency braking of any of the platooning vehicles without collision.

Cooperative platooning

Given the vehicle dynamics (1.2), and the state and input bounds (1.3), the control problem we consider to solve is to minimize the overall fuel consumption (1.5), while guaranteeing platoon safety (1.6). This can be summarized by the following optimal

control problem:

$$\begin{aligned} & \text{minimize} && \text{platoon fuel consumption (1.5),} \\ & \text{subj. to} && \text{vehicle dynamics (1.2),} \\ & && \text{state and input bounds (1.3),} \\ & && \text{safety constraint (1.6).} \end{aligned}$$

where $i = 1, \dots, N_v$. The cooperative platooning problem is addressed in Part I of the thesis.

Non-cooperative platooning

For non-cooperative platooning, the following vehicle exploits the predicted trajectory of the lead vehicle. If inter-vehicular communication is available, this trajectory can be computed by the lead vehicle and communicated to the following vehicle. If it is not available, it has to be computed by the following vehicle. We refer to the preceding vehicle predicted trajectory as

$$(\hat{v}_1(\cdot), \hat{s}_1(\cdot)). \tag{1.7}$$

Given vehicle dynamics (1.2), the state and input bounds (1.3), and the preceding vehicle predicted trajectory (1.7), the control problem we address how to minimize the vehicle fuel consumption, (1.4), while guaranteeing the platoon safety (1.6). This can be summarized by the following optimal control problem:

$$\begin{aligned} & \text{minimize} && \text{vehicle fuel consumption (1.4),} \\ & \text{subj. to} && \text{preceding vehicle predicted trajectory (1.7),} \\ & && \text{vehicle dynamics (1.2),} \\ & && \text{state and input bounds (1.3),} \\ & && \text{safety constraint (1.6).} \end{aligned}$$

where $N_v = 2$, $i = 2$ in (1.2), (1.3), and (1.4) and $(v_1(\cdot), s_1(\cdot)) = (\hat{v}_1(\cdot), \hat{s}_1(\cdot))$ in (1.6). The non-cooperative platooning problem is addressed in Part II of the thesis.

1.6 Thesis outline and contribution

In this section, we outline the thesis and its contributions.

Chapter 2: Background

This chapter provides the background on fuel-efficient freight transportation and the role of platooning in such a system. We first introduce the technologies that enable

vehicle platooning. Second, we give an overview of the literature related to vehicle platooning. The majority of these works address the problems of platooning and look-ahead control separately. Third, we present the general problem of creating a fuel-efficient freight transportation system, which ranges from how the goods should be dispatched to optimized truck usage. We present a system architecture aimed to divide this complex problem into solvable subproblems. Lastly, we briefly introduce the mathematical tools that we use to solve this control problem, namely dynamic programming and model predictive control. This chapter is partially based on the following publication:

- B. Besselink, V. Turri, S. H. van de Hoef, K.-Y. Liang, A. Alam, J. Mårtensson, and K. H. Johansson. Cyber-physical control of road freight transport. *Proceedings of the IEEE*, 104(5): 1128–1141 (2016).

Chapter 3: Modeling

In this chapter we present a vehicle model suitable for the design of controllers for fuel-efficient and safe platooning. Particular attention is given in modeling components that play an essential role for the fuel consumption, namely the gravitational, rolling, aerodynamic, braking, and traction forces. The vehicle model also includes a high-level powertrain model that describes the engine, the clutch, the gearbox and the transmission. This model details how the fuel is converted into traction force and provides a way to describe the dynamics of gear shifts and freewheeling, i.e., driving in neutral gear. The chapter ends with an overview of a system architecture.

Chapter 4: Control architectures for platooning

In this chapter we develop two control architectures for heavy-duty vehicle platoons. Key aspects include the use of topography information and the ability to take external traffic into account. In order to acquire a good understanding of the effect of road altitude variation on the platoon dynamics, the chapter starts with an analysis of a platooning experiment conducted on public roads. The insights collected from the analysis are used to motivate the following two architectures for vehicle platooning: (i) A control architecture for cooperative control of platoons. In this setting, platooning vehicles cooperate in order to minimize the overall fuel consumption of the platoon, while guaranteeing safety. (ii) A control architecture for the non-cooperative control of platoons. Here, each vehicle greedily minimizes its own fuel consumption given the prediction of the preceding vehicle trajectory. The experiment analyzed in this chapter is based on the following publication:

- A. Alam, B. Besselink, V. Turri, J. Mårtensson, and K. H. Johansson. Heavy-duty vehicle platooning for sustainable freight transportation: A cooperative

method to enhance safety and efficiency. *IEEE Control Systems Magazine*, 35(6): 34–56 (2015).

Part I – Cooperative platooning

Chapter 5: Cooperative fuel-efficient and safe platooning

This chapter proposes a two-layer cooperative controller for vehicle platooning. Each layer is based on an optimal control problem formulation aimed at optimizing the platoon behavior. The top layer, denoted platoon coordinator, is based on dynamic programming, and computes a reference speed profile defined over space for all vehicles of the platoon. It ensures the feasibility of the speed trajectory, which is fuel-optimal by explicitly taking topography information into account. The lower layer, denoted vehicle control layer, is based on a distributed model predictive control framework that safely tracks the reference speed trajectory. Safety is guaranteed by specifically designed constraints that ensure the recursive feasibility of the model predictive controller. The proposed controller is tested in an in-depth simulation study that can be divided into three parts: (i) We evaluate the fuel consumption of a two-vehicle platoon for multiple vehicle control strategies. The results show the potential of the platoon coordinator to reduce the fuel consumption for a fairly hilly road by up to 12% for following vehicles with respect to standard platooning controller from the literature. (ii) We test the reaction of a three-vehicle platoon to multiple maneuvers of the leading vehicle. The results show how the platooning vehicles successfully handle harsh braking of the leading vehicle without collision and how disturbances attenuate along the platoon. (iii) The overall two-layer controller is tested by simulating a three-vehicle platoon driving along the same road as in the experiment presented in the previous chapter, outperforming the experimentally tested controller. The platoon exhibits a smooth behavior and the controller is able to compensate for disturbances acting on the control input. This chapter is based on the following publications:

- V. Turri, B. Besselink, and K. H. Johansson. Cooperative look-ahead control for fuel-efficient and safe heavy-duty vehicle platooning. *IEEE Transactions on Control Systems Technology*, 25(1): 12–28 (2017a).
- V. Turri, B. Besselink, J. Mårtensson, and K. H. Johansson. Fuel-efficient heavy-duty vehicle platooning by look-ahead control. In *Proceedings of IEEE 53rd Conference on Decision and Control*, 654–660. Los Angeles, CA, USA (2014).

Chapter 6: Gear management in cooperative platooning

In this chapter we discuss the problem of how to efficiently manage gear shifts in heavy-duty vehicle platoons. Gears have a strong impact on the vehicle fuel

consumption, and on the reference speed and inter-vehicular distance tracking. Selecting the wrong gear can cause the engine to run in a fuel-inefficient operating point. A gear shift taking place at the wrong moment, e.g., during an uphill stretch, can lead to a large deviation from the speed reference, which can be hard to recover from. Here, we discuss a modification of the control architecture presented in the previous chapter: a gear management layer that optimizes the gear selection and the gear shift timing is introduced. The underlying optimal control problem aims at minimizing the vehicle fuel consumption and the speed and inter-vehicular reference tracking deviations. The gear management is tested in a simulation study that compares it to alternative solutions. The study shows how the proposed solution properly manages the gear shifting task guaranteeing fuel-efficiency and the smooth behavior of the platoon. This chapter is based on the following publication:

- V. Turri, B. Besselink, and K. H. Johansson. Gear management for fuel-efficient heavy-duty vehicle platooning. In *Proceedings of IEEE 55th Conference on Decision and Control*, 1687–1694. Las Vegas, NV, USA (2016).

Part II – Non-cooperative platooning

Chapter 7: Fuel-optimal vehicle-following control

In this chapter, we study the vehicle-following control problem for heavy-duty vehicles. The problem is formulated as an optimal control problem that exploits road topography information and the predicted trajectory of the preceding vehicle to compute the optimal state and input trajectories for the vehicle under control. The vehicle model includes the longitudinal vehicle dynamics and a powertrain model that captures both the gear shifts and freewheeling (cruising in neutral gear) dynamics. This allows for exploring the benefits of combining the fuel savings given by a short inter-vehicular distance with those given by a pulse and glide control strategy. The control is computed via dynamic programming and is tested in a simulation study where the performance for multiple scenarios and controller setups are compared. In particular, we compare the behavior and fuel savings of a heavy-duty vehicle using the proposed control strategy with that of a reference vehicle-following controller that tracks a constant distance. The results show that the proposed control strategy is able to reduce the fuel consumption by up to 18% by keeping a minimum distance of 20 m with respect to the driving alone scenario, and up to 7% with respect to the use of the constant-distance vehicle-following controller. This chapter is based on the following publication:

- V. Turri, O. Flårdh, J. Mårtensson, and K. H. Johansson. Fuel-optimal look-ahead adaptive cruise control for heavy-duty vehicles. In *Proceedings of IEEE American Control Conference*. Milwaukee, WI, USA (2018). To appear.

Chapter 8: Low complexity vehicle-following control

In this chapter, we discuss a vehicle-following controller for passenger cars. The controller receives a prediction of the preceding vehicle trajectory and directly manipulates the inputs of the low-level vehicle controllers. This requires the vehicle-following controller (i) to exploit long previews of the preceding vehicle trajectory and (ii) to run fast enough for real-time. These conditions are conflicting as the exploitation of a long preview suggests a long prediction horizon, while the fast computation calls for a short one. To address this conflict, we propose an optimal control formulation that uses a relatively short horizon and compensates for that by redefining the cost function and introducing a specific terminal state constraint. In particular, the cost function is redefined to include terms that promote the long term fuel-efficient behavior of the vehicle. The terminal state set includes all states that, given a conservative prediction of the preceding vehicle future trajectory, will not require braking action after the end of the prediction horizon. The proposed vehicle-following controller is tested in both real vehicle experiments and simulations. The experiments show that the proposed controller avoids unnecessary braking and can significantly improve fuel economy and ride comfort. Remarkably, the proposed terminal set can conveniently exploit long previews, while keeping the length of the prediction horizon limited to a few seconds, thus making the real-time implementation realistic. The simulation study shows how the vehicle behavior is comparable when using the proposed controller and when using a similar controller that uses a significant longer horizon, representing an approximation of the acausal optimum. This chapter is based on the following publication:

- V. Turri, Y. Kim, J. Guanetti, K. H. Johansson, and F. Borrelli. A model predictive controller for non-cooperative eco-platooning. In *Proceedings of IEEE American Control Conference*, 2309–2314. Seattle, WA, USA (2017b).

Chapter 9: Conclusion and future work

This chapter contains a summary of the work presented in the thesis and highlights potential future research directions.

Other publications

The following publications are not part of the thesis, but inspired some of the presented work:

- V. Turri, A. Carvalho, H. E. Tseng, K. H. Johansson, and F. Borrelli. Linear model predictive control for lane keeping and obstacle avoidance on low curvature roads. In *Proceedings of IEEE 16th International Annual Conference on Intelligent Transport*, 378–383. The Hague, The Netherlands (2013).

-
- K.-Y. Liang, S. van de Hoef, H. Terelius, V. Turri, B. Besselink, J. Mårtensson, and K. H. Johansson. Networked control challenges in collaborative road freight transport. *European Journal of Control*, 30: 2–14 (2016).
 - D. Nigicser, V. Turri, J. Mårtensson, A. A. Mustafa, and E. S. da Silva. Predictive vehicle motion control for post-crash scenarios. In *Proceedings of 14th International Symposium on Advanced Vehicle Control*. Beijing, China (2018). To appear.

Contribution by the author

In the above works, the order of the authors reflects their contribution, where the first had the most important contribution. In all the publications the thesis author participated actively in the discussions and derivations of the theory and results, as well as in the paper writings.

Background

This chapter establishes the required background to the rest of the thesis. We first introduce the technologies that enable look-ahead vehicle platooning and the existing longitudinal control functionalities that relate to it. Then, we give an overview of the literature related to look-ahead vehicle platooning. There exist only few works that address the fuel-efficient vehicle platooning control by explicitly taking road topography information into account. Such overview, therefore, mainly focuses on the works that deal with the problems of platooning control and look-ahead vehicle control, separately. Afterwards, we give a broader perspective on the potential for increasing fuel-efficiency in the freight transport sector. We propose a system architecture for fuel-efficient freight transportation aimed at maximizing the benefits from platooning. Such architecture deals with problems ranging from how to fuel-optimally route vehicles over the road network exploiting platoon possibilities, to how to efficiently control the vehicle actuators. Lastly, we introduce the concepts of dynamic programming and model predictive control that will be exploited in the platoon controllers proposed in the thesis.

The chapter is organized as follows: in Section 2.1 we present the technologies that enable the safe and fuel-efficient implementation of vehicle platooning. Sections 2.2 and 2.3 provide a literature overview on vehicle platooning control and look-ahead vehicle control, respectively. The fuel-efficiency problem from the whole freight transport sector perspective is discussed in Section 2.4 and a system architecture centered on platooning is introduced. Section 2.5 presents a short overview on the concepts of dynamic programming and model predictive control. Lastly, Section 2.6 summarizes the chapter.

2.1 Technologies enabling platooning

In order to safely operate heavy-duty vehicles at a short inter-vehicular distance, as necessary for a reduced aerodynamic drag, the longitudinal dynamics automation

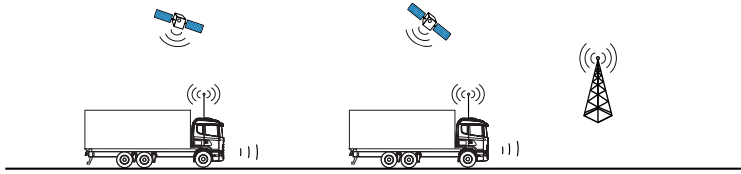


Figure 2.1: Advances in technology provide the tools for realizing safe and fuel-efficient vehicle platooning. On-board sensors, e.g. radars, lidars and cameras, allow to measure the distance and the relative speed with respect to the preceding vehicle. GPS data fused with speed and acceleration measurements can generate estimation of the current vehicle state with a precision of centimeters. Wireless sensor units allow the platooning vehicles to share state information between them and to communicate with a back-end office or cloud services.

based on information received through communication or collected by on-board sensors is needed. In this section we present the existing technologies that enable platooning. In particular, we discuss the longitudinal control functionalities and the technologies at the base of the environment perception and vehicle connectivity.

2.1.1 Longitudinal control functionalities

The first step towards the automation of the longitudinal relative vehicle dynamics happened with the introduction of the adaptive cruise control (ACC), see e.g. Vahidi and Eskandarian (2003). ACC relies on information collected by on-board sensors such as inter-vehicular distance and relative speed. In the early days of ACC, this information was collected by a radar placed in the front of the vehicle. Nowadays, other sensors, e.g. lidars and multiple cameras, work alongside the radar in order to provide more accurate information. This information, combined with estimated states of the own vehicle, is used to control the powertrain and braking system in order to track a certain spacing policy while ensuring safety. While this setup has been proved successful for the vehicle-following control problem, it showed its limit when multiple contiguous vehicles in a platoon formation use it to regulate the inter-vehicular spacing. In particular, as ACC only relies on local information, the acceleration of the head of the vehicle string can only be detected with a certain delay by the tail of the platoon. This can produce unwanted behaviors such as the amplification of distance errors and control effort along the platoon, giving rise to the so-called string instability.

The introduction of wireless units in vehicles enables the communication between different vehicles, known as vehicle-to-vehicle communication, and between vehicles and infrastructure, known as vehicle-to-infrastructure communication, see Figure 2.1. The inter-vehicular communication allows each vehicle to have a more complete

and accurate knowledge of the platoon state. By fusing GPS data with speed and acceleration measurements, each vehicle can estimate its state with a precision of centimeters (Ryu and Gerdes, 2004) and, thanks to inter-vehicular communication, this information can be shared with the rest of the platoon. Inter-vehicular communication allows vehicles to also share or agree on parameters that are critical for platooning, such as vehicle mass, braking capability and actuator limitations. The inter-vehicular communication framework has allowed the development of more advanced longitudinal control functionalities, known as cooperative adaptive cruise control (CACC).

Vehicle-to-infrastructure communication, on the other hand, allows vehicles to receive information on the road ahead, e.g., topography information or traffic status. Topography information can be exploited to improve the fuel-efficiency of vehicles. By including such information in a look-ahead control (LAC) framework the speed of single vehicles can in fact be adjusted to minimize their fuel consumption, for example, by avoiding unnecessary braking during downhills. The same idea can be extended to platooning vehicles for which the speed can be coordinated to reach a high level of fuel-efficiency. We will refer to this control as cooperative look ahead control (CLAC). Vehicle-to-infrastructure communication, finally, can also be exploited to communicate with off-board systems, such as a back-end office or cloud services, see e.g. Whaiduzzaman et al. (2014) and van Dooren et al. (2017). This provides the means for implementing more complex tasks related to platooning, e.g., the coordination of vehicles on a road network in order to create platoons as it will be discussed in Section 2.4.

2.1.2 Environment perception

The longitudinal control functionalities rely on information about the surrounding environment collected by multiple on-board sensors, e.g., radars, lidars and cameras.

Nowadays, vehicles are equipped with multiple radars that carry out different functions. Those used for the control of the longitudinal dynamics are placed in the front of the vehicle and are typically categorized as short, middle and long range radar sensors, depending on the specifications. The radar uses the reflection of electromagnetic waves with wavelength in the order of a few millimeters to measure the distance and the relative speed of an object. The distance is computed by processing the emitted signal together with the received one, while the relative speed measurement relies on the Doppler effect (Wenger, 2005). The distance range varies between 0.15 and 200 m, while the accuracy can be down to 0.02 m and 0.1 m/s for distance and relative speed measurements, respectively (Hasch et al., 2012). Radar has a fundamental role in automotive applications because of its robustness against environmental influences such as extreme temperatures, bad light and weather conditions.

One of the first uses of lidar technology for automotive control dates back to the

2005 Grand DARPA Challenge, where the winning team from Stanford University equipped their vehicle with five lidars (Thrun et al., 2006). A lidar emits ultraviolet light and estimates the distance to an object by measuring the time it takes for the light beam to reach the object and be reflected back to the sensor. By simultaneously emitting multiple laser beams or scanning the field of view using a spinning mirror, the lidar is able to return a 3D map of the environment (Zhao et al., 2015). Thanks to an accuracy in the order of centimeters and a refresh time down to tenths of a second, the lidar can provide detailed 3D maps of the surrounding environment ideal for navigation purposes and safety functionalities (Gutelius, 2014).

Cameras are typically used to identify and classify objects critical for the vehicle automation, including both moving objects, e.g., other vehicles, pedestrians and cyclists, and road features, e.g., lane markings and traffic lights. Used in pairs, cameras also allow to measure distances to objects and can be successfully used for ACC applications (Zhao et al., 2015). Collision warning functionalities have been also been developed using single cameras that rely on the scale-change of objects to trigger the warning (Dagan et al., 2004).

Typically the information collected by radars, lidars and cameras is fused in order to obtain an accurate and real-time environment model with a high-level of redundancy thanks to sensor diversity. This model is essential for the successful control of autonomous vehicles. How to model the environment in a suitable way for autonomous vehicle control is still an open problem and the subject of ongoing research, see e.g. Berkeley DeepDrive (2018) and MIT SelfDrivingCars (2018).

2.1.3 Vehicle connectivity

Extensive research has been conducted on wireless vehicle communications, see Sichertiu and Kihl (2008) and Willke et al. (2009). Some of the main challenges faced in these works are related to communication reliability (Ramachandran et al., 2007), the requirement for limited delay (Bilstrup et al., 2008) and communication security (Raya and Hubaux, 2005). These are considered significant problems in inter-vehicular communication especially because of the intrinsic decentralized nature and highly dynamic characteristics of vehicle networks. Multiple standards are currently under study by telecommunication companies and institutions in order to implement reliable wireless vehicle communication.

The IEEE 802.11p is an amendment to the IEEE 802.11 standard approved in 2010 aimed at adding wireless access in vehicular environments IEEE-SA (2010). It defines the wireless medium access control (MAC) and physical layer specifications in order to enable data exchange between (high-speed) vehicles and infrastructure. For the implementation of the IEEE 802.11p standard the United States Federal Communications Commission and the European Telecommunications Standards Institute have allocated part of the 5.9GHz band, although the frequency range is not exactly the same. The ITS-G5 technology that is expected to roll out in the

next few years is based on the IEEE 802.11p protocol and will provide cellular and inter-vehicular connectivity to vehicles (ETSI, 2012).

2.2 Platooning control

Although the commercial deployment of platoons is at a research stage and expected to happen in the next few years (Peloton, 2018; Scania, 2018; Ahola, 2018), the concept of platooning has a long history. The first public presentation of an automated convoy of vehicles driving at a short inter-vehicular distance dates back to 1939 during the World Fair in New York. At this exposition, General Motors showed a film entitled *To New Horizons* (General Motors, 1939) which presents a future where cars are able to maintain a safe distance by using automated radio control and where curved road sides help the driver to keep the vehicle within its lane. Early works on the dynamical behavior of a string of (manually driven) vehicles start to appear in the fifties. In Pipes (1953), a simple model of the driver is used to explain the delayed start of a string of vehicles when the light turns green at an intersection. Only in the sixties, the platoon concept, intended as a string of automatically controlled vehicles, started to gain a certain attention from the control community. An early work (Levine and Athans, 1966) proposed an optimal control approach for the automation of the longitudinal dynamics of a string of vehicles. The solution of the optimal control problem resulted in a feedback law that required the exchange of information between all platooning vehicles. Approaches that required the communication between a smaller number of vehicles have been later proposed, see, e.g., Chu (1974) and Sheikholeslamn and Desoer (1990).

In the remainder of the section, we review a selection of works on platooning control most relevant to this thesis, grouping them according to their main focus, i.e., string stability, fuel-efficiency, and safety.

2.2.1 String stability

An aspect that has been deeply studied since the early days of platooning research is string stability. The notion of string stability was first introduced by Peppard (1974) and refers to the ability of the controlled vehicle string to attenuate disturbances as they propagate through the string. A formal definition of string stability is given in Swaroop and Hedrick (1996) and an overview of its various interpretations existing in literature is presented in Ploeg et al. (2014). In order to achieve string stability, Peppard (1974) proposes a PID controller that exploits real-time information from both the preceding and following vehicles in order to track a constant space gap.

Sheikholeslamn and Desoer (1990) were able to show that string stability cannot be achieved by only using real-time information from the preceding vehicles (known as the predecessor-following strategy) while tracking a constant space gap. In their work, therefore, they propose a different control framework that is able to obtain

string stability by exploiting the real-time information from both the preceding and leading vehicle. In Seiler et al. (2004), an explanation for these results is given, based on properties of the transfer function between the position errors of contiguous vehicles. In order to overcome the intrinsic string instability of predecessor-following strategies based on the space gap policy, Ioannou and Chien (1993) proposed the use of a speed-dependent spacing policy. They show that string stability can be achieved in a predecessor-following strategy setup by using a constant headway gap policy, i.e., tracking a gap proportional to the vehicle speed (where the proportional constant is referred to as headway time) in addition to the fixed space gap. Although this approach allows to reach string-stability also in an ACC framework (where inter-vehicular communication is not available), Swaroop et al. (1994) pointed out that the constant headway gap policy requires traction forces that are inversely proportional to the headway time. A small headway gap can therefore lead to the saturation of the inputs and to the consequent deterioration of the platoon performance. Swaroop et al. (1994) observed that the proportionality constant can be reduced by introducing local communication between contiguous vehicles (and therefore switching to a CACC framework) and feeding back the acceleration of the preceding vehicle. These results have been verified by Naus et al. (2010) and Ploeg et al. (2011) by conducting platooning experiments involving two and six vehicles, respectively. In particular, they show how it is possible to significantly reduce the constant headway gap by switching from an ACC configuration to a CACC one. Yanakiev and Kanellakopoulos (1995) show that string stability can be guaranteed also for the more complex dynamics of heavy-duty vehicles, when a constant headway gap policy is used or the reference speed of the leading vehicle is shared between vehicles.

More recently, a decentralized framework based on model predictive control has been proposed in Dunbar and Murray (2006) and Dunbar and Caveney (2012) for heterogeneous vehicle platooning. Because of the non-linearities intrinsic to the model predictive controller, the platoon string stability could not be studied by a frequency domain analysis. Instead, the authors use a Lyapunov-based argument to prove string stability of the platoon when each vehicle exploits the communicated predicted trajectory of the preceding vehicle and the reference trajectory of the leading one in a model predictive controller. Besselink and Johansson (2017) study the string stability problem for platoons tracking a speed trajectory defined in the spatial domain. The authors show that by using a constant time gap policy corresponding to the tracking of a unique spatially-defined speed trajectory, string stability can be guaranteed. Here, we point out that string stability is however not a guarantee for safety. Even if disturbances attenuate along the string of vehicles, the harsh braking of any of the platooning vehicles can lead to a position deviation equal to the reference distance and result therefore into collision.

Until the nineties the research on platooning has been mainly theoretical. The

Partners for Advanced Transportation Technology (PATH) project (Shladover, 2007), founded in 1986 in California, USA, brought a new boost to the field. The original aim of the project was the study of the potential of platooning for an increased highway throughput. Within this project, Varaiya (1993) proposed a solution based on platoons of 15 vehicles driving at an inter-vehicular distance of 2 m and platoons separated by 60 m. Due to the short inter-vehicular distance, it is argued that, even if collisions occur, they would have a small impact because of the small relative speed between vehicles. This solution allows to increase the highway throughput up to three times. In Horowitz and Varaiya (2000), a system architecture that splits the described control task in manageable subproblems is proposed. During the project numerous experimental tests involving vehicle platoons of up to eight vehicles using inter-vehicular communication have been conducted (Hedrick et al., 1994; Rajamani et al., 2000). In these tests, the string stability has been guaranteed by the exploitation of the leading and preceding vehicles speed and acceleration shared by inter-vehicular communication, while tracking a constant space gap.

2.2.2 Fuel-efficiency

Although the environmental aspect was not the original focus of the PATH project, the fuel consumption reduction potential of vehicle platooning has been studied. Tests conducted in a wind tunnel with passenger car models suggest a reduction of approximately 20% of the aerodynamic drag experienced by following vehicles for a platoon of four vehicles spaced by half vehicle length (Zabat et al., 1995). Experiments conducted on real heavy-duty vehicles show average fuel consumption reductions that vary from about 11% at 3-4 meters spacing to about 8% at 8-10 meters spacing (Browand et al., 2004). With the beginning of the PATH project and the related successful experimental results, there was an increased interest of the research community towards more practical aspects of platooning, e.g., traffic impact, safety, user acceptance and fuel-efficiency (Bergenheim and Huang, 2010; Bergenheim et al., 2012; Tsugawa, 2013; Shladover, 2012). In particular, because of the noteworthy results on the reduction of fuel consumption for heavy-duty vehicle platooning, the potential for increased fuel-efficiency has been further studied for heavy-duty vehicles. In more recent tests that involved two-vehicle platoons, fuel consumption reduction of approximately 10% while driving at the inter-vehicular distance of 10 meters have been confirmed (Bonnet and Fritz, 2000; Alam et al., 2010; Roeth, 2013; Lammert et al., 2014).

Remark 2.2.1. The variability of the reported results in the fuel consumption reduction is attributed to multiple factors. The reviewed works suggest that the shape of the heavy-duty vehicles is a main factor, as experiments conducted with flat-nosed tractors (Bonnet and Fritz, 2000; Alam et al., 2010) returned higher fuel-saving than those conducted with long-nosed tractors (Roeth, 2013; Lammert et al., 2014).

Other factors are vehicle parameters (e.g., mass and tire roll coefficient), external factors (e.g., wind, weather condition, and road surface state), and measurement noise.

The so-far-discussed experiments have been conducted in controlled environments, where the influence of neither external traffic nor altitude variations have been considered. Lank et al. (2010) report tests conducted within the KONVOI project (Wille et al., 2007) where a platoon of four heavy-duty vehicles is driven on a public highway. The authors state that, while fuel savings were registered during preliminary experiments conducted along a test track, no fuel consumption reduction occurred during the public road experiments due to traffic interference. Alam et al. (2015) report another test conducted along public highway involving a three-vehicle platoon. The experiment results show the platooning potential of reducing fuel consumption of about 5% along nearly flat road stretches. However, when the road exhibited a larger altitude variation, the performance of the platoon degraded and the fuel consumption of following vehicles increased to about 4% with respect to driving alone, due to repeated braking actions. An in-depth analysis of this increase in fuel consumption is presented in Section 4.1. This analysis provides the fundamental insights for the development of the control formulations presented in the next chapters. Other research works that study the impact of altitude variations on platoon performance and propose control frameworks to address it are discussed in Section 2.3.

2.2.3 Safety

As vehicle platoons are expected to drive on public roads, they need to cope with the presence of external vehicles. Unexpected events such as accidents or vehicle cuts-in, can require emergency braking of any vehicle in the platoon. According to the definition of safety given in Section 1.5, platooning vehicles should be therefore able to react to the maximum deceleration of any of the other vehicles, without collision occurring.

In Chien and Ioannou (1992), the authors derive a formulation of the safety distance, i.e., the minimal allowed inter-vehicular distance, that agrees with our definition of safety. The obtained expression takes the maximum vehicle deceleration and detection delays into account and can be formulated as

$$d_{\text{safe}} = \lambda_1(v_i^2 - v_{i-1}^2) + \lambda_2 v_i + \lambda_3, \quad (2.1)$$

where v_{i-1} and v_i represent the speed of the preceding and current vehicles, respectively, and λ_1 , λ_2 and λ_3 are suitable parameters. Similar expressions of the safety distance have been derived in Doi et al. (1994) and Yasuhiko et al. (1995), and are used to formulate a binary logic to control the braking action in a adaptive cruise controller. Seiler et al. (1998b) propose a sliding mode controller to track a braking

speed profile corresponding to the safety distance. Collision avoidance and collision warning functionalities based on a similar distance model have been also developed by Honda and Mazda (Seiler et al., 1998*a*).

Works within the PATH project have addressed the safety problem for platoon operations. In Li et al. (1997) and Alvarez and Horowitz (1997), the authors propose control laws for the safe merging and splitting maneuvers in platoons. More recently, Alam et al. (2014) propose a game-based approach to compute the safe state set for CACC frameworks where communication is allowed. The authors show how in such setting it is safe to drive at full speed with a inter-vehicular distance of 1.2 m. In van Nunen et al. (2016), the safety problem in the scenario of inter-vehicular connectivity failure in CACC is addressed. The authors propose a maneuver mechanism that allows to maintain safety when connectivity is lost. In van Nunen et al. (2017), multiple safety indicators are tested in experiments involving a platoon of two vehicles driving with a headway gap of 0.5 s. The authors state that, in such scenario, indicators that rely on inter-vehicular communication are able to distinguish between threatening and safe situations, while those that use only radar information fail in that. A systemic literature review on safety in vehicle platooning is presented in Axelsson (2017).

2.3 Look-ahead control

The works on platooning control reviewed in the previous section are based on feedback control. In this section, we discuss existing works on longitudinal vehicle control that use a look-ahead control framework to improve the performance of the controller. Look-ahead control allows to exploit information about known future disturbances acting on the vehicles. These disturbances can be, for example, the altitude variation of the road ahead or the predicted behavior of preceding vehicles. By taking this preview information into account in the synthesis of the control inputs it is potentially possible to improve the fuel economy and safety of vehicles.

In the remainder of the section we first present look-ahead control approaches used to reduce the fuel consumption of single vehicles. Then, we focus on look-ahead control strategies for non-cooperative and cooperative platooning. Here, we remind that in this thesis we refer to cooperative platooning when vehicles act together to reach a common goal, whereas we refer to non-cooperative platooning when each vehicle greedily optimizes its own fuel consumption by exploiting prediction of the preceding vehicle trajectory. In the latter, the prediction can be computed by the preceding vehicle and communicated to the following vehicle, or it can be computed by the following vehicle itself.

2.3.1 Single vehicle

The first works that studied how to include preview information to improve the energy economy of a single vehicle, focused on rail vehicle control. Kokotovic and Singh (1972) propose a control law based on the Pontryagin maximum principle to optimally accelerate and decelerate an electric train equipped with regenerative braking. An extensive review of energy-efficient look-ahead control for trains is presented in Liu and Golovitcher (2003).

An early work that explores how to exploit terrain topography information to improve the fuel economy of a passenger vehicle has been authored by Schwarzkopf and Leipnik (1977). This work formulates an optimization problem based on non-linear vehicle dynamics aimed at minimizing the vehicle fuel consumption and proposes an analytical solution for constant road grade based on the maximum principle. In Hooker (1988), an approach based on dynamic programming that is able to handle generic road profiles has been proposed. However, due to the complexity of the algorithm, only short road segments could be considered. In order to overcome this limitation, a variation of this technique was proposed in Monastyrsky and Golownykh (1993). In this work, thanks to the reformulation of the problem in the spatial domain and the relaxation of the time constraint, a significant reduction of the computational complexity was reached. In detail, the reduction of the dimension of the state space allowed to consider much more complex scenarios. A similar approach has been taken in Hellström et al. (2006), where a predictive cruise control for heavy-duty vehicles based on topography information and speed limits of the road ahead computes the fuel-optimal speed profile. Experimental tests in Hellström et al. (2009) have shown the ability of such a controller to reduce the fuel consumption of a heavy-duty vehicle driving over a hilly road by up to 3.5%. Solutions of the optimal control problem for the fuel-efficient control of heavy-duty vehicles via the Pontryagin maximum principle have also been proposed, see e.g. He et al. (2016) and Henriksson et al. (2017).

In Johannesson et al. (2015), a three-layer control architecture is proposed to handle the fuel-optimal control of a hybrid truck. The layers are responsible for the generation of the fuel-optimal speed profile, the scheduling of the gear and the powertrain mode, and the tracking of the optimal speed profile, respectively. Because of the good scalability of such architecture, we propose in Chapter 6 a similar breakdown of the control tasks for the supervision of a heavy-duty vehicle platoon.

2.3.2 Cooperative platooning

As discussed in the previous subsection, the exploitation of topography information to control single heavy-duty vehicles has been extensively studied and it results in valuable fuel savings. However, only in the last years the research community

has started to address the problem for heavy-duty vehicle platoons. Because of the extra constraints on the vehicle dynamics due to the short inter-vehicular distance, look-ahead control is expected to lead to larger benefits to platoons compared to single vehicles.

A first study of the impact of altitude variation on heavy-duty vehicle platoons and the potential benefits of the inclusion of topography information in platoon control is presented in Alam et al. (2013). The authors propose a control strategy that collects the fuel-optimal speed trajectory computed by each vehicle individually and selects the one that is feasible for all the vehicles as a reference for the whole platoon. In Németh and Gáspár (2013), a similar approach is used. In this work, a common reference speed trajectory is also computed by combining the optimal speed trajectories of each vehicle. The combination is done by minimizing the deviations of the optimal trajectories of each vehicle from the common speed trajectory of the whole platoon. Kaku et al. (2013) propose a nonlinear model predictive control framework based on a detailed model of the platoon that uses a relatively short horizon. Simulation results show the capability of the proposed controller to fuel-efficiently adjust the platoon vehicle speed while driving over a synthetic hill. However, the relatively short horizon necessary for limiting the problem complexity is in general too restrictive to be used for realistic road profiles. Murgovski et al. (2016) divide the fuel-efficient control problem into two subproblems within a hierarchical control architecture. The higher layer uses simplified vehicle models and solves a quadratic programming problem to compute reference speed trajectories. The lower layer solves a dynamic programming problem and computes the optimal gear shift sequence for each platooning vehicle. The simulation study shows the capability of the proposed architecture to fuel-efficiently control the platooning vehicles.

In Chapters 5 and 6 we present a novel control architecture that addresses the cooperative look-ahead control problem for fuel efficient and safe heavy-duty vehicle platooning. The proposed architecture, similarly to Murgovski et al. (2016), divides the overall fuel-efficient control problem into manageable subproblems.

2.3.3 Non-cooperative platooning

In recent years, look-ahead control has been also explored in order to improve the fuel economy in vehicle-following control problems for passenger cars. Bu et al. (2010) propose a model predictive control formulation for adaptive cruise control where the preceding vehicle communicates its state and control input. Experiments reported in the paper show how the shared information lead to a smoother and more reactive platoon behavior. Li et al. (2011) propose a model predictive control formulation that aims at promoting a smooth, fuel-efficient and safe behavior of a vehicle following another one whose future behavior is estimated. The authors report the ability of the proposed controller to save approximately 6% and 2% of fuel

in simulated city and highway scenarios, respectively, compared to feedback-based controllers. In Li et al. (2013), the authors test the controller through real vehicle experiments and report similar fuel savings by using a prediction horizon of 5 s. In Li et al. (2012), the authors identify the most fuel-optimal driving strategies for passenger cars and translate them into a rule-based controller. They show how it is possible to combine vehicle-following and pulse and glide control strategies in a rule-based controller to reduce the vehicle fuel consumption.

Stanger and del Re (2013) address the vehicle-following problem from a fuel-efficiency perspective. They propose a nonlinear model predictive controller that aims at directly minimizing the fuel consumption. A simulation study tests the controller with different prediction horizons under the assumption of perfect knowledge of the preceding vehicle trajectory. Simulation results show how, with a horizon of 15 – 20 s, the following vehicle saves approximately 20%. In Lang et al. (2014), the authors propose a nonlinear autoregressive model to predict the trajectory of the preceding vehicle in a moderate non-congested traffic scenario and they show how the accuracy of the prediction highly influences the vehicle fuel consumption. Moser et al. (2018) use a conditional linear Gaussian model to estimate the probability distribution of the preceding vehicle trajectory and they exploit it in a stochastic model predictive control framework. Simulation results show a significant reduction in the vehicle fuel consumption compared to the use of a deterministic model predictive control strategy.

None of the reviewed works, however, addresses the vehicle-following control problem for heavy-duty vehicles where the fuel economy can largely benefit from short inter-vehicular distances, but it can be also influenced by road altitude variations. In Chapter 7 we address this problem and we show how the inclusion of topography information in the optimal control problem formulation is beneficial for further reducing fuel consumption.

2.4 Fuel-efficient road freight transportation

In this section we discuss an architecture for the promotion and the control of heavy-duty vehicle platoons aimed at a more sustainable road freight transportation.

As argued in Section 2.2, platooning has a great potential for increasing the fuel-efficiency of heavy-duty vehicles. However, in order to fully exploit the benefits of platooning, the formation of platoons needs to be promoted and coordinated, see Figure 2.2. Heavy-duty vehicles represent a small portion of the road traffic and their locations can be sparsely distributed over the road network. In order to achieve this, the route, departure time and speed profile of each vehicle need to be adjusted. This is not a easy task. Each vehicle has its own mission defined by a specific starting point, final destination, and a certain time constraint. Therefore, the coordination of heavy-duty vehicles cannot be performed in a naive way. Increasing

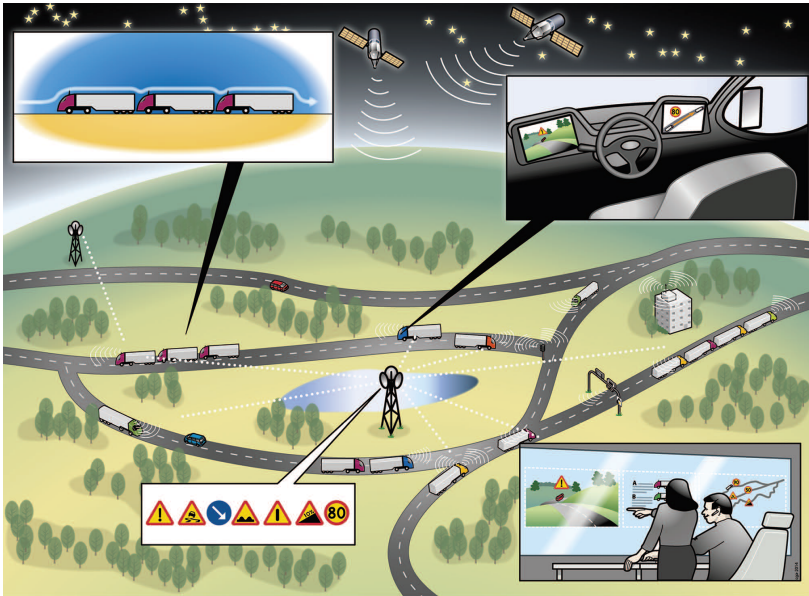


Figure 2.2: Illustration of a heavy-duty vehicles coordination problem. Vehicles with different destinations and time constraints need to be coordinated in order to form platoons. The coordination should be based on fuel-efficiency criteria and platoons should be formed only when favorable.

the average speed to join a platoon that is going to split after only a few kilometers can be less efficient than simply maintaining the original average speed and continue driving alone. Therefore it is evident that the starting time, the route and the speed trajectory of each heavy-duty vehicle need to be planned and coordinated intelligently in order to fully exploit the benefits of platooning.

In order to address the resulting optimization problem aimed at fully exploiting the benefit of platooning, we propose a system architecture that splits this large problem into manageable subproblems. The system architecture is depicted in Figure 2.3 and is composed of three layers, namely, the fleet layer, the platoon layer, and the low-level vehicle control layer. Each layer is detailed in the following paragraphs.

The fleet layer is responsible for the coordination of a large fleet of vehicles potentially belonging to multiple fleet owners. Explicitly taking information on destinations and time requirements of all vehicles in the fleet into account, it defines the routes and meeting times and points for the creation of new platoons or the merging of existing ones. Since traffic and slopes have a significant impact on the fuel-consumption of heavy-duty vehicles, topography information and historical and real-time traffic information can be also included. This problem can be cast in a large

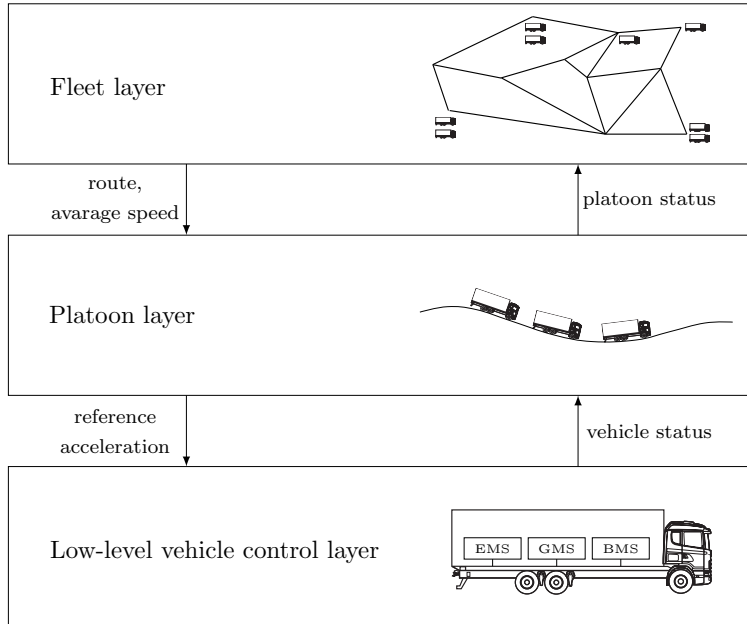


Figure 2.3: Three-layer system architecture for a fuel-efficient freight transport system. The aim of this architecture is to split in solvable subproblems the complex problem of coordinating and controlling heavy-duty vehicles to fully exploit the benefits of platooning.

optimization problem and suggestions on how to solve it have been proposed in the recent years, see e.g. (van de Hoef et al., 2015), (Larson et al., 2015), (Liang et al., 2016a), (Čičić et al., 2017) and (van De Hoef et al., 2018). van de Hoef et al. (2015) propose a centralized approach based on the sequential computation of optimal paths for each vehicle and the optimization of each vehicle’s average speed in order to enable the formation of platoons. Larson et al. (2015), instead, solve the problem by employing controllers distributed over the road network. A control unit located in each node of the network decides if it is fuel-efficient for the approaching vehicles to adapt their speed in order to form platoons. The functionality of the fleet layer can also be extended upwards to include the logistics problem, i.e., how the flow of goods needs to be distributed between the available vehicles while taking limitations on size into account, weight and the type of cargo in each vehicle. Alternative approaches aimed at stimulating the formation of platoon have been also studied. For example, Farokhi and Johansson (2013) propose a game-theoretic approach that exploits dynamic congestion fees depending on the vehicle category, i.e., passenger car or heavy-duty vehicle, in order to encourage vehicles belonging to the same category to drive at the same time.

The platoon layer is responsible for the fuel-efficient and safe control of the platoon. It receives requirements on average speed from the cooperation layer and computes the fuel-optimal acceleration of each vehicle. Such computation relies on an optimal control framework that explicitly takes topography information into account and guarantees the safety of platoon operations. The existing results on this topic have been reviewed in Section 2.3. A novel approach that addresses the problem is proposed in Chapter 5 and extended in Chapter 6.

The low-level vehicle control layer controls the vehicle actuators. Its implementation relies on control units typically available in commercial heavy-duty vehicles. These units are the engine management system, the gear management system and the braking management system. A detailed treatment of these control units is given in Section 3.3.

2.5 Optimal control

In this section, we briefly introduce the two optimal control approaches that will be used in the platoon control formulations presented in this thesis, namely dynamic programming and model predictive control. In this thesis, dynamic programming is preferred to solve optimal control problems that are highly non-linear or that contain discrete states. Model predictive control is preferred to address control problems that use a (quasi-)linear vehicle model, have a short horizon and need to be solved in a relatively short time.

2.5.1 Dynamic programming

Dynamic programming is a method to solve an optimal control problem by breaking it down into a collection of simpler optimal control subproblems. By exploiting the overlap of these subproblems, it significantly reduces the number of required arithmetic calculations. The theory of dynamic programming has been formulated in the fifties by Bellman (1957), although it has its origin in the work of Hamilton and Jacobi on calculus of variations. For more recent references see Bertsekas (1995) and Liberzon (2012). In this section we present the dynamic programming concept applied to a discrete system.

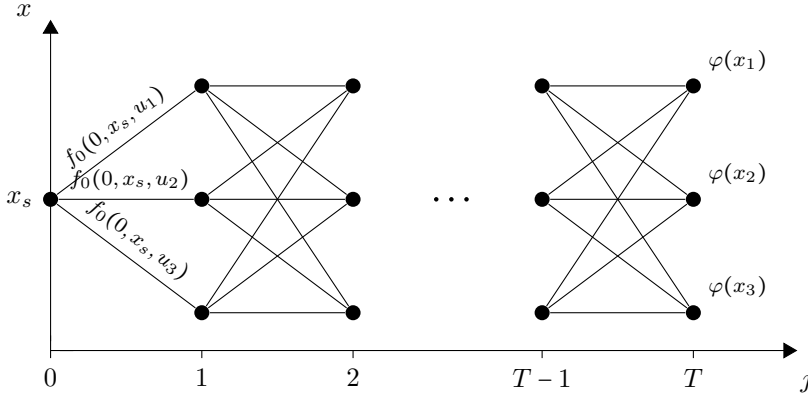


Figure 2.4: Discrete optimal control problem.

Consider the optimal control problem of the form

$$J^*(x_s) = \text{minimize } \sum_{j=0}^{T-1} f_0(j, x(j), u(j)) + \varphi(x(T)), \quad (2.2a)$$

$$\text{subj. to } x(j+1) = f(j, x(j), u(j)), \quad (2.2b)$$

$$x(j) \in \mathcal{X} = \{x_1, \dots, x_N\}, \quad (2.2c)$$

$$u(j) \in \mathcal{U} = \{u_1, \dots, u_M\}, \quad (2.2d)$$

$$x(0) = x_s, \quad (2.2e)$$

where x is the model state that belongs to a finite set \mathcal{X} of N elements, see constraint (2.2c), and u is the control input that belongs to a finite set \mathcal{U} of M elements, see constraint (2.2d). The independent variable j represents the enumeration of the stages of the optimal control problem and, in general, may not have anything to do with time (e.g., in the platoon controller of Chapter 4 it represents a spatial discretization). The variable x_s represents the initial state. Finally, the relation (2.2b) represents the system model, while the cost function (2.2a) weighs functions of the state and the control input. The problem is visualized in Figure 2.4.

The most naive approach to address this problem consists in enumerating all the possible trajectories starting from x_s at stage 0 going forward up to stage T , associating to each trajectory the cost and comparing the costs in order to select the optimal one. The complexity of this approach can be easily computed and results in $\mathcal{O}(M^T T)$ arithmetic operations. In the case of a large number of stages T , this method can result in an extremely long computation time.

The dynamic programming approach relies on the so-called “principle of optimality”, which can be stated as follows:

Principle of optimality: Let $\{x_j^*\}_{j=0}^T$ and $\{u_j^*\}_{j=0}^{T-1}$ be the optimal state and control trajectories for the problem (2.2), respectively. Then, each control subtrajectory $\{u_j^*\}_{j=k}^{T-1}$ is optimal for the subproblems obtained by the optimization on the form (2.2) but with initial condition $(k, x^*(k))$ (i.e., starting at time k and state $x^*(k)$).

Let $\bar{J}^*(k, x(k))$ be the cost associated to the optimal control trajectory $\{u_j^*\}_{j=k}^{T-1}$ with initial condition $(k, x(k))$ and refer to it as the optimal cost-to-go. Note that the optimal cost-to-go $\bar{J}^*(0, x_s)$ corresponds to the optimal cost $J^*(x_s)$ for the complete problem (2.2).

According to the principle of optimality, given a stage k , one of the N optimal control subtrajectories $\{u_j^*\}_{j=k}^{T-1}$ with initial condition $(k, x(k))$ will belong to the optimal control trajectory $\{u_j^*\}_{j=0}^{T-1}$. Following this observation, the principle of optimality can be exploited by starting from the final stage T and proceeding backwards. At the stage T , the optimal cost-to-go for all the possible initial conditions $(T, x(T))$ is simply defined as the final cost function, i.e., $\bar{J}^*(T, x(T)) = \varphi(x(T))$. At the generic stage k , the optimal cost-to-go with initial condition $(k, x(k))$ can be defined as the minimum of the costs given by the summation of the cost to reach a certain state at stage $k+1$ from $x(k)$ and the optimal cost-to-go with the new state as initial condition, i.e.,

$$\bar{J}^*(k, x(k)) = \min_{u(k) \in \mathcal{U}} \{f_0(k, x(k), u(k)) + \bar{J}^*(k+1, f(k, x(k), u(k)))\}. \quad (2.3)$$

This equation provides a recursive relation between the optimal cost-to-go of contiguous stages and is known as the Bellman equation. If we apply it to all possible initial conditions $(k, x(k))$ proceeding backwards until stage 0 and we save the corresponding optimal control subtrajectory $\{u_j^*\}_{j=k}^{T-1}$, we will be eventually able to compute the optimal cost $J^*(x_s) = \bar{J}^*(0, x_s)$ and the corresponding optimal control trajectory $\{u_j^*\}_{j=0}^{T-1}$.

As for each stage and each possible state we have to compare M summations, the complexity of the dynamic programming approach can be easily computed and results in $\mathcal{O}(NMT)$ arithmetic operations. Comparing this with the complexity of the naive approach, we can conclude that dynamic programming is significantly more efficient in the case of large T . Furthermore, dynamic programming intrinsically provides a feedback law, as it computes the optimal control trajectory for every stage k and state $x(k)$. Note, however, that, although the complexity is linear in the number of possible states N , N can be an extremely large number, as it grows exponentially with the dimension of the state. This is known as the *curse of dimensionality*.

2.5.2 Model predictive control

Model predictive control (MPC) is a control framework that relies on the iterative solution of optimal control problems based on the predicted state to compute the instantaneous control input. The prediction of the state is based on the system model and this explains the name *model predictive control*. MPC has its origins in the seventies in the process industry, where it was used to control chemical plants and oil refineries (Richalet et al., 1978). The slow dynamics of such systems were favorable to the MPC requirement of solving optimization problems in real-time and the limited computational power of the contemporary hardware. With the increase of the computational power of the last decades, MPC has become attractive for other industries as well, for instance, the automotive industry (Hrovat et al., 2012; Del Re et al., 2010). In this section we introduce the MPC concept. For a detailed treatment of the topic, see Borrelli et al. (2017).

At each time instant k , the following optimal control problem is solved:

$$\text{minimize} \quad \sum_{j=k}^{k+N_{\text{MPC}}-1} f_0(j, x(j|k), u(j|k)) + \varphi(x(k+N_{\text{MPC}}|k)), \quad (2.4a)$$

$$\text{subj. to} \quad x(j+1|k) = f(j, x(j|k), u(j|k)), \quad (2.4b)$$

$$x(j|k) \in \mathcal{X}, \quad (2.4c)$$

$$u(j|k) \in \mathcal{U}, \quad (2.4d)$$

$$x(k|k) = x(k), \quad (2.4e)$$

where $x(j|k)$ and $u(j|k)$ denote the predicted state and control input at time j computed at time k , respectively, while $x(k)$ denotes current state. The variable N_{MPC} denotes the prediction horizon. The relation (2.4b) represents the prediction model, while the constraints (2.4c) and (2.4d) provide bounds on the predicted state and control input, respectively. The cost function (2.4a) weighs a function of the predicted state and control input from the current time k to the end time $k+N_{\text{MPC}}$. The solution of the optimal control problem (2.4) returns the optimal state and control input trajectory $\{x^*(\cdot|k)\}_{j=k}^{N_{\text{MPC}}}$ and $\{u^*(\cdot|k)\}_{j=k}^{N_{\text{MPC}}-1}$, respectively, as displayed in Figure 2.5. The MPC algorithm only applies the first element of the optimal control input trajectory $u^*(k|k)$ to the system. At the next time instant $k+1$, a new optimal control problem of the form (2.4) is cast and solved, and this is repeated for each time instant.

The re-resolution at each step of the optimal control problem (2.4), provides feedback in the MPC framework, making it robust to disturbances and model uncertainties. Another significant advantage of the MPC framework is the possibility to introduce constraints on the future state and control input.

Due to the non-linearities in the formulation (2.4), the presented framework is typically referred as nonlinear MPC. In the case of a linear prediction model,

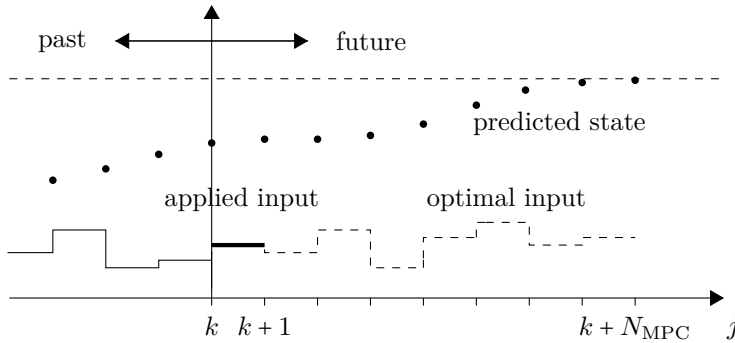


Figure 2.5: Illustration of the MPC concept. At each time instant k , an optimal control problem based on the predicted state is solved. The solving returns the optimal predicted state and the optimal control input trajectories. Of the optimal control input trajectory only the first element is applied to the system. At the time instant $k + 1$, a new optimal control problem is formulated and solved.

polytopic constraints on state and control input, and quadratic cost function, we will talk instead of linear MPC. In this case the optimal control problem (2.4) can be recast as a quadratic program for which efficient numerical algorithms are available. A distributed version of MPC has been successfully used to control vehicle platoons, see Dunbar and Murray (2006) and Dunbar and Caveney (2012). In these works, the platooning vehicles share their optimal state trajectory with the following vehicle. Each following vehicle exploits the received information by including it in its MPC formulation. The authors also provide conditions on the controller parameters that guarantee string stability of the platoon.

2.6 Summary

Although only the recent advances in technology provided the basis for the commercial implementation of platooning control, the topic has been researched extensively. The first works on vehicle platooning date back to the sixties and mainly focus on studying the string stability of the platoon. Only in the nineties, with the beginning of the PATH project, researchers started to address more practical aspects of platooning. Among these aspects, the fuel-efficient control of heavy-duty vehicle platoons gained a certain attention. Thanks to the shape of these vehicles, the short inter-vehicular distance results in a significant reduction of the overall aerodynamic drag and the fuel consumption. Although the large impact of slopes on the fuel consumption of heavy-duty vehicles is well known (as proved by the large number of works on look-ahead control for single vehicles), few works address the inclusion of

topography information in the design of fuel-efficient heavy-duty vehicle platooning.

In this chapter we first presented the technologies that enable vehicle platooning. Second, we provided an overview of the works that address vehicle platooning and look-ahead vehicle control. Third, the problem for the overall fuel-efficient transportation system was discussed. Lastly, we introduced the concepts of dynamic programming and MPC that will be at the base of the controllers proposed in the next chapters.

Hheavy-duty vehicles are complex systems with a large number of interacting dynamics. For example, due to the large weight, their braking and powertrain systems have to generate and transfer extremely high torques. This requires the coordination of multiple braking actuators and the damping of oscillations arising in the powertrain. The control system architecture of heavy-duty vehicles is therefore highly distributed and hierarchical.

In this chapter we present a vehicle model suitable for the design of controllers for fuel-efficient and safe platooning. Particular attention is given in modeling those components that play an essential role in the vehicle fuel consumption, as the gravitational, rolling, aerodynamic, braking and traction forces. The vehicle model also includes a high-level powertrain model that describes the engine, the clutch, the gearbox and the transmission. This model details how the fuel is converted into traction force and provides a way to describe gear shifts and freewheeling. Finally, we provide an overview of a heavy duty vehicle system architecture. This explanation will be useful to understand the overall functioning of the truck and to identify the units and other control systems which the proposed platoon controllers will interact with.

The chapter is organized as follows. In Section 3.1 we introduce the model of the longitudinal dynamics of a single vehicle and the platoon. Section 3.2 introduces the powertrain model, including the engine, gearbox and transmission. In Section 3.3, we describe the vehicle system architecture in which the platoon controller is expected to operate. Lastly, Section 3.4 provides a summary of the chapter.

3.1 Longitudinal vehicle dynamics

In this section we present the models of the longitudinal dynamics of a vehicle and the platoon that will be used in the formulation of the platooning controllers presented in the next chapter. An overview of the longitudinal forces acting on a heavy-duty

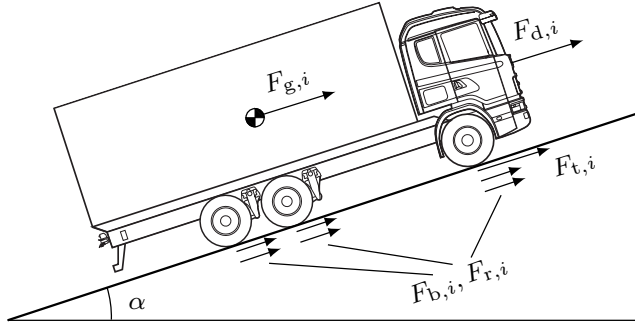


Figure 3.1: Illustration of the forces acting on the heavy-duty vehicle along the longitudinal direction. The sign convention for all forces is according to the direction of travel.

vehicle is shown in Figure 3.1. Using Newton's second law, see e.g. (Guzzella and Sciarretta, 2007), the dynamics of vehicle i can be expressed as

$$\begin{aligned} m_i \dot{v}_i &= F_{t,i} + F_{b,i} + F_{g,i}(\alpha(s_i)) + F_{r,i} + F_{d,i}(v_i, d_i), \\ \dot{s}_i &= v_i, \end{aligned} \quad (3.1)$$

where $v_i \geq 0$ and s_i form the state of the vehicle and denote its speed and longitudinal position of the vehicle front, respectively. We collect them in the state vector $x_i = [v_i \ s_i]^T$. $F_{t,i}$ and $F_{b,i}$ denote the forces generated by the actuators, i.e., the traction and braking forces, whereas $F_{d,i}$ and $F_{r,i}$ denote the resistive forces acting on the vehicle, i.e., the drag and rolling resistances; $F_{g,i}$ represents the gravitational force defined as the component of the gravity vector in the vehicle longitudinal direction. The parameter m_i represents the mass of vehicle i , while the variable $\alpha(s_i)$ is the road grade and is defined as a function of the vehicle's longitudinal position. Finally d_i denotes the distance of vehicle i to the preceding one.

The model of a platoon of N_v vehicles can be obtained by combining the vehicle model (3.1) for $i = 1, \dots, N_v$ and the distance definition

$$d_i = \begin{cases} \infty, & \text{if } i = 1, \\ s_{i-1} - s_i - l_{i-1}, & \text{if } i \geq 2, \end{cases} \quad (3.2)$$

where l_i denotes the length of vehicle i .

In the remainder of this section, we describe each one of the forces acting on the vehicle.

Traction force

The traction force $F_{t,i}$ is the longitudinal force generated by the powertrain. The powertrain is constituted by different components, i.e., the engine, the clutch, the gearbox and the final drive, that transform the fuel into traction energy. A high-level model of the powertrain that relates the traction force to the engine fuel flow is presented in Section 3.2.

Braking force

The braking system of a heavy-duty vehicle is composed of several actuators. Following the same reasoning as for the powertrain, here we assume that the braking force is a control input and the corresponding acceleration is tracked by a low-level controller. The braking actuators acting on each axle can generate a maximum torque $T_{a,\max}$ (Alam, 2014). This torque is transferred to the road surface through the wheels and the tires. The minimum (according to the sign convention) potential braking force is therefore equal to $-T_{a,\max}n_a r$, where n_a and r denote the number of axles and the radius of the wheels, respectively. Due to the limited friction between the tires and the road surface, there is however a threshold on the minimum braking force that can be transferred to the ground. Assuming an equal distribution of the vehicle mass on the axles, this threshold can be approximated as $-\mu m_i g_a$, where μ and g_a denote the (positive) road friction coefficient and the gravitational acceleration, respectively (Pacejka, 2012). Therefore, depending on the mass of the vehicle, the minimum braking force can be limited by either the maximum torque that the braking actuators can generate or the minimum force that the wheels are able to transfer on the ground. This constraint can be modeled as follows:

$$F_{b,\min,i} \leq F_{b,i} \leq 0, \quad (3.3)$$

where $F_{b,\min,i}$ is defined as

$$F_{b,\min,i} = \max\{-T_{a,\max}n_a r, -\mu m_i g_a\}.$$

Depending on the vehicle parameters, the braking capability of the vehicles in the platoon can vary significantly. Therefore, in order to guarantee safety, a framework that is able to handle heterogeneous platoons is needed.

Gravitational force

Here, we denote the gravitational force with the component of the gravity vector in the vehicle longitudinal direction. Depending on the road grade, such force can be

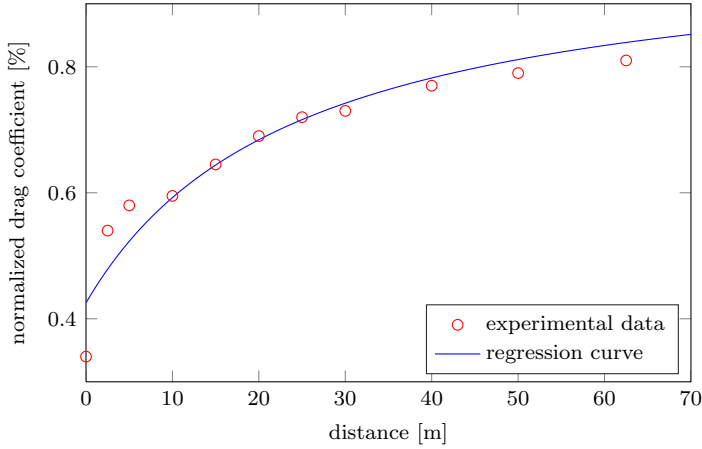


Figure 3.2: Experimental data from Hucho (1987) and regression curve of the normalized drag coefficient experienced by a heavy-duty vehicle as function of the distance to the preceding vehicle.

either a resistive or assistive force and its expression can be formulated as

$$F_{g,i}(\alpha(s_i)) = -m_i g_a \sin \alpha(s_i). \quad (3.4)$$

Due the large mass of heavy-duty vehicles, even small road grade generates a significant gravitational force. Therefore, it is common that these vehicles are not able to keep constant speed during an uphill or downhill road stretch without exceeding the engine power limits and without braking.

Rolling resistance

The rolling resistance is generated by the interaction between tires and the road surface. It is a resistive force and is mainly due to the asymmetric deformation of the tires during compression and expansion (Pacejka, 2012). It is approximately proportional to the vertical load on the tires and is typically modeled as

$$F_{r,i} = -c_{r,i} m_i g_a, \quad (3.5)$$

where $c_{r,i}$ denotes the rolling resistance coefficient of vehicle i . This parameter can be influenced by different factors, as the pressure, temperature and width of the tires.

Aerodynamic drag

The aerodynamic drag is a resistive force due to the interaction between the vehicle and the surrounding air. It grows quadratically in magnitude with the vehicle speed and gets reduced when driving at a short distance to a preceding vehicle. This phenomenon is due to a slipstream effect between the vehicles that results in a reduced pressure on the second vehicle and reduced air vortices behind the first one. Thanks to the slipstream effect the aerodynamic drag experienced by both vehicles decreases as the inter-vehicular distance shrinks, although such reduction is more significant for follower vehicles. The reduction in the aerodynamic drag is the reason why race bikers or migratory birds try to keep a compact formation while moving and provides a strong motivation for heavy-duty vehicle platooning. The aerodynamic drag can be modeled as

$$F_{d,i}(v_i, d_i) = -\frac{1}{2}\rho A_v C_d(d_i) v_i^2, \quad (3.6)$$

where ρ is the air density, A_v is the cross-sectional area of the vehicle and C_d is the aerodynamic drag coefficient (here assumed as vehicle-independent). In order to capture the reduction of the aerodynamic drag with the inter-vehicular distance, the drag coefficient C_d is defined as a function of the distance to the preceding vehicle d_i . The effect of the short inter-vehicular distance on the preceding vehicles has been neglected since it is significantly smaller than that one on the follower vehicles (see the experimental data in Figure 1.5). The literature reports measurements on air drag coefficient and fuel consumption based on both real experiments (Hucho, 1987; Bonnet and Fritz, 2000; Lammert et al., 2014) and fluid dynamics simulation (Norrby, 2014). All these works show a reduction of the air drag coefficient for short inter-vehicular distances. However, how the reduction relates to the inter-vehicular distance varies. The variability has been attributed to weather conditions (e.g, temperature, humidity or wind) and the shape of the vehicles. In this work we refer to the experimental data presented in Hucho (1987). The dependence of the drag coefficient C_d on the distance d_i is therefore modeled as

$$C_d(d_i) = C_{d,0} \left(1 - \frac{C_{d,1}}{C_{d,2} + d_i} \right), \quad (3.7)$$

where the parameters $C_{d,1}$ and $C_{d,2}$ are obtained by regressing the experimental data presented in Hucho (1987). The experimental data and the regression curve are displayed in Figure 3.2.

3.2 Powertrain model

The powertrain is responsible for generating the traction force $F_{t,i}$. A schematic of the powertrain is displayed in Figure 3.3. The main components of the powertrain are

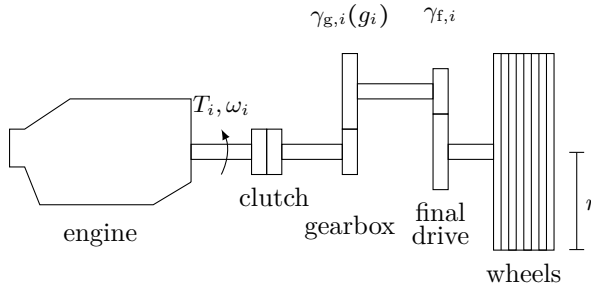


Figure 3.3: Illustration of the powertrain components.

the engine, the clutch, the gearbox and the final drive. The fuel is first transformed in rotational torque by the engine. Then, the clutch and gearbox work together to amplify the torque and diminish the rotational speed of a factor dependent on the gear. Finally, the final drive and the wheels convert the torque into traction force.

In order to obtain a manageable model, the following assumptions have been introduced:

- (i) The engine inertia is negligible with respect to the mass of the vehicle.
- (ii) the engine fuel consumption can be defined as a static map of the engine speed and torque.
- (iii) Transmission shafts are rigid.
- (iv) No power loss takes place in the gearbox and the transmission.

These assumptions allow to limit the number of states of the powertrain model making possible to use it for our control purpose. In the remainder of this section, the models of the fuel, the gearbox-clutch and the transmissions are presented.

Fuel model

The fuel-efficiency of an engine is typically represented by the brake specific fuel consumption (BSFC) that denotes the ratio between the fuel flow and the produced power. The BSFC map of an engine is obtained by gridding the torque/speed space and measuring the engine fuel consumption and the generated power for each grid point. An example of a BSFC map is displayed in Figure 3.4. This map represents a 400 hp engine of a heavy duty vehicle Sandberg (2001). For the correct operational of the engine, its speed is bounded between a minimum and a maximum value, i.e.,

$$\omega_{\min,i} \leq \omega_i \leq \omega_{\max,i}, \quad (3.8)$$

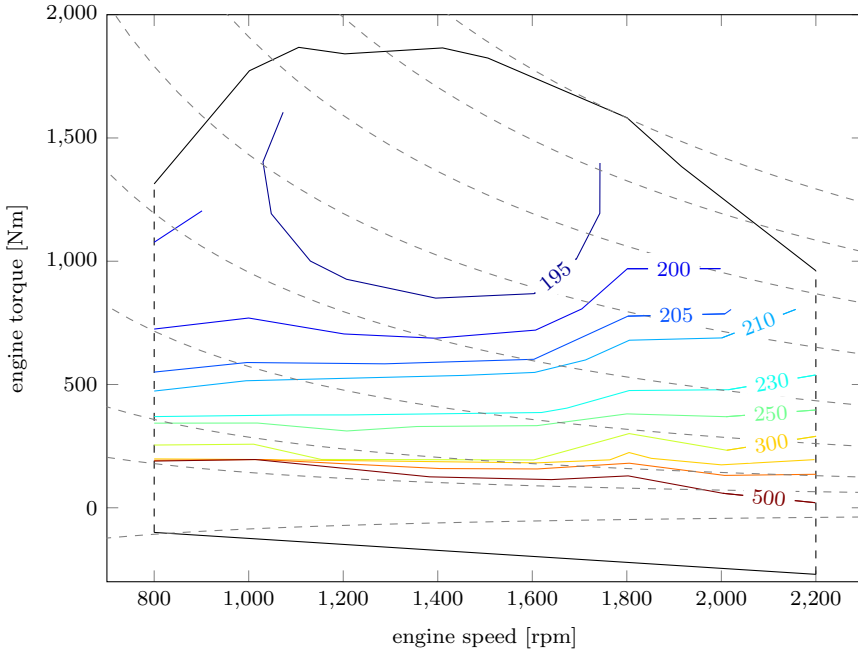


Figure 3.4: BSFC map for a 400 hp engine regenerated from Sandberg (2001) and expressed in g/kWh. The black lines denote the maximum and minimum engine torque, while the contour color lines denote operation points with same BSFC.

represented by the black dashed lines in Figure 3.4. The torque is also bounded by speed-dependent minimum and maximum functions, i.e.,

$$T_{\min,i}(\omega_i) \leq T_i(\omega_i) \leq T_{\max,i}(\omega_i), \quad (3.9)$$

indicated by solid black lines. The minimum engine torque $T_{\min,i}$ is the torque generated by the engine $T_{e,i}$ when no fuel is injected. This is typically strictly negative and can be roughly approximated by a affine function of the engine speed ω_i as the consequence of rotational friction. The maximum engine torque $T_{\max,i}$, instead, is the result of the physical limits of the engine and typically shows three distinct trends. At low engine speeds, it exhibits a approximately linear dependency on the engine speed due to the limit on the injected fuel per stroke. At middle range engine speed, it is constant due to the maximum torque that the engine components can handle. At high speed, it exhibits a hyperbolic trend due to the maximum heat that the engine can dissipate. Finally, the contour colored lines in Figure 3.4 represent operation points with same BSFC, while the dotted lines represent the collection of operation points with equal generated power.

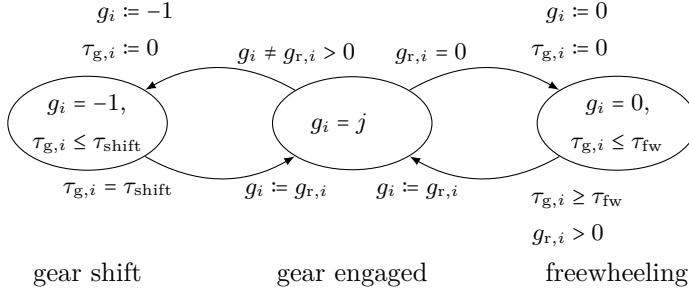


Figure 3.5: Timed automaton describing the gearbox-clutch dynamics.

In this work, we model the fuel consumption by expressing the fuel flow ψ_i defined as amount of fuel per seconds as function of the engine speed ω_i and the engine torque T_i , i.e.,

$$\psi_i = \varphi_i(\omega_i, T_i). \quad (3.10)$$

Such function can be easily derived from the engine BFSC map of vehicle i .

Gearbox-clutch model

We now present the gearbox and clutch dynamics summarized by the timed automaton displayed in Figure 3.5. This model aims to correctly capture the timing of gear shifts and freewheeling, i.e., coasting in neutral gear.

The state of the automaton is $g_i \in \{-1, 0\} \cup \mathcal{G}_{a,i}$, where $\mathcal{G}_{a,i} = \{j \in \mathbb{N} | j \in [g_{\min,i}, g_{\max,i}]\}$ represents the set of the admissible gears. If $g_i \in \mathcal{G}_{a,i}$, the clutch disks are closed and gear g_i is engaged. If $g_i = 0$, the clutch disks are open and the vehicle is freewheeling. Finally, if $g_i = -1$, the clutch disks are open and a gear shift is taking place. The control input is $g_{r,i} \in \{0\} \cup \mathcal{G}_{a,i}$. If $g_{r,i} \in \mathcal{G}_{a,i}$, gear $g_{r,i}$ is requested, while, if $g_{r,i} = 0$, freewheeling is requested. The time requirements on the gear shifts and the freewheeling are ensured by edge guards and location invariants defined as function of the automaton clock $\tau_{g,i}$.

The gearbox starts in the engaged gear condition modeled by the central macro-state in the automaton of Figure 3.5 that collects all the state $g_i \in \mathcal{G}_{a,i}$. From this macro-state, two transitions are possible:

- if the requested gear $g_{r,i}$ switches to 0, the gearbox jumps to the freewheeling state, i.e., $g_i = 0$. In order to avoid a premature deterioration of powertrain components and driver discomfort, the fast switching between engaged gear and freewheeling is limited by requiring that the freewheeling is maintained for a time longer than τ_{fw} . This is achieved by resetting the automaton clock $\tau_{g,i}$, when the gearbox jumps to $g_i = 0$, and by defining the location invariant $\tau_{g,i} \leq \tau_{fw}$ for the freewheeling state and the guard $\tau_{g,i} \geq \tau_{fw}$ on the edge leaving

the freewheeling state. If we are not interested in exploiting freewheeling, the requested gear set can be redefined as $g_{r,i} \in \mathcal{G}_{a,i}$.

- if the requested gear $g_{r,i}$ switches to a value in the set $\mathcal{G}_{a,i}$ different from g_i , the gearbox jumps to the gear-shift state, $g_i = -1$. The gearbox stays in the gear-shift state for a time of τ_{shift} , before jumping to the engaged gear macro-state with $g_i = g_{r,i}$.

It is important to understand the distinction between the input $g_{r,i}$ and the gearbox-clutch state g_i . While the required gear $g_{r,i}$ can vary between the allowed values at any time, the state g_i is constrained by the automaton dynamics to switch value in well-defined patterns.

Transmission model

To complete the powertrain model, we now present the static relation between the engine variables and the chassis variables as function of the gearbox-clutch state g_i .

The torque T_i generated by the engine acts on the engine side of the clutch. If the clutch disks are open (i.e, $g_i \in \{-1, 0\}$), no torque is transmitted by the gearbox-clutch group. If a gear is engaged (i.e, $g_i \in \mathcal{G}_{a,i}$), the torque is amplified by a factor $\gamma_{g,i}$ depending on the specific engaged gear g_i . The torque on the gearbox shaft is transmitted to the wheel shaft by the final drive that amplifies it by a constant factor $\gamma_{f,i}$. Finally, the torque on the wheel shaft is transferred to the road by the wheels. The longitudinal force $F_{t,i}$ generated by the road/wheel contact can be therefore summarized by

$$F_{t,i}(g_i, T_i) = \begin{cases} 0, & \text{if } g_i \in \{-1, 0\}, \\ \frac{\gamma_{g,i}(g_i)\gamma_{f,i}}{r} T_i, & \text{if } g_i \in \mathcal{G}_{a,i}, \end{cases} \quad (3.11)$$

where r is the wheel radius.

In a similar way, under the assumption of no slip between wheels and road surface, the engine speed can be defined as function of g_i and the vehicle speed as

$$\omega_i(g_i, v_i) = \begin{cases} \omega_{\min,i}, & \text{if } g_i \in \{-1, 0\}, \\ \frac{\gamma_{g,i}(g_i)\gamma_{f,i}}{r} v_i, & \text{if } g_i \in \mathcal{G}_{a,i}. \end{cases} \quad (3.12)$$

Note that, when the clutch is open, the engine is assumed to rotate at the minimum allowed engine speed $\omega_{\min,i}$.

3.3 Vehicle system architecture

The correct functioning of a heavy-duty vehicle is guaranteed by a large number of system units that communicate with each other through the controller area network

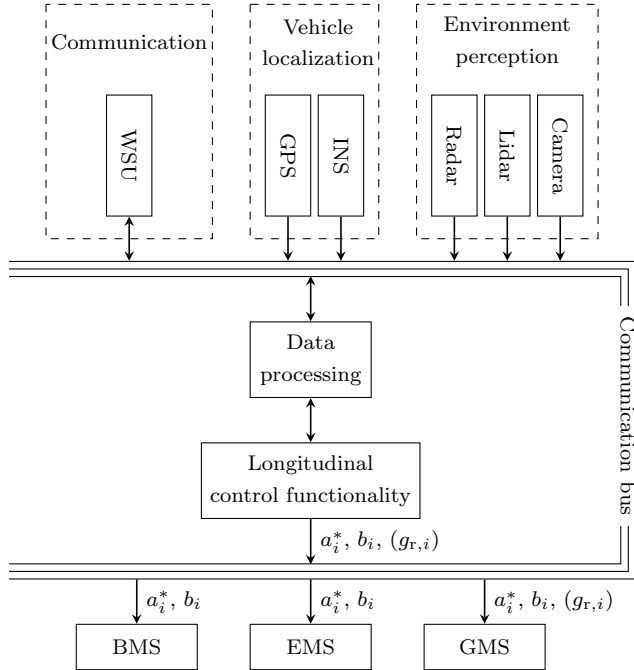


Figure 3.6: Vehicle system architecture for vehicle platooning.

(CAN) bus or Ethernet. In this section, we present an abstraction of the vehicle system architecture that includes the units that play a role in the control of the platoon longitudinal dynamics.

The vehicle system architecture that enables vehicle platooning is displayed in Figure 3.6. The units at the top of figure represent the interfaces of the vehicle to the outside world. In detail, the global positioning system (GPS) returns the absolute position of the vehicle, while the inertial navigation system (INS) provides information about the linear and angular vehicle accelerations. By fusing the data from the two systems, the controller has access to an estimate of the own vehicle state with a precision of centimeters (Ryu and Gerdes, 2004). The radars, lidars and cameras provide data about the surrounding environment. This information can be processed to create a real-time dynamic map of the environment that includes accurate measures of the distance to the preceding vehicle and its relative speed. The wireless sensor unit (WSU) shares real-time information with the other platooning vehicles and allows the communication with external vehicles and off-board systems, such as a back-end office or cloud services. While the GPS and radar are consolidated technologies in vehicles, the lidar, cameras and WSU are still uncommon and the focus of ongoing research.

The blocks at the bottom of Figure 3.6 represent the units controlling the vehicle longitudinal actuators. They take as input the reference acceleration a_i^* and a boolean variable b_i that indicates whether a_i^* is a traction or braking acceleration. The brake management system (BMS) tracks the reference braking acceleration by coordinating multiple actuators ranging from the strong brake disk to the weaker exhaust and retarder brakes. Furthermore, in case of harsh braking, the BMS is responsible for correctly distributing the braking force between the brake discs and guaranteeing that the wheels do not lock. The engine management system (EMS) generates the required traction acceleration by controlling the engine fuel flow. Because of the large torques created in the powertrain, it also ensures that no excessive oscillations are generated. Finally, the gear management system (GMS) controls the gearbox and the clutch by engaging the requested gear. If no gear request interface exists, it can also operate autonomously by monitoring the engine speed and the requested torque and selecting the gears according to predefined thresholds.

The information from the sensor blocks is elaborated in the *data processing* block and transferred to the *longitudinal control functionality* block. Here, multiple control functionalities can be implemented depending on the availability of preview information, the presence of other vehicles, and the existence of a cooperation framework, see Table 3.1:

- Cruise control (CC): this is the most common longitudinal control functionality available in commercial vehicles. It relies on feedback control that regulates the engine fuel flow in order to track a reference speed. If the road is nearly flat the vehicle speed remains constant.
- Look-ahead control (LAC): when the road exhibits relevant altitude variations and topography information are available to the vehicle, this information can be exploited by look-ahead control to adapt the vehicle speed according to present and future road grades in order to improve fuel-efficiency.
- Adaptive cruise control (ACC): if the vehicle under control comes in proximity of another vehicle, information collected by the on-board sensors (i.e., distance and relative speed) are used to track a desired gap policy.
- Look-ahead adaptive control (LAAC): if topography information and/or an estimation of the preceding vehicle future trajectory are available, they can be used to adapt the inter-vehicular gap. The future trajectory of the preceding vehicle can be estimated according to the road topography or can be communicated by the preceding vehicle itself.
- Cooperative adaptive cruise control (CACC): if a cooperative framework is available, multiple vehicles, driving at a short inter-vehicular distance, can cooperate to ensure a smooth, fuel-efficient and safe behavior of the platoon.

Table 3.1: Longitudinal control functionalities.

	driving alone	non-cooperative platooning	cooperative platooning
w/o preview information	CC	ACC	CACC
w/ preview information	LAC	LAAC	CLAC

- Cooperative look-ahead control (CLAC): The availability of preview information about the road ahead such as topography information can be incorporated in the platoon controller in order to reach a higher degree of fuel-efficiency.

In this thesis, we study the platooning control problem when preview information about the road topography is available. In details, in Chapters 5 and 6, we address the CLAC problem, while, in Chapters 7 and 8, we address the LAAC problem.

3.4 Summary

In this chapter we presented the model of the longitudinal vehicle dynamics that will be used, with possible simplification, in the controller formulations presented in the next chapters. As one of the main focus of this thesis is vehicle fuel consumption, a particular attention has been given in correctly modeling the powertrain. This model describes the relation between the consumed fuel and the traction force as a function of the gearbox-clutch dynamics. Lastly, we have presented an abstraction of the vehicle system architecture that describes the units and the low level vehicle controllers that play a significant role in the overall platoon control.

Control architectures for platooning

In this chapter we develop two control architectures suitable for the fuel-efficient and safe control of heavy-duty vehicle platoons. Key aspects include the use of topography information and the ability to take external traffic into account. In order to acquire a good understanding of the effect of road altitude variation on the platoon dynamics, the chapter starts with an analysis of a platooning experiment conducted on open road. The insights collected from the analysis are used to motivate the following two control architectures for vehicle platooning:

- A control architecture for the cooperative control of platoons. In this setting, platooning vehicles cooperate in order to minimize the overall fuel consumption of the platoon and guarantee safety.
- A control architecture for the non-cooperative control of platoons. Here, each vehicle greedily minimizes its own fuel consumption given the estimation of the preceding vehicle trajectory.

The chapter is structured as follows. In Section 4.1, we present the insights gained by the analysis of the platooning experiment. In Sections 4.2 and 4.3, we propose the control architectures for cooperative and non-cooperative platooning, respectively. Finally, Section 4.4 summarizes the chapter.

4.1 Motivational experiment

In this section we present and analyze the data collected from a platooning experiment conducted on open roads. For the full description of the experiment results, refer to Alam et al. (2015). The experiment provides fundamental insights that will be incorporated in the design of the control architectures detailed in the remainder of the chapter.



Figure 4.1: The three trucks used in the experiment. Photo provided by courtesy of Scania AB.

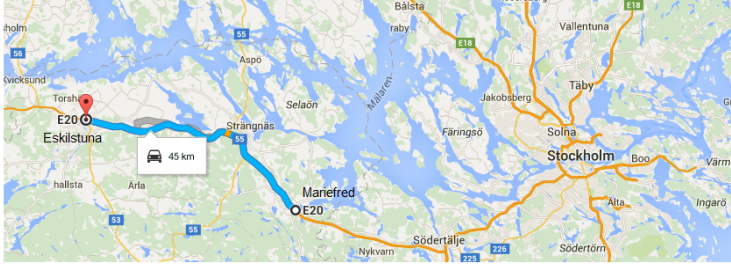
Table 4.1: Vehicle parameters.

m_1	first vehicle mass	t	37.5
m_2	second vehicle mass	t	38.4
m_3	third vehicle mass	t	39.5
l_i	vehicle length	m	18
$c_{r,i}$	rolling coefficient	-	0.006
A_v	cross-sectional vehicle area	m ²	10
$C_{d,0}$	nominal drag coefficient	-	0.6
$C_{d,1}$	first drag reduction coefficient	m ⁻¹	12.8
$C_{d,2}$	second drag reduction coefficient	m	19.7

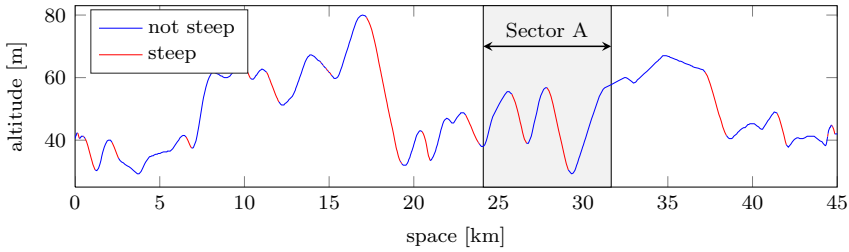
4.1.1 Experiment setup

In this experiment, a platoon of three heavy-duty vehicles is driven over a 45 km highway stretch between the Swedish cities of Mariefred and Eskilstuna. The vehicles, depicted in Figure 4.1, have the same 480 hp engine type and a mass of approximately 38 tonnes. The measured and estimated vehicles parameters are reported in Table 4.1. The highway stretch map and topography information are shown in Figure 4.2. The red color in Figure 4.2b is used to highlight (i) the uphill sections where the slope is too steep for a nominal vehicle of 40 tonnes with a 480 hp engine to maintain a constant speed of 21.5 m/s and (ii) the downhill sections where the slope is too steep for the same vehicle to maintain constant speed without braking. The steep downhill sections represent 22% of the total length, while, because of the large power to weight ratio of the vehicle, no steep uphill stretches are present.

The platoon control architecture is decentralized and does not make use of topography information. Each vehicle controller has two modes, i.e., a traction mode where the computed reference acceleration is tracked by the engine management



(a) Road map (Map data ©2018 Google).



(b) Road topography.

Figure 4.2: The 45 km highway stretch between the Swedish cities of Mariefred and Eskilstuna. The red color in (b) highlights the uphill and downhill sections for which the slope is too steep for a vehicle of 40 tonnes with a 480 hp engine to maintain a constant speed of 21.5 m/s without exceeding the maximum engine power and without braking.

system (EMS), and a braking mode where the reference acceleration is tracked by the braking management system (BMS). The leading vehicle controller tracks a reference speed of 21.5 m/s using the commercial cruise control and it switches to braking mode only when the speed limit of 23.6 m/s is reached. The following vehicle controllers track a reference headway gap of 1 s (i.e., the reference distance from the preceding vehicle is computed as the product of the vehicle speed and the 1 s headway gap) and it switches to braking mode only when the headway gap is smaller than a certain threshold.

4.1.2 Experiment results

The platoon exhibited different behavior depending on the steepness of the road. Along road stretches with small altitude variation, the platoon control behaved smoothly and reduction of the fuel consumption was recorded. The second and third vehicles were able to save on average 4.1% and 6.5% of fuel, respectively. However, in the sections where the road exhibited a larger altitude variation, the performance of the platoon degraded and the controllers of the following vehicles repeatedly

switched to the braking mode.

In order to understand how the road grade variation affects the platoon performance, in the remainder of the section we focus on the behavior of the platoon driving along the two steep hills highlighted in Figure 4.2b as Sector A. For the sake of simplicity, only the behavior of the first and second vehicles is reported in Figure 4.3, since the third vehicle shows patterns similar to the second one. In this sector, the fuel consumption of the second vehicle actually increases of about 4% compared to the driving alone scenario.

In order to identify the causes of the control performance deterioration, the measured speed and input trajectories are replicated in simulation according to the vehicle model (3.1) with the parameters reported in Table 4.1. The simulated braking, gravitational, rolling and aerodynamic forces have been integrated over time according to

$$E_{\square,i} = \int_0^{t_{\text{sec}}} F_{\square,i}(t)v_i(t) dt \quad (4.1)$$

to obtain the energy consumption associated with each force. Here, t_{sec} represents the time that platoon takes to drive along the sector, while the placeholder \square represents the subindexes b, g, r and d. The total energy consumption is defined as the summation of the single components, i.e.,

$$E_i = \sum_{\square \in \{b, g, r, d\}} E_{\square,i}. \quad (4.2)$$

In Figure 4.4, we show the energy consumed by the two vehicles divided into the different components and normalized with respect to the first vehicle energy E_1 . Due to the difference of approximately 1 tonne between the vehicle masses, the gravitational and rolling forces are slightly higher for the second vehicle. On the other hand, thanks to the slipstream creation, the energy dissipated by the aerodynamic force of the second vehicle is 31% smaller compared to the one of the first vehicle. The largest difference, however, is due to the braking action. The second vehicle dissipates by braking approximately 130% more energy with respect to the first vehicle. This leads to an overall energy consumption increase of about 6% of the second vehicle with respect to the first one. This result is in line with the measured 4% increase in the second vehicle fuel consumption with respect to the scenario where the same vehicle was driving alone (taking into account the mass difference of the vehicles).

In order to understand the cause of the increased braking action, in the remainder of the section, we focus the attention back to the experimental results displayed in Figure 4.3. To facilitate the analysis we identify three segments denoted as Segments 1, 2 and 3 in Figure 4.3, where the braking action takes place:

- Segment 1. As soon as the first downhill begins, the controller of the first vehicle requires zero traction torque to the engine. Due to the large gravitational

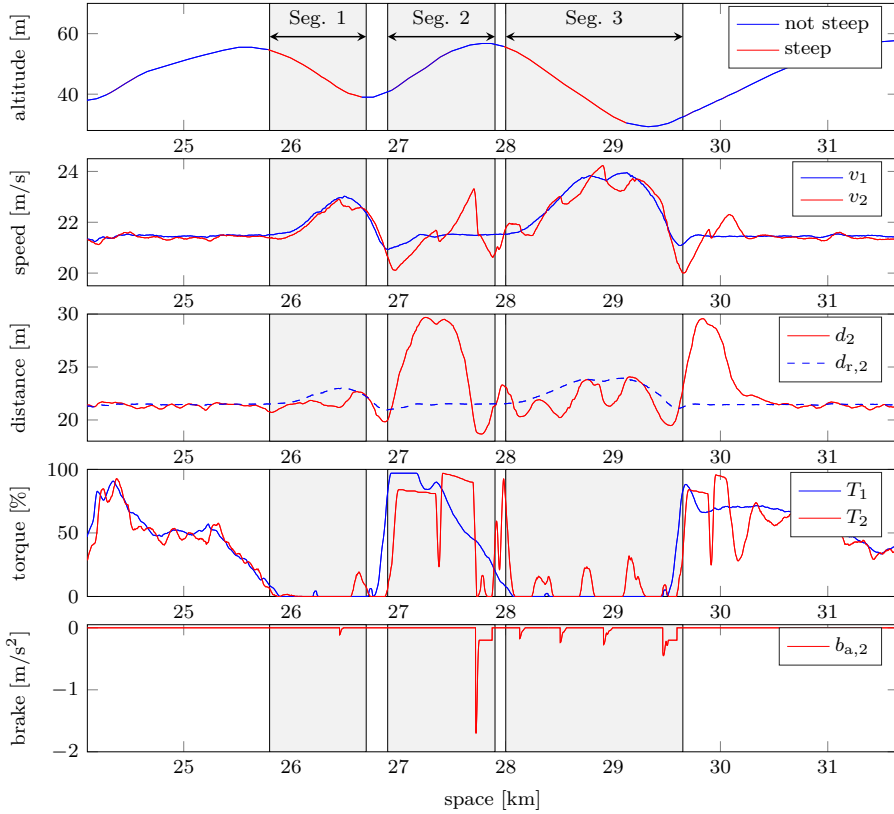


Figure 4.3: Experimental results for the first two vehicles of the three-vehicle platoon driving over the Sector A highlighted in Figure 4.2b. The first plot shows the road topography, whereas the second plot shows the speed of the two vehicles; the third plot shows the real and reference distances (according to a headway gap policy) between the vehicles; finally the fourth and fifth plots show the normalized engine torque for both vehicles and the braking acceleration for the second vehicle (the braking action of the lead vehicle is not available), respectively.

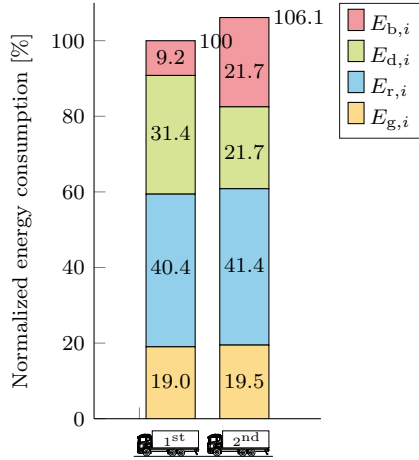


Figure 4.4: Normalized energy consumption of the two vehicles divided into the different components, i.e., energies associated with the gravitational, rolling, aerodynamic and braking forces.

force, the first vehicle still accelerates. Since the downhill is not long enough, the maximum speed limit is not reached and no switching to the braking mode takes place. This behavior is known as coasting (driving without any fuel injection nor braking action). The second vehicle, which is tracking a reference headway gap, starts coasting soon after the first vehicle. However, due to the reduced aerodynamic resistance acting on it, the gap between the vehicles shrinks until the minimum headway gap is reached. At this point, the second vehicle brakes.

- Segment 2. While trying to compensate for the headway gap error built up during the downhill, the speed of the second vehicle deviates from the one of the first truck. Soon after the uphill starts, both vehicles full-throttle. However, the speed difference at the beginning of the uphill results in a large deviation in the headway gap. Furthermore, to generate larger torque, the gear management of the second vehicle requires a downshift, leading to an increased time for closing the gap. Once the gap is closed, the controller of the second vehicle requires a significant braking torque to promptly reduce the large relative speed between the vehicles.
- Segment 3. In the second downhill, the second vehicle states oscillate as a result of the input saturation and the two controller modes. The controller of the second vehicle repeatedly switches between the two modes and this results in an inefficient behavior, where throttling and braking phases alternate. Finally, at the end of the downhill, both vehicles reach the speed limit and brake.

According to the above discussion, we witness the limitations of the implemented distributed feedback control. Because of the large weight to power ratio typical for trucks, small road grades lead the vehicle to operate in saturation for a significant amount of time. As a result, the controller fails in smoothly controlling the vehicle in scenarios where large vehicle state deviations are not possible, as in platooning.

In order to improve the system performance, we propose the use of look-ahead platoon control. The developed optimization allows to explicitly include the tight input bounds and the preview information about the road ahead, i.e., road grade and speed limits. The look-ahead framework can foresee inefficient behaviors and avoid them. For example, by reducing the throttling before the full gap closure, the second vehicle braking could have been avoided in Segment 2 and the first part of Segment 3 of Figure 4.3. The harsh braking in the final part of Segment 3 could have been prevented by starting the coasting phase when still climbing the preceding uphill.

4.2 Cooperative platooning

In this section, we discuss a cooperative framework suitable for the control of heavy-duty vehicle platoons driving along roads with varying topography. With the cooperative term, we indicate that the platooning vehicles operate together in order to reach the common goal of smooth, fuel-efficient and safe platoon behavior.

As we concluded in the previous section, varying topography has a large impact on platoons. A way to address the problem is to exploit look-ahead control that makes use of preview information about the road topography to adapt the vehicle speeds and inter-vehicular distances. The look-ahead control problem that we wish to solve can be summarized by the following receding horizon formulation:

$$\begin{aligned}
 & \text{minimize} && \text{platoon fuel consumption} \\
 & \text{subj. to} && \text{vehicle dynamics,} \\
 & && \text{state and input bounds,} \\
 & && \text{safety constraint.}
 \end{aligned} \tag{4.3}$$

We choose the actuator inputs for each vehicle such that the fuel consumption of the whole platoon is minimized under guaranteed safety. Directly solving the optimization problem in a model predictive control framework, however, presents two relevant issues:

- *Communication complexity.* Regardless of whether the problem is solved by a cloud service or by the computer of one of the vehicles, the optimal control inputs need to be communicated to all vehicles. Since this communication is wireless, however, there is no strict guarantee that all vehicles will receive it. Packet losses and communication outages should be taken into consideration.

Although the intermittent interruption of communication between vehicles is not a crucial concern for fuel-efficiency, it is for safety. The trajectory time variations for improving the fuel consumption highlighted in the previous section are relatively slow and, therefore, do not require high-rate communication. However, safety guarantee requires the prompt reaction of vehicles to unexpected platoon state changes. The platoon safety, therefore, needs to be ensured by local controllers using locally collected information, as distance to the preceding vehicle and relative speed.

- *Computational complexity.* The optimization problem (4.3) has to predict a number of states that grows linearly with the number of platooning vehicles. This prediction should be done over a relative long horizon of the order of a couple of kilometers. For example, the harsh braking in the final part of Segment 3 in Figure 4.3 should have been predicted when the platoon was still climbing the preceding uphill in order to be avoided. Furthermore, the prediction model has to be non-linear due to the powertrain, and the gravitational and aerodynamic forces. Because of these considerations, the optimization problem (4.3) is rather large and complex, and, in addition, needs to be solved in a short time.

The controller that ensures safety needs to run locally in each vehicle. However, the controller that coordinates the vehicles for overall platoon fuel-efficiency needs to interact with all vehicles. We propose therefore to divide the optimal control problem (4.3) into two hierarchical subproblems that use different update period and horizon length. A centralized controller first optimizes the behavior of the whole platoon according to the common goal of fuel-efficiency. Then, local controllers track the identified optimal trajectory, while ensuring the safety of the platoon. We refer to the first controller as *platoon coordinator* and the latter ones as *vehicle controllers*. The control architecture is depicted in Figure 4.5. In the remainder of the section, we present an overview of the tasks that each controller should solve.

Platoon coordinator

The platoon coordinator aims at defining a common behavior of the platooning vehicles that is fuel-efficient by taking topography information directly into account. It is a centralized controller that can run in one of the vehicles or off-board on a cloud service. It operates in a receding horizon fashion by repeatedly computing the optimal behavior. As the vehicle controllers are supposed to track the fuel-optimal trajectories, the refresh time of the platoon coordinator can be relatively large, of the order of a few seconds. In order to capture the slow dynamics induced by the road topography, it should have a prediction horizon of about one/two kilometers.

An overview of the optimal control problem solved by the platoon coordinator is displayed in the upper block of Figure 4.6. In order to predict the vehicle trajectory

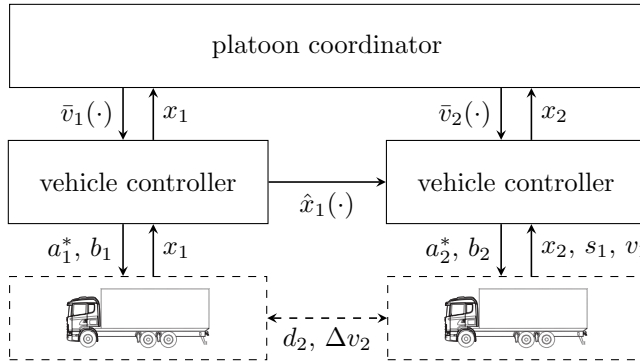


Figure 4.5: Control architecture for cooperative platooning.

and estimate the platoon fuel consumption, the optimal control problem relies on advanced vehicle models. They should include the non-linear longitudinal dynamics and input and state bounds of all vehicles. The platoon coordinator computes the reference speed trajectories for all vehicles that minimize the overall platoon fuel consumption and fulfill the average speed requirements. In the next chapter, we propose a specific platoon coordinator that addresses these points and scales well with the number of vehicles.

Vehicle controller

The vehicle control layer aims at tracking the reference speed profile computed by the platoon coordinator while ensuring safety.

An overview of the optimal control problem solved by each vehicle controller is displayed in the lower block of Figure 4.6. The vehicle controller receives the predicted state trajectory of the preceding vehicle through wireless communication, and current state information about the preceding vehicle by fusing measurements of the inter-vehicular distance and relative speed collected by on-board sensors (e.g., radar, lidar and cameras) with the vehicle own state. Using a simplified vehicle model and the predicted trajectory of the preceding vehicle, the vehicle controller computes the references for the low-level controllers (i.e., the braking, engine and gear management systems presented in Section 3.3) by minimizing a tracking error from the reference behavior. Furthermore, it guarantees safety by exploiting the locally collected information and, if available, the communicated one. Safety is guaranteed by ensuring that, in case the emergency braking of any of the platooning vehicles, all the following vehicles can reduce their speed without collision.

The gear selection can be directly taken into account in the platoon control architecture or outsourced to the low-level gear management system. Chapter 5 discusses a vehicle controller based on distributed model predictive control. Chap-

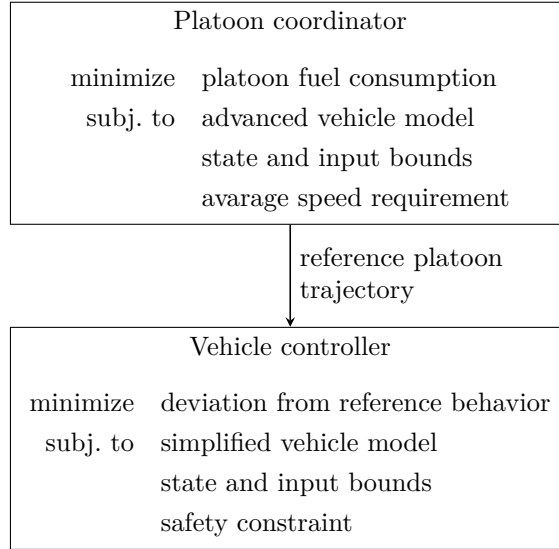


Figure 4.6: Overview of the optimal control problems solved in the platoon coordinator and the vehicle controllers.

ter 6 presents a controller that takes gear selection directly into account in the optimization.

Remark 4.2.1. The platoon coordinator is important only if the road presents significant altitude variations (i.e., the vehicles cannot maintain constant speed during uphill due to limited engine power or during downhill due to the large mass). In this case the proposed control architecture is an example of the cooperative look-ahead control (CLAC) presented in Section 3.3. If the road does not present significant altitude variations, the platoon coordinator can be omitted and the reference behavior can be set to constant speed. In this case the control architecture is an example of the cooperative adaptive cruise control (CACC) presented in Section 3.3.

4.3 Non-cooperative platooning

In this section we discuss the vehicle platooning problem when no cooperation between vehicles is possible or desired. This is a common problem when a heavy-duty vehicle encounters, along the road, another heavy-duty vehicle with which no framework for cooperation exists. Because of the lack of cooperation, this problem typically involves two heavy-duty vehicles. Here, the first vehicle drives ignoring the presence of a follower. Its longitudinal dynamics can be controlled manually by the

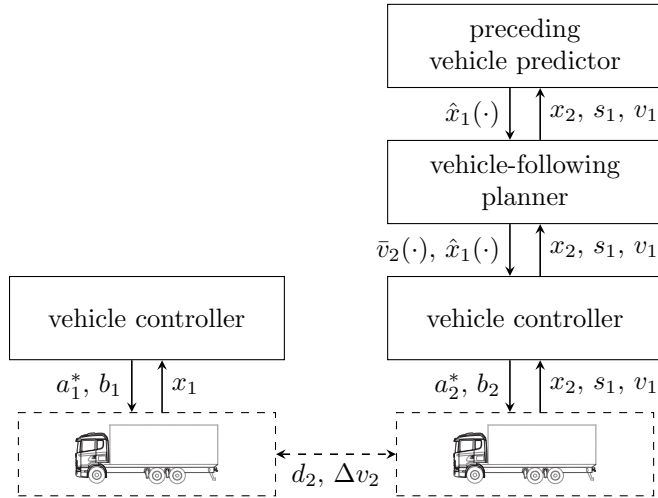


Figure 4.7: Control architecture for non-cooperative platooning.

driver or automatically by employing the cruise control or the look-ahead control introduced in Section 3.3. The second vehicle aims at fuel-optimally following the first vehicle. This is achieved by seeking the right trade-off between keeping a short inter-vehicular distance for the creation of the slipstream effect, efficiently using the powertrain and avoiding braking. The non-cooperative platooning problem is also referred to as ad-hoc platooning or vehicle-following to stress that the main challenges lie in the second vehicle. The tasks that have to be accomplished are mainly twofold:

- (i) Prediction of the trajectory of the preceding vehicle. Depending on the availability of inter-vehicular communication, we distinguish between the two following cases:
 - If inter-vehicular communication is available, the prediction task can be executed by the preceding vehicle and the predicted trajectory can be communicated to the following one.
 - If inter-vehicular communication is not available, the prediction of the preceding vehicle is carried by the following vehicle. This prediction should be based on historical and current information collected by on-board sensors, such as vehicle distance and relative speed. Few works addressed this prediction problem, see e.g. Lang et al. (2014) and Moser et al. (2018), but, to the best knowledge of the author, no work exploited topography information about the road ahead to obtain a more accurate estimation. This is an open problem that is discussed in Chapter 9.

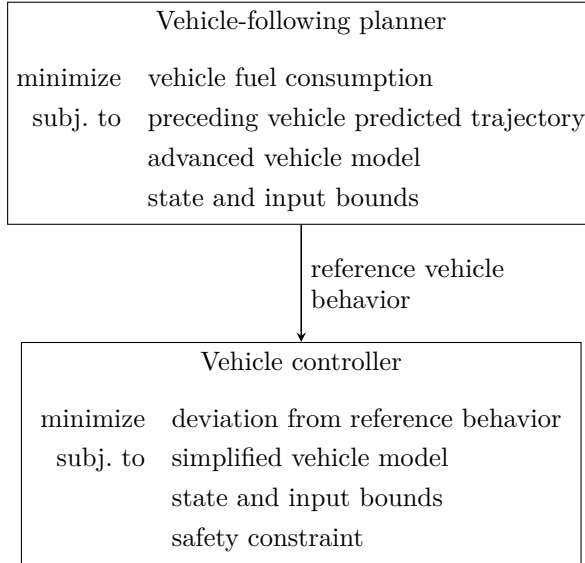


Figure 4.8: Overview of the optimal control problems solved in the vehicle-following planner and the vehicle controller.

- (ii) Exploitation of the preceding vehicle predicted trajectory. This task can be formulated as the following optimal control problem that needs to be solved by the following vehicle:

$$\begin{aligned}
 &\text{minimize} && \text{vehicle fuel consumption} \\
 &\text{subj. to} && \text{preceding vehicle predicted trajectory,} \\
 &&& \text{vehicle dynamics,} \\
 &&& \text{state and input bounds,} \\
 &&& \text{safety constraint.}
 \end{aligned} \tag{4.4}$$

In this thesis we address the control problem summarized in the second bullet point. Figure 4.7 displays the control architecture for the non-cooperative platooning control problem. Here, the optimal control problem (4.4) is addressed by the two control layers, named *vehicle-following planner* and *vehicle controller*. An overview of the optimal control problems solved by these two controllers is displayed in Figure 4.8 and explained in the remainder of the section.

Vehicle-following planner

The vehicle-following planner computes the reference behavior of the vehicle under control. As displayed in the upper block of Figure 4.8, this computation is the result of the minimization of the vehicle fuel consumption under predicted preceding vehicle behavior. The prediction is done by exploiting the estimated trajectory of the preceding vehicle and topography information, and using a model of the vehicle under control. As the vehicle-following planner is not handling safety critical aspects and the trajectory of the preceding vehicle is expected to be slowly varying, the optimization refresh time can be relatively large, of the order of a few seconds.

Vehicle controller

The vehicle controller for non-cooperative platooning solves a similar problem to that one addressed by the vehicle controller for cooperative platooning presented in the previous section, i.e., tracking a reference behavior while ensuring safety. The main difference lies in the fact that the vehicle controller for non-cooperative platooning uses a locally computed estimation of the future behavior of the preceding vehicle, instead of the communicated one by the preceding vehicle itself.

In Chapter 7, we propose an implementation of the vehicle-following planner based on dynamic programming. It uses a detailed model of the longitudinal dynamics and transmission to compute the optimal gear sequence and traction force request. In Chapter 8 we present a lower-complexity controller based on model predictive control that aims at solving both the vehicle-following planner and the vehicle controller problems in a single formulation.

4.4 Summary

In this chapter we first presented the analysis of a platooning experiment conducted on a Swedish highway. The insight gained by this analysis gave us the suggestion to design two control architectures: one for cooperative platooning and one for non-cooperative platooning. Both architectures were based on look-ahead control that allows to exploit preview information on the road topography and preceding vehicle behavior in the control computation. In cooperative platooning, the fuel-efficiency is managed by the platoon coordinator that aims at minimizing the fuel consumption of the whole platoon. In the non-cooperative architecture, instead, the fuel-efficiency is managed by the vehicle-following planner that aims at minimizing the following vehicle own fuel consumption. In both architectures, the tracking of the fuel-efficient behavior is handled by local vehicle controllers, which also ensure safety.

Part I

Cooperative platooning

Cooperative fuel-efficient and safe platooning

In this chapter, we discuss a formulation and implementation of the cooperative control architecture for fuel-efficient and safe platooning introduced in Chapter 4. Each layer is based on an optimal control problem formulation aimed at optimizing the platoon behavior. The higher layer, denoted as platoon coordinator, is based on a dynamic programming framework, which computes a reference speed profile defined over space for all vehicles of the platoon. It ensures the feasibility of the speed trajectory and its fuel-optimality by explicitly taking topography information into account. The lower layer, denoted as vehicle control layer, is based on a distributed model predictive control framework that safely tracks the reference speed trajectory. Safety is guaranteed by specifically designed constraints that ensure the recursive feasibility of the model predictive controller.

The proposed control architecture is tested in an in-depth simulation study that can be divided into three parts: (i) We evaluate the platoon coordinator performance by means of simulations where the fuel consumption of a two-vehicle platoon under multiple vehicle control strategies is compared. The results show the potential of the platoon coordinator to reduce the fuel consumption for a fairly hilly road of up to 12% for following vehicles with respect to standard platooning controllers. (ii) We test the reaction of a three-vehicle platoon to multiple maneuvers of the leading vehicle. The results show how the platooning vehicles successfully handle harsh braking of the leading vehicle without collision and how disturbances attenuate along the platoon. The vehicles successfully manage to brake without collision occurring. (iii) The functioning of the overall control architecture is tested by simulating a three-vehicle platoon driving in the same scenario as the experiment presented in Section 4.1, outperforming the controller tested previously. The platoon exhibits a smooth behavior and the controller is able to compensate for small disturbances acting on the control input.

The chapter is organized as follows. In Section 5.1, we present the cooperative platooning control architecture tailored to our implementation and we state the

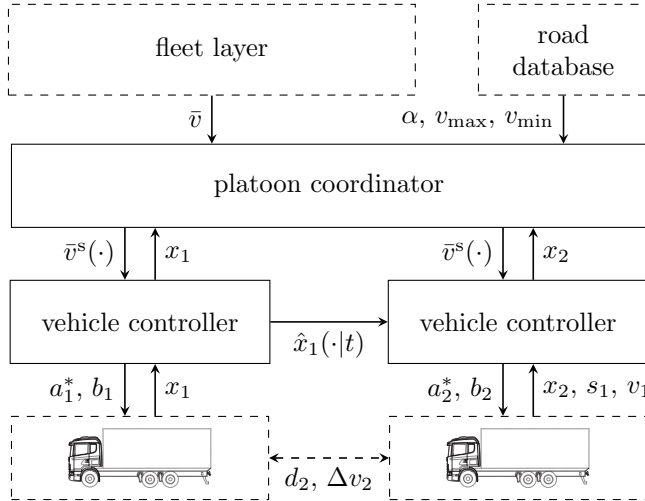


Figure 5.1: Control architecture for cooperative platooning.

control problems solved by the two layers. Sections 5.2 and 5.3 detail the platoon coordinator and the vehicle control layers, respectively. Sections 5.4 and 5.5 provide an independent evaluation of the performance of the two layers. Finally, Section 5.6 evaluates the performance of the overall closed-loop system and Section 5.7 concludes the chapter.

5.1 Control architecture and problem statement

In this section, we discuss the control architecture for cooperative platooning shown in Figure 5.1 and we state the problem formulations for the two platoon coordinator and the vehicle control layer.

The fleet layer displayed in Figure 5.1 is responsible for routing the single vehicles and platoons, and for defining their average speed over each road section, in order to promote the fuel-efficient platoon formation. The platoon coordinator receives the average speed requirement and defines the reference speed trajectory for all vehicles in the same platoon exploiting available information on the road ahead, i.e., road altitude profile and speed limits. Finally, the vehicle controllers safely tracks the reference speed profile.

5.1.1 Platoon coordinator problem statement

The platoon coordinator is responsible for the overall fuel-efficient operation of the platoon. It defines reference speed trajectories for the platooning vehicles that (i)

minimize the fuel consumption of the whole platoon, (ii) are feasible for all vehicles and (iii) satisfy the average speed condition required by the fleet layer.

In Section 5.2, we propose a platoon coordinator formulation that scales well with the length of the platoon. This is achieved by requiring platooning vehicles to follow the same speed profile defined over space. As road attributes, e.g., the beginning of an uphill or a downhill, or speed limit, affect the platooning vehicles at specific space, it is natural to impose speed variations in the space domain instead of the time domain. To this end, the platoon coordinator computes a unique space-defined speed profile for the whole platoon. If we define the optimal control problem over space, it means that we can reduce the number of predicted states from a number that grows linearly with the number of vehicles to a fixed number of states independent from the number of vehicles.

A consequence of the space-defined speed profile for the whole platoon is that vehicles are spaced by a constant time gap. That means that the time interval that passes between two consecutive vehicles going through the same point is constant, i.e.,

$$s_i(t) = s_{i-1}(t - \tau_i). \quad (5.1)$$

where s_i and τ_i denote the position of vehicle i and the time gap, respectively. This can be easily proved by computing the time derivative of the left-hand side of equation (5.1), leading to

$$\frac{ds_i(t)}{dt} = v_i(t) = v_i^s(s_i(t)), \quad (5.2)$$

where $v_i^s(s)$ denotes the speed of vehicle i at space s , and the right-hand side of equation (5.1), leading to

$$\begin{aligned} \frac{ds_{i-1}(t - \tau_i)}{dt} &= v_{i-1}(t - \tau_i) \\ &= v_{i-1}^s(s_{i-1}(t - \tau_i)) = v_{i-1}^s(s_i(t)). \end{aligned} \quad (5.3)$$

For the proposed platoon coordinator, we relax the strict average speed requirement by weighting the platoon travel time in the cost function. As the traveled time can be defined as the integral of a function of the vehicle speed, i.e.,

$$\int_0^{S_{\text{final}}} \frac{1}{v_i^s(s)} ds, \quad (5.4)$$

the space-dependent state time is no more used in the optimal control formulation and its dynamics can be therefore omitted. This allows to further reduce the computational complexity of the optimal controller. The optimization problem of the platoon coordinator is synthesized in the upper block of Figure 5.2. Due to the non-linearities of the vehicle model, the optimal control problem is solved by

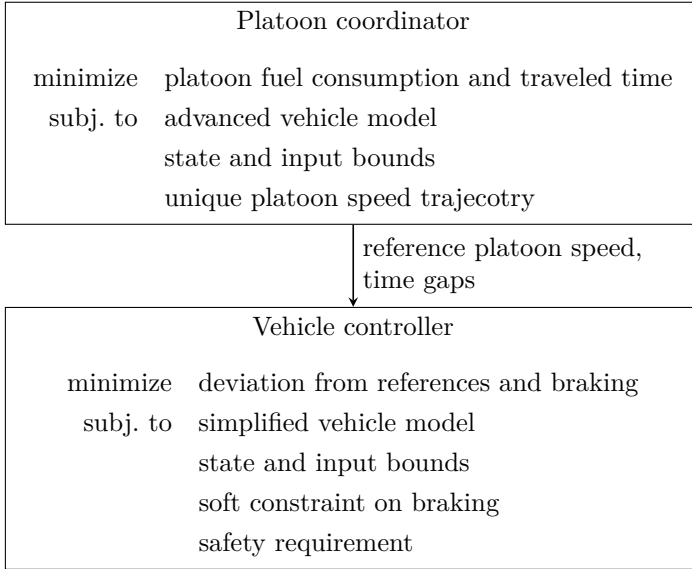


Figure 5.2: Overview of the optimal control problems solved in the proposed formulations of the platoon coordinator and the vehicle controllers.

dynamic programming. Details are given in Section 5.2.

5.1.2 Vehicle control layer problem statement

The vehicle control layer is responsible for the safe tracking of the reference platoon speed profile generated by the platoon coordinator. In Section 5.3, we propose a vehicle control layer based on model predictive control. Each vehicle controller receives (i) the reference speed trajectory from the platoon coordinator $\bar{v}^s(\cdot)$, (ii) the predicted future trajectory from the preceding vehicle $\hat{x}_{i-1}^*(\cdot|t)$ and (iii) measurements of the preceding vehicle current states (i.e., its position s_{i-1} and speed v_{i-1}), obtained by fusing information from on-board sensors (i.e., inter-vehicular distance d_i , relative speed Δv_i , vehicle position s_i , and vehicle speed v_i).

The model predictive controller of each vehicle uses a simplified linear model of the vehicle, namely a double integrator. In order to fuel-efficiently and safely track the reference speed trajectory, the optimal control formulation aims at minimizing the deviation from the reference trajectory and from the constant time gap, while avoiding unnecessary braking. The latter condition is obtained by introducing a soft constraint on avoiding the braking action and heavily penalizing the slack variable associated with the soft constraint in the cost function. The safety of the platoon is defined as the requirement of all vehicles being able to decelerate without reaching

collision when one or multiple vehicles in the platoon unexpectedly full-brake. The safety is ensured by defining specifically designed safety constraint enforced in each vehicle controller.

The optimization problem of the vehicle controller is synthesized in the lower block of Figure 5.2. Details are given in Section 5.3.

5.2 Platoon coordinator

The parameters that characterize the dynamic programming formulation are the horizon length H_{DP} , the discretization space Δs_{DP} and the recomputation frequency f_{DP} . We also define the number of steps in the horizon as $N_{\text{DP}} = \lfloor H_{\text{DP}}/\Delta s_{\text{DP}} \rfloor$. In the remainder of the section we present the platoon model, the powertrain model, model constraints and the cost function that are used in the dynamic programming formulation.

5.2.1 Platoon model

The platoon coordinator relies on a discretized version of the vehicle model (3.1), where the discretization is carried out in the spatial domain using the implicit Euler approximation. The discretized vehicle model is:

$$v_i^s(z_k) \frac{v_i^s(z_k) - v_i^s(z_{k-1})}{\Delta s_{\text{DP}}} = F_{t,i}^s(z_k) + F_{b,i}^s(z_k) - m_i g_a (\sin(\alpha(z_k)) + c_{r,i}) - \frac{1}{2} \rho A_v C_d (d_i^s(z_k)) (v_i^s(z_k))^2, \quad (5.5a)$$

$$v_i^s(z_k) \frac{t_i^s(z_k) - t_i^s(z_{k-1})}{\Delta s_{\text{DP}}} = 1, \quad (5.5b)$$

where z_k is the discretized space variable, and $v_i^s(z_k)$, $t_i^s(z_k)$, $F_{t,i}^s(z_k)$, $F_{b,i}^s(z_k)$ and $d_i^s(z_k)$ are the speed, time, traction and braking forces, and distance to the preceding vehicle, all expressed as function of space, respectively. The definition of the vehicle parameters is introduced in Chapter 3 and synthesized in Table 5.1. In the dynamic programming formulation we refer to equation (5.5a) as

$$v_i^s(z_{k-1}) = f_i^s(v_i^s(z_k), u_i^s(z_k)), \quad (5.6)$$

where $u_i^s(z_k)$ is the input vector defined as $u_i^s(z_k) = [F_{t,i}^s(z_k), F_{b,i}^s(z_k)]^T$. As argued in Section 5.1, the space-defined time dynamics (5.5b) are ignored since they are not used in the constraints or cost function.

The inter-vehicular distance (3.2) cannot be explicitly expressed in the space domain. We therefore approximate it with a function of the current vehicle speed

$v_i^s(z_k)$ according to

$$d_i^s(z_k) = v_i^s(z_k)\tau_i - l_{i-1}. \quad (5.7)$$

This approximation is valid if the (fuel-optimal) speed profile exhibits slow dynamics, as would be expected.

5.2.2 Powertrain model

Here, we derive a simplified model of the powertrain that captures the relation between the instantaneous fuel consumption and the generated traction power P_i defined as the product of the traction force and the vehicle speed:

$$P_i = F_{t,i}v_i. \quad (5.8)$$

In order to obtain a model that can be effectively used in the cost function definition of the platoon coordinator, the gearbox-clutch dynamics have been simplified by assuming that:

- (i) the gear ratio $\gamma_{g,i}$ defined in Section 3.2 can be chosen on a continuous and unlimited span,
- (ii) no delays occur in gear ratio changes.

These simplifications, combined with the requirement that all vehicles follow the same speed profile defined over space, allow to obtain a dynamic programming formulation that scales linearly with the number of vehicles.

According to the transmission models (3.11)–(3.12) presented in Chapter 3 and the power definition (5.8), the engine torque T_i can be rewritten as

$$T_i = \frac{P_i}{\omega_i} \quad (5.9)$$

and the fuel model (3.10) can be redefined as function of the engine speed ω_i and the generated power P_i , as

$$\psi_i = \varphi_i\left(\omega_i, \frac{P_i}{\omega_i}\right). \quad (5.10)$$

Thanks to the introduced assumptions, the gear ratio $\gamma_{g,i}$ and, consequently, the engine speed ω_i can be chosen optimally such that the fuel flow is minimized for a given generated traction power P_i , i.e.,

$$\psi_i = \min_{\omega_i} \varphi_i\left(\omega_i, \frac{P_i}{\omega_i}\right) = q_i(P_i). \quad (5.11)$$

This pre-optimization give as the simplified powertrain model $q_i(\cdot)$ that will be used in the cost function definition.

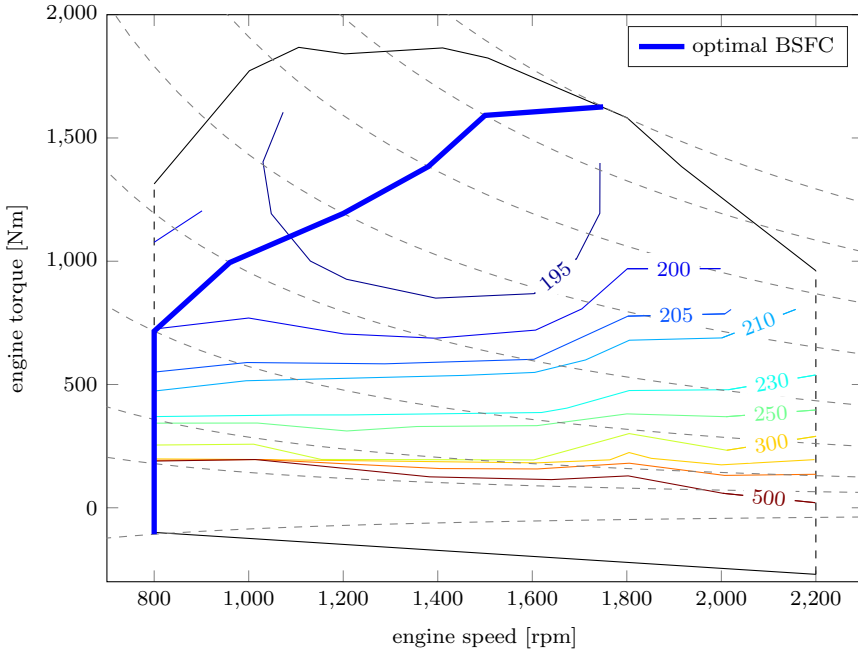


Figure 5.3: BSFC map of the 400 hp engine introduced in Section 3.2. The thick blue line represents the collection of the optimal operation points associated to the simplified powertrain model $q(\cdot)$.

To understand the meaning of the simplified model in Figure 5.3 we reproduce the BSFC map of the 400 hp engine first presented in Section 3.2. The thick blue line in Figure 5.3 highlights the operation points (pairs of engine speed and torque) associated with the simplified powertrain model (5.11). The simplified engine model $q_i(\cdot)$ and the optimal engine speed corresponding to such engine are displayed in Figure 5.4. We can notice how $q_i(\cdot)$ exhibits a nearly affine trend. We therefore extract a linearized powertrain model (displayed in Figure 5.4 as a red line) that will be used to define the terminal cost in the platoon coordinator cost function. We will refer to such model as

$$\psi_i = q_{1,i}P_i + q_{0,i}. \quad (5.12)$$

From Figure 5.3, we can finally extract the minimum and maximum engine power bounds, $P_{\min,i}$ and $P_{\max,i}$, respectively, that will be enforced as model constraints.

5.2.3 Model constraints

The vehicle dynamics are constrained by the following bounds on input and state.

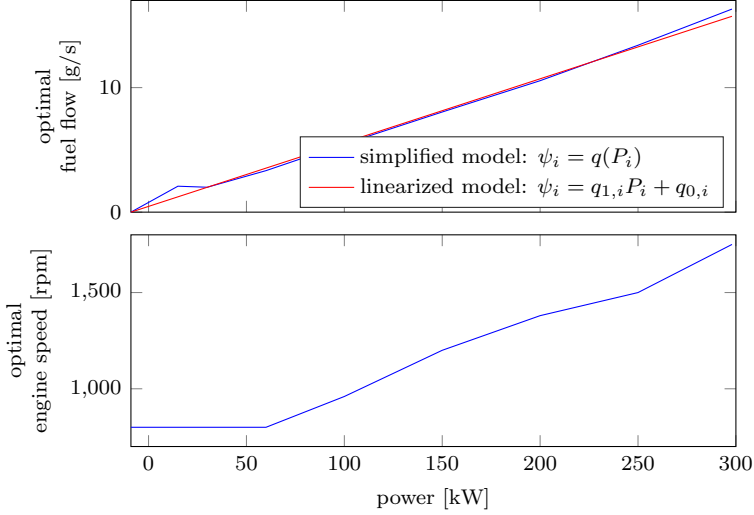


Figure 5.4: The plots show the optimal fuel flow and engine speed as function of the generated power. In the first plot we also display the fuel model expressed in (5.12) obtained by the regression of the raw data.

Input constraints

According to the engine power bounds derived in the previous subsection and according to equation (3.3), the traction and braking forces are bounded by:

$$P_{\min,i} \leq F_{t,i}^s(z_k)v_i^s(z_k) \leq P_{\max,i}, \quad (5.13a)$$

$$F_{b,\min,i} \leq F_{b,i}^s(z_k) \leq 0, \quad (5.13b)$$

Speed constraints

In order to take into account speed limits, the speed is constrained by the following space-dependent bounds:

$$v_{\min}(z_k) \leq v_i^s(z_k) \leq v_{\max}(z_k). \quad (5.14)$$

Moreover, as argued in Section 5.1, all vehicles are required to follow the same speed profile by enforcing the following constraint:

$$v_i^s(z_k) = v^s(z_k), \quad i = 1, \dots, N_v. \quad (5.15)$$

We will refer to $v^s(\cdot)$ as the platoon speed.

5.2.4 Cost function

The cost function is defined as a weighted summation of a term representing the platoon fuel consumption and a term representing the traveled time, i.e.,

$$J_{\text{DP}}(v^{\text{s}}(\cdot), u^{\text{s}}(\cdot)) = J_{\text{fuel}}(v^{\text{s}}(\cdot), u^{\text{s}}(\cdot)) + \beta J_{\text{time}}(v^{\text{s}}(\cdot)), \quad (5.16)$$

where $u^{\text{s}}(\cdot)$ concatenates the inputs of all vehicles, i.e., $u^{\text{s}}(\cdot) = [u_1^{\text{s}}(\cdot), \dots, u_{N_v}^{\text{s}}(\cdot)]^{\text{T}}$. Here, β represents the trade-off between fuel consumption and traveled time, but can be also interpreted as the Lagrangian multiplier of the relaxed average speed constraint. It can be analytically computed according to a simplified platoon model where speed constraints are ignored similarly to what is proposed in Hellström et al. (2006), or controlled. In this work, we opt for the latter option where, in detail, β is controlled by a slow PI controller that tracks the average speed \bar{v} required by the fleet layer depicted in Figure 5.1.

The fuel consumption term $J_{\text{fuel}}(v^{\text{s}}(\cdot), u^{\text{s}}(\cdot))$ is computed according to the powertrain model (5.11) and includes a terminal term representing the kinematic energy of the platoon at the end of the horizon. The final kinematic energy has been scaled according to the linearized powertrain model (5.12). The fuel consumption term can be computed as

$$\begin{aligned} J_{\text{fuel}}(v^{\text{s}}(\cdot), u^{\text{s}}(\cdot)) &= \sum_{i=1}^{N_v} \sum_{j=k}^{k+N_{\text{DP}}-1} \frac{q(F_{\text{t},i}^{\text{s}}(z_j)v^{\text{s}}(z_j)) \Delta s_{\text{DP}}}{v^{\text{s}}(z_j)} \\ &\quad - \sum_{i=1}^{N_v} p_{1,i} \frac{m_i(v^{\text{s}}(z_{j+N_{\text{DP}}-1}))^2}{2}. \end{aligned} \quad (5.17)$$

The traveled time term $J_{\text{time}}(v^{\text{s}}(z_j))$ is computed by integrating the time dynamics (5.5b), resulting in

$$J_{\text{time}}(v^{\text{s}}(\cdot)) = \sum_{j=k}^{k+N_{\text{DP}}-1} \frac{\Delta s_{\text{DP}}}{v^{\text{s}}(z_j)}. \quad (5.18)$$

5.2.5 Dynamic programming formulation

We now have all the elements to state the dynamic programming formulation:

$$\underset{u^s(\cdot)}{\text{minimize}} \quad J_{\text{DP}}(v^s(\cdot), u^s(\cdot)) \quad (5.19\text{a})$$

$$\text{subj. to} \quad v_i^s(z_{j-1}) = f_i^s(v_i^s(z_j), u_i^s(z_j)), \quad (5.19\text{b})$$

$$P_{\min,i} \leq F_{t,i}^s(z_k) v_i^s(z_k) \leq P_{\max,i}, \quad (5.19\text{c})$$

$$F_{b,\min,i} \leq F_{b,i}^s(z_k) \leq 0, \quad (5.19\text{d})$$

$$v_{\min}(z_k) \leq v_i^s(z_k) \leq v_{\max}(z_k), \quad (5.19\text{e})$$

$$v_i^s(z_j) = v^s(z_j) \in \mathcal{V}^s(z_j), \quad (5.19\text{f})$$

$$z_k = s_1(t), \quad (5.19\text{g})$$

$$v^s(z_k) = v_1(t), \quad (5.19\text{h})$$

for $j = k, \dots, k + N_{\text{DP}} - 1$, where equations (5.19g) and (5.19h) represent the initial conditions of the dynamic programming formulation.

5.3 Vehicle control layer

The parameters that characterize the model predictive control MPC formulation are the horizon length H_{MPC} , the discretization time Δt_{MPC} and the re-computation frequency f_{MPC} . We define the number of steps in the horizon as $N_{\text{MPC}} = \lfloor H_{\text{MPC}} / \Delta t_{\text{MPC}} \rfloor$. We also assume a maximum delay in vehicle communication and in the measurement collection by the on-board sensors of Δt_{MPC} . In the remainder of the section, we present the vehicle model, the model constraints, the safety constraint and the cost function that are used in the MPC formulation.

5.3.1 Vehicle model

In the MPC formulation the vehicle is described by the double integrator dynamics

$$x_i(t_{j+1}|t_k) = Ax_i(t_j|t_k) + Ba_i(t_j|t_k), \quad (5.20)$$

where

$$A \triangleq \begin{bmatrix} 1 & 0 \\ \Delta t_{\text{MPC}} & 1 \end{bmatrix}, \quad B \triangleq \begin{bmatrix} \Delta t_{\text{MPC}} \\ 0 \end{bmatrix}.$$

The state x_i represents the vector concatenating the vehicle speed and position, i.e., $x_i = [v_i, s_i]^T$, while the control input a_i represents the vehicle acceleration. The variables $x_i(t_j|t_k)$ and $a_i(t_j|t_k)$ denote the predicted state and control input trajectories of vehicle i associated with the update time t_k . We also introduce three

additional trajectories associated with each update time t_k that will be used in the MPC formulation:

- the optimal state trajectory $x_i^*(t_j|t_k)$,
- the reference state trajectory $\bar{x}_i(t_j|t_k)$,
- the assumed state trajectory $\hat{x}_i(t_j|t_k)$,

for $j = k, \dots, k + N_{\text{MPC}} - 1$ and the corresponding input control trajectories defined likewise. While the predicted and optimal trajectories are functions of the optimization variable, the reference and assumed trajectories are precomputed. More precisely the reference trajectories $\bar{x}_i(t_j|t_k) = [\bar{v}_i(t_j|t_k), \bar{s}_i(t_j|t_k)]^T$ and $\bar{a}_i(t_j|t_k)$ are computed from the reference platoon trajectory $\bar{v}^s(\cdot)$ and the current position $s(t_k)$ of the vehicle. In particular, $\bar{s}_i(t_j|t_k)$ is defined recursively as

$$\bar{s}_i(t_j|t_k) = \begin{cases} s_i(t_j), & j = k, \\ \bar{s}_i(t_{j-1}|t_k) + \Delta t_{\text{MPC}} \bar{v}^s(\bar{s}_i(t_{j-1}|t_k)), & j > k, \end{cases} \quad (5.21)$$

while $\bar{v}_i(t_j|t_k)$ is defined as

$$\bar{v}_i(t_j|t_k) = \bar{v}^s(\bar{s}_i(t_j|t_k)). \quad (5.22)$$

The control input reference trajectory $\bar{a}_i(t_j|t_k)$ is defined as finite differences of $\bar{v}_i(t_j|t_k)$, i.e.,

$$\bar{a}_i(t_j|t_k) = \frac{\bar{v}_i(t_{j+1}|t_k) - \bar{v}_i(t_j|t_k)}{\Delta t_{\text{MPC}}}. \quad (5.23)$$

The assumed state and control input trajectories are computed from the optimal and real trajectories of the vehicle as

$$\hat{x}_i(t_j|t_k) = \begin{cases} x_i(t_j), & j < k, \\ x_i^*(t_j|t_{k-1}), & k \leq j < k + H_{\text{MPC}}, \end{cases} \quad (5.24)$$

and $\hat{a}_i(t_j|t_k)$ likewise. The assumed trajectories represent the most accurate knowledge of the past and future state and control input trajectories of each vehicle. Using a similar framework to the one presented in Dunbar and Murray (2006), such trajectories are communicated by each vehicle to the following one. In this way, the assumed trajectories of the preceding vehicle can be exploited in each vehicle controller formulation in order to track the required gap policy. Note that the dependence of the assumed trajectories to the optimal trajectories computed the previous step, see definition (5.24), reflects the assumption of a maximum delay in vehicle communication of Δt_{MPC} .

5.3.2 Model constraints

In order to take the bounds on the braking force (3.3) and the engine power (5.13b) into account, as done in the platoon coordinator layer, the control input a_i is bounded by the following non-linear constraint:

$$a_{\min,i}(x_i(t_j|t_k), \hat{x}_{i-1}(t_j|t_k)) \leq a_i(t_j|t_k) \leq a_{\max,i}(x_i(t_j|t_k), \hat{x}_{i-1}(t_j|t_k)), \quad (5.25)$$

for $j = k, \dots, k + N_{\text{MPC}} - 1$, where

$$a_{\min,i}(x_i, \hat{x}_{i-1}) = \frac{1}{m_i} (F_{\text{b},\min,i} + F_{\text{ext},i}(x_i, \hat{x}_{i-1})), \quad (5.26a)$$

$$a_{\max,i}(x_i, \hat{x}_{i-1}) = \frac{1}{m_i} \left(\frac{P_{\max,i}}{v_i} + F_{\text{ext},i}(x_i, \hat{x}_{i-1}) \right). \quad (5.26b)$$

Here $F_{\text{ext},i}$ denotes the summation of the external forces acting on the vehicle defined as

$$F_{\text{ext},i}(x_i, \hat{x}_{i-1}) = -m_i g_a \sin \alpha(s_i) - m_i g_a c_{\text{r},i} - \frac{1}{2} \rho A_{\text{v}} C_d (\hat{s}_{i-1} - s_i - l_{i-1}) v_i^2. \quad (5.27)$$

The control input a_i is additionally bounded by the soft constraint introduced in Section 5.1 that ensures that braking action happens only if necessary, i.e., when the safety constraint activates, or if it is required by the platoon coordinator. This is formulated as follows:

$$a_i(t_j|t_k) + \varepsilon_i(t_k) \geq \min(a_{\text{coast},i}(x_i(t_j|t_k), \hat{x}_{i-1}(t_j|t_k)), \bar{a}_i(t_j|t_k)), \quad (5.28a)$$

$$\varepsilon_i(t_k) \geq 0, \quad (5.28b)$$

for $j = k, \dots, k + N_{\text{MPC}} - 1$, where $a_{\text{coast},i}$ is the coasting acceleration, i.e., the vehicle acceleration when fuel is not injected, defined as

$$a_{\text{coast},i}(x_i, \hat{x}_{i-1}) = \frac{1}{m_i} \left(\frac{P_{\min,i}}{v_i} + F_{\text{ext},i}(x_i, \hat{x}_{i-1}) \right). \quad (5.29)$$

and ε_i is the slack variable associated with the soft constraint. Here, we remark that the dependence of the input constraints on the assumed trajectory of the preceding vehicle is due to the aerodynamic drag reduction with the inter-vehicular distance reduction.

Finally, the speed is bounded according to constraint (5.14) as

$$v_{\min}(s_i(t_j|t_k)) \leq v_i(t_j|t_k) \leq v_{\max}(s_i(t_j|t_k)). \quad (5.30)$$

5.3.3 Safety constraint

The platoon is intended to operate on public highways where other vehicles are present. The designed controller, therefore, should be able to cope with cases where the platoon behavior deviates from the predicted one because of internal disturbances (e.g., gear shifts) or external events (e.g., high traffic or a vehicle full-braking). In this section we focus on the safety problem, leaving to further work the study of how such events should be handled (i.e., autonomously or by switching to manual driving).

The platoon is considered safe if, regardless of the action of any vehicle in the platoon, there exists an input for all the following vehicles such that a collision can be avoided. The safety of the platoon is guaranteed by ensuring that the state of each vehicle lies within a safety set and it is firstly studied by considering two adjacent vehicles and later extended to the entire platoon. In here we consider the following continuous-time vehicle dynamics:

$$\dot{\tilde{x}}_i = \begin{bmatrix} \dot{\tilde{v}}_i \\ \dot{\tilde{s}}_i \end{bmatrix} = f(\tilde{x}_i, \tilde{a}_i) = \begin{bmatrix} \tilde{a}_i \\ \tilde{v}_i \end{bmatrix}, \quad (5.31)$$

where \tilde{v}_i , \tilde{s}_i and \tilde{a}_i are the speed, position and acceleration of vehicle i , respectively.

Let now focus on the dynamics of two adjacent vehicles described by

$$\begin{bmatrix} \dot{\tilde{x}}_{i-1} \\ \dot{\tilde{x}}_i \end{bmatrix} = F(\tilde{x}_{i-1}, \tilde{x}_i, \tilde{a}_{i-1}, \tilde{a}_i) = \begin{bmatrix} f(\tilde{x}_{i-1}, \tilde{a}_{i-1}) \\ f(\tilde{x}_i, \tilde{a}_i) \end{bmatrix}, \quad (5.32)$$

where the acceleration of the current vehicle \tilde{a}_i is the control input, while the acceleration of the preceding vehicle \tilde{a}_{i-1} is the exogenous input that can be regarded as a disturbance. We also introduce the admissible set

$$\tilde{\mathcal{X}} = \{[\tilde{x}_{i-1}^T, \tilde{x}_i^T]^T : \tilde{v}_{i-1} \geq 0, \tilde{v}_i \geq 0, \tilde{s}_{i-1} - \tilde{s}_i \geq l_{i-1}\} \quad (5.33)$$

as the set of all admissible states, where l_i denotes the length of vehicle i . In order to obtain a closed form of the safety set, the following conservative approximations of the exogenous and control inputs are introduced:

$$\tilde{a}_{i-1} \in \mathcal{A}^p(\tilde{x}_{i-1}) = \begin{cases} [\underline{a}_{\min, i-1}, \bar{a}_{\max, i-1}], & \text{if } \tilde{v}_{i-1} > 0, \\ [0, \bar{a}_{\max, i-1}], & \text{if } \tilde{v}_{i-1} = 0, \end{cases} \quad (5.34a)$$

$$\tilde{a}_i \in \mathcal{A}^f(\tilde{x}_i) = \begin{cases} [\bar{a}_{\min, i}, \underline{a}_{\max, i}], & \text{if } \tilde{v}_i > 0, \\ [0, \underline{a}_{\max, i}], & \text{if } \tilde{v}_i = 0, \end{cases} \quad (5.34b)$$

where $\underline{a}_{\min, i}$, $\bar{a}_{\min, i}$, $\underline{a}_{\max, i}$ and $\bar{a}_{\max, i}$ are lower and upper bounds on the minimum and maximum possible accelerations of vehicle i , respectively. Such bounds are

computed under reasonable assumptions on the vehicles and road properties, i.e., the vehicles' speed is limited ($0 \leq \tilde{v}_i \leq v_{\max}$) and the road slope α is bounded ($|\alpha| \leq \alpha_{\max}$). For example, the bounds $\underline{a}_{\min,i}$ and $\bar{a}_{\min,i}$ represent the minimum braking acceleration in the best and worst case environmental conditions. They can be computed as

$$\underline{a}_{\min,i} = \min_{0 \leq v \leq v_{\max}, |\alpha| \leq \alpha_{\max}, d \geq 0} a_{\min,i}(v, \alpha, d), \quad (5.35a)$$

$$\bar{a}_{\min,i} = \max_{0 \leq v \leq v_{\max}, |\alpha| \leq \alpha_{\max}, d \geq 0} a_{\min,i}(v, \alpha, d), \quad (5.35b)$$

where $a_{\min,i}(v, \alpha, d)$ denotes the minimum braking acceleration defined as

$$a_{\min,i}(v, \alpha, d) = \frac{F_{b,\min,i}}{m_i} - g_a \sin(\alpha) - c_{r,i} g_a - \frac{\rho A_v C_d(d) v^2}{2m_i}. \quad (5.36)$$

Note that, due to the definition of the bounds and because of the dominance of the $F_{b,\min,i}/m_i$ term in the definition of $a_{\min,i}$, the following inequalities hold:

$$\underline{a}_{\min,i} \leq \bar{a}_{\min,i} \leq 0, \quad (5.37a)$$

$$\underline{a}_{\max,i} \leq \bar{a}_{\max,i}. \quad (5.37b)$$

A similar approach can be taken for computing the bounds on the maximum traction acceleration $\underline{a}_{\max,i}$ and $\bar{a}_{\max,i}$.

In order to guarantee the safety of the subsystem (5.32), we should guarantee that the state $[\tilde{x}_{i-1}^T, \tilde{x}_i^T]^T$ always lies in a safety set \mathcal{S}_i included in $\tilde{\mathcal{X}}$, for any admissible trajectory of the preceding vehicle. We now define the safety set $\mathcal{S}_i \subseteq \tilde{\mathcal{X}}$, displayed in Figure 5.5, as

$$\mathcal{S}_i = \{[\tilde{x}_{i-1}^T, \tilde{x}_i^T]^T : g_j(\tilde{x}_{i-1}, \tilde{x}_i) \geq 0, j = 1, \dots, 4\}, \quad (5.38)$$

where, in this section, $g_j(\cdot, \cdot)$, $j = 1, \dots, 4$, represent the boundary functions of \mathcal{S}_i and are defined as

$$\begin{aligned} g_1(\tilde{x}_{i-1}, \tilde{x}_i) &= \tilde{s}_{i-1} - \tilde{s}_i - l_{i-1} - \frac{\tilde{v}_{i-1}^2}{2\underline{a}_{\min,i-1}} + \frac{\tilde{v}_i^2}{2\bar{a}_{\min,i}}, \\ g_2(\tilde{x}_{i-1}, \tilde{x}_i) &= \tilde{s}_{i-1} - \tilde{s}_i - l_{i-1}, \\ g_3(\tilde{x}_{i-1}, \tilde{x}_i) &= \tilde{v}_{i-1}, \\ g_4(\tilde{x}_{i-1}, \tilde{x}_i) &= \tilde{v}_i. \end{aligned} \quad (5.39)$$

We now state and prove the following result:

Lemma 1. Given the dynamical system (5.32) and the constraints (5.34a) and (5.34b) on the exogenous and control inputs respectively, there exists a con-

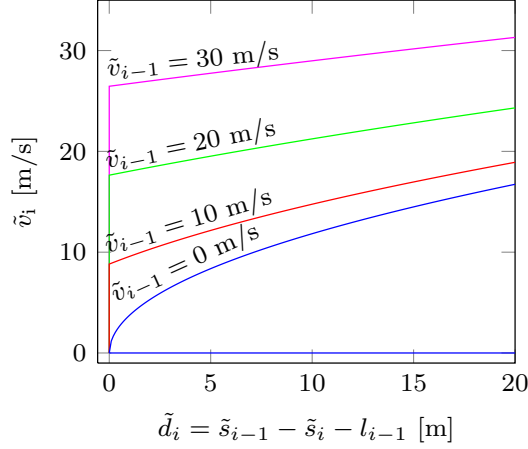


Figure 5.5: Projection of the boundary $\partial\mathcal{S}_i$ of the safety set $\mathcal{S}_i \subseteq \tilde{\mathcal{X}}$ on the $(\tilde{d}_i, \tilde{v}_i)$ plane for $\tilde{v}_{i-1} = 0, 10, 20, 30$ m/s. The variable \tilde{d}_i denotes the distance between the two adjacent vehicles. The bounds on the minimum braking acceleration has been chosen such that $\underline{a}_{\min, i-1} < \bar{a}_{\min, i}$.

trol law $\tilde{a}_i = \varphi([\tilde{x}_{i-1}^T, \tilde{x}_i^T]^T) \in \mathcal{A}^f(\tilde{x}_i)$ such that for all $[\tilde{x}_{i-1}^T(t_0), \tilde{x}_i^T(t_0)]^T \in \mathcal{S}_i$ and $\tilde{a}_{i-1} \in \mathcal{A}^p(\tilde{x}_{i-1})$, the condition $[\tilde{x}_{i-1}^T(t), \tilde{x}_i^T(t)]^T \in \mathcal{S}_i$ holds for all $t \geq t_0$.

In other words, \mathcal{S}_i is a robust controlled invariant set (Blanchini, 1999).

Proof. By using Nagumo's theorem for robust controlled invariant sets (Blanchini, 1999), the lemma can be proven by showing that for all $[\tilde{x}_{i-1}^T, \tilde{x}_i^T]^T \in \partial\mathcal{S}_i$ (defined as the boundary of \mathcal{S}_i), there exists an $\tilde{a}_i \in \mathcal{A}^f$ such that, for all $\tilde{a}_{i-1} \in \mathcal{A}^p$, the relation

$$\nabla g_j(\tilde{x}_{i-1}, \tilde{x}_i)^T F(\tilde{x}_i, \tilde{x}_{i-1}, \tilde{a}_{i-1}, \tilde{a}_i) \geq 0 \quad (5.40)$$

holds for all j such that $g_j(\tilde{x}_{i-1}, \tilde{x}_i) = 0$. Because of the structure of the problem, the control input \tilde{a}_i is chosen as maximum braking, i.e.,

$$\tilde{a}_i = \begin{cases} \bar{a}_{\min, i}, & \text{if } \tilde{v}_i > 0, \\ 0, & \text{if } \tilde{v}_i = 0, \end{cases} \quad (5.41)$$

for any $[\tilde{x}_{i-1}^T, \tilde{x}_i^T]^T \in \partial\mathcal{S}_i$ and $\tilde{a}_{i-1} \in \mathcal{A}^p(\tilde{x}_{i-1})$. We organize the proof by considering the $[\tilde{x}_{i-1}^T, \tilde{x}_i^T]^T \in \partial\tilde{\mathcal{S}}_i$ defined by the activation of each $g_j(\tilde{x}_{i-1}, \tilde{x}_i) \geq 0$:

- for $[\tilde{x}_{i-1}^T, \tilde{x}_i^T]^T$ such that $g_1(\tilde{x}_{i-1}, \tilde{x}_i) = 0$, and $g_j(\tilde{x}_{i-1}, \tilde{x}_i) \geq 0$, for $j \in \{2, 3, 4\}$,

$$\begin{aligned} \nabla g_1(\tilde{x}_{i-1}, \tilde{x}_i)^\top F(\tilde{x}_{i-1}, \tilde{x}_i, \tilde{a}_{i-1}, \tilde{a}_i) &= \left(1 - \frac{\tilde{a}_{i-1}}{\underline{a}_{\min, i-1}}\right) \tilde{v}_{i-1} - \left(1 - \frac{\tilde{a}_i}{\bar{a}_{\min, i}}\right) \tilde{v}_i, \\ &= \left(1 - \frac{\tilde{a}_{i-1}}{\underline{a}_{\min, i-1}}\right) \tilde{v}_{i-1} \geq 0, \end{aligned}$$

where the equality and inequality hold because of the definition of \tilde{a}_i in (5.41) and $g_3(\tilde{x}_{i-1}, \tilde{x}_i) \geq 0$.

- for $[\tilde{x}_{i-1}^\top, \tilde{x}_i^\top]^\top$ such that $g_2(\tilde{x}_{i-1}, \tilde{x}_i) = 0$, and $g_j(\tilde{x}_{i-1}, \tilde{x}_i) \geq 0$, for $j \in \{1, 3, 4\}$,

$$\nabla g_2(\tilde{x}_{i-1}, \tilde{x}_i)^\top F(\tilde{x}_{i-1}, \tilde{x}_i, \tilde{a}_{i-1}, \tilde{a}_i) = \tilde{v}_{i-1} - \tilde{v}_i \geq 0,$$

where the inequality holds by noticing that the combination of $g_1(\tilde{x}_{i-1}, \tilde{x}_i) \geq 0$, $g_2(\tilde{x}_{i-1}, \tilde{x}_i) = 0$ and the relation (5.37a) gives $\tilde{v}_{i-1} \geq (\underline{a}_{\min, i} / \bar{a}_{\min, i}) \tilde{v}_i$.

- for $[\tilde{x}_{i-1}^\top, \tilde{x}_i^\top]^\top$ such that $g_3(\tilde{x}_{i-1}, \tilde{x}_i) = 0$, and $g_j(\tilde{x}_{i-1}, \tilde{x}_i) \geq 0$, for $j \in \{1, 2, 4\}$,

$$\nabla g_3(\tilde{x}_{i-1}, \tilde{x}_i)^\top F(\tilde{x}_{i-1}, \tilde{x}_i, \tilde{a}_{i-1}, \tilde{a}_i) = \tilde{a}_{i-1} \geq 0,$$

where the inequality holds because of (5.34a). The same can be verified in a similar way for $[\tilde{x}_{i-1}^\top, \tilde{x}_i^\top]^\top$ such that $g_4(\tilde{x}_{i-1}, \tilde{x}_i) = 0$ and $g_j(\tilde{x}_{i-1}, \tilde{x}_i) \geq 0$ for $j \in \{1, 2, 4\}$. \square

The choice of the safety set guarantees that the following vehicle can react to the emergency braking maneuver of its predecessor, such that both vehicles come to a standstill without colliding. We now extend the result in Lemma 1 to the safety of the whole platoon. More precisely, we prove that whatever a vehicle does, there exists an input for all the following vehicles, such that collision can be avoided. This is formalized by the following theorem:

Theorem 1. Consider a vehicle with index $i_0 < N_v$ and all its following vehicles $i \in \mathcal{I} = \{i_0 + 1, \dots, N_v\}$ satisfying the dynamics in (5.31). Then, there exists a control law $\tilde{a}_i = \varphi(\tilde{x}_i, \tilde{x}_{i-1}) \in \mathcal{A}^f(\tilde{x}_i)$, $i \in \mathcal{I}$ such that for all $[\tilde{x}_{i-1}^\top(t_0), \tilde{x}_i^\top(t_0)]^\top \in \mathcal{S}_i$ and $\tilde{a}_{i_0} \in \mathcal{A}^p(\tilde{x}_{i_0})$, the condition $[\tilde{x}_{i-1}^\top(t), \tilde{x}_i^\top(t)]^\top \in \mathcal{S}_i$ holds for all $t \geq t_0$ and all $i \in \mathcal{I}$.

Proof. The application of Lemma 1 for $i = i_0 + 1$ proves the existence of an input $\tilde{a}_i \in \mathcal{A}^f(\tilde{x}_i)$ that ensures that $[\tilde{x}_{i-1}^\top(t), \tilde{x}_i^\top(t)]^\top \in \mathcal{S}_i$ for all $t \geq t_0$. Then, by noting that $\mathcal{A}^f(\tilde{x}_i) \subseteq \mathcal{A}^p(\tilde{x}_i)$ according to (5.37), it follows that $\tilde{a}_i \in \mathcal{A}^p(\tilde{x}_i)$. The theorem is then proven by induction over the vehicle index, hereby repetitively applying Lemma 1. \square

This result is adapted to the MPC formulation in order to take communication delays and the discretized nature of MPC into account. In detail, at each time t_j along the prediction, we have access to the preceding vehicle real state at time t_{j-1} (according to the assumption of maximum delay in vehicle to vehicle communication and radar measurements of Δt_{MPC}). Furthermore, at each time t_j along the prediction, we want to ensure that the predicted state at time t_{j+1} (that will be the current one in the next MPC iteration) is safe. According to these considerations, we can translate the safety set \mathcal{S}_i into the following safety constraints on each following vehicle state:

$$s_i(t_{j+1}|t_k) - \frac{v_i^2(t_{j+1}|t_k)}{2\bar{a}_{\min,i}} \leq \hat{s}_{i-1}(t_{j-1}|t_k) - \frac{\hat{v}_{i-1}^2(t_{j-1}|t_k)}{2\underline{a}_{\min,i-1}} - l_{i-1}, \quad (5.45a)$$

$$s_i(t_{j+1}|t_k) \leq \hat{s}_{i-1}(t_{j-1}|t_k) - l_{i-1}, \quad (5.45b)$$

for $i = 2, \dots, N_v$. The constraints (5.45a) and (5.45b) correspond to the boundaries of \mathcal{S}_i characterized by g_1 and g_2 , respectively, as defined in equation (5.39). The constraints corresponding to g_3 and g_4 have been here omitted since they require the vehicles to drive in the forward direction, which is true by assumption. Note that the constraint (5.45b) is not necessary if the bounds on the minimum braking acceleration of contiguous vehicles satisfies the constraint $\underline{a}_{\min,i-1} \leq \bar{a}_{\min,i}$ (this is the case, for example, when the platooning vehicles have the same maximum braking capability, i.e., $F_{b,\min,i} = F_{b,\min}$ for all i). In this case, in fact, the vehicle dynamics (5.31) and the definition of the safety set (5.38)–(5.39) prohibit reaching the boundary characterized by g_2 (see Figure 5.5). Finally we remark that, for safety purpose, only the safety constraints for $j = k$ is necessary. In fact it guarantees that, if at the update time t_k the current state of each following vehicle is safe, then it is going to be safe also at the update time t_{k+1} . However, the safety constraints for $j > k$ give optimal trajectories that are safe over the whole horizon and therefore produce a more fuel-efficient behavior of the platoon. In the MPC formulation, we refer to the safety constraints (5.45a)–(5.45b) as $f_{\text{safe}}(x_i(t_{j+1}|t_k), \hat{x}_{i-1}(t_{j-1}|t_k)) \geq 0$.

Remark 5.3.1. Here, the safety constraint has been considered only for following vehicles. However, note that in case of a moderately-congested traffic scenario, if a prediction of the future trajectory of the vehicles preceding the platoon (e.g., by using a traffic model) is available, the safety constraint can be also introduced in the lead vehicle controller. This would allow to fuel-efficiently follow the external traffic.

5.3.4 Cost function

The objective of the vehicle control layer is to follow the reference speed trajectory and the gap policy defined by the platoon coordinator, while avoiding unnecessary

braking. This is formulated by the following cost function:

$$\begin{aligned}
 J_{\text{MPC}}(a_i(\cdot, t_k), \varepsilon_i(t_k)) = & \sum_{j=k}^{k+N_{\text{MPC}}-1} \|x_i(t_j|t_k) - \hat{x}_{i-1}(t_{j-T_i}|t_k)\|_{(1-\zeta_i)Q}^2 \\
 & + \|a_i(t_j|t_k) - \hat{a}_{i-1}(t_{j-T_i}|t_k)\|_{(1-\zeta_i)R}^2 \\
 & + \|x_i(t_j|t_k) - \bar{x}_i(t_j|t_k)\|_{\zeta_i Q}^2 \\
 & + \|a_i(t_j|t_k) - \bar{a}_i(t_j|t_k)\|_{\zeta_i R}^2 \\
 & + \|\varepsilon_i(t_k)\|_P^2,
 \end{aligned} \tag{5.46}$$

where

$$\zeta_i = \begin{cases} 1, & \text{if } i = 1, \\ \bar{\zeta} \in [0, 1], & \text{if } i = 2, \dots, N_v, \end{cases} \tag{5.47}$$

T_i represents the discretized version of the time gap τ_i (i.e., $T_i = \lfloor \tau_i / \Delta t_{\text{MPC}} \rfloor$) and the notation $\|\cdot\|_S$ is defined as $\|x\|_S^2 = x^T S x$. In detail, the first and second terms in (5.46) penalize the deviation of the predicted state and input trajectories from the delayed assumed trajectories of the preceding vehicle. The third and fourth terms penalize the deviation of the predicted state and input trajectories from the reference ones. Here, the parameter $\bar{\zeta}$ defines the trade-off between the tracking of the reference trajectories and the gap policy. The fifth term penalizes the slack variable associated to the soft constraint on braking action (5.28a). The weights Q , R and P are chosen in order to reach a good balance between the tracking of the state and input trajectories and actuator excitation. In particular, P is chosen relatively large such that only the activation of the safety constraint $f_{\text{safe}}(x_i(t_{j+1}|t_k), \hat{x}_{i-1}(t_{j-1}|t_k)) \geq 0$ can require a significant braking force. This ensures the fuel-efficient and safe tracking of the reference trajectories.

By penalizing both the deviations from the reference trajectories and from the constant time gap policy, we aim at reaching a good attenuation of disturbances along the platoon. Rigorously guaranteeing string stability in distributed model predictive control settings is challenging as such controllers result in control laws that are nonlinear. However, if the perturbations are small enough such that the model predictive control constraints do not activate, the controller behaves as a linear-quadratic (LQ) regulator. This allows to exploit the extensive research on string stability based on transfer function analysis and apply it to our formulation. If $\bar{\zeta} = 0$, all vehicles but the leader only track the time gap to the preceding vehicle. In the case of perfect tracking, as discussed in Besselink and Johansson (2017), this leads to a marginally string stable scenario where perturbations do not amplify or attenuate along the platoon. On the other hand, if $\bar{\zeta} = 1$, each vehicle tracks the same reference trajectory and completely ignores what the preceding vehicle is doing. That means that perturbations will completely die after one vehicle. Here, we argue

that by correctly choosing $\bar{\zeta}$, it is possible to successfully achieve the attenuation of disturbances along the platoon.

5.3.5 Model predictive control formulation

Combining the vehicle model, the input/state constraints, the safety constraint and the cost function, the MPC problem can be formulated as:

$$\underset{a_i(\cdot|t_k)}{\text{minimize}} \quad J_{\text{MPC}}(a_i(\cdot|t_k), \varepsilon_i(t_k)) \quad (5.48a)$$

$$\text{subj. to} \quad x_i(t_{j+1}|t_k) = Ax_i(t_j|t_k) + Ba_i(t_j|t_k), \quad (5.48b)$$

$$a_i(t_j|t_k) \geq a_{\min,i}(x_i(t_j|t_k), \hat{x}_{i-1}(t_j|t_k)), \quad (5.48c)$$

$$a_i(t_j|t_k) \leq a_{\max,i}(x_i(t_j|t_k), \hat{x}_{i-1}(t_j|t_k)), \quad (5.48d)$$

$$a_i(t_j|t_k) + \varepsilon_i(t_k) \geq \min(a_{\text{coast},i}(x_i(t_j|t_k), \hat{x}_{i-1}(t_j|t_k)), \bar{a}_i(t_j|t_k)), \quad (5.48e)$$

$$v_{\min}(s_i(t_j|t_k)) \leq v_i(t_j|t_k) \leq v_{\max}(s_i(t_j|t_k)), \quad (5.48f)$$

$$f_{\text{safe}}(x_i(t_{j+1}|t_k), \hat{x}_{i-1}(t_{j-1}|t_k)) \geq 0, \text{ if } i \geq 2, \quad (5.48g)$$

$$\varepsilon_i(t_k) \geq 0, \quad (5.48h)$$

$$x_i(t_k|t_k) = x_i(t), \quad (5.48i)$$

for $j = k, \dots, k + N_{\text{MPC}} - 1$, where equation (5.48i) represents the initial condition of the MPC problem. In our implementation, we have replaced the time-dependent predicted state $x_i(t_j|t_k)$ in constraints (5.48c)–(5.48f) with the assumed state $\hat{x}_i(t_j|t_k)$, transforming those non-linear constraints in linear constraints. The modification allows to recast the MPC problem into a quadratic constraint quadratic programming (QCQP) problem for which efficient solvers exist.

The output of the vehicle controller are the desired acceleration $a_i^*(t_k)$ defined as $a_i^*(t_k) = a_i^*(t_k|t_k)$, where $a_i^*(\cdot|t_k)$ is the optimal input trajectory, and a boolean variable b_i defined as

$$b_i(t_k) = \begin{cases} 1, & \text{if } a_i^*(t_k) < a_{\text{coast},i}(x_i(t_k|t_k), \hat{x}_{i-1}(t_k|t_k)), \\ 0, & \text{if } a_i^*(t_k) \geq a_{\text{coast},i}(x_i(t_k|t_k), \hat{x}_{i-1}(t_k|t_k)), \end{cases} \quad (5.49)$$

that indicates if the desired acceleration defines a traction or braking force. According to such variable, the acceleration will be either tracked by the braking management system or the engine and gear management systems presented in Section 3.3 and displayed in Figure 3.6.

5.4 Evaluation of the platoon coordinator

In this section, we evaluate the performance of the platoon coordinator presented in Section 5.2. In this analysis, we compare the fuel and energy consumption of a

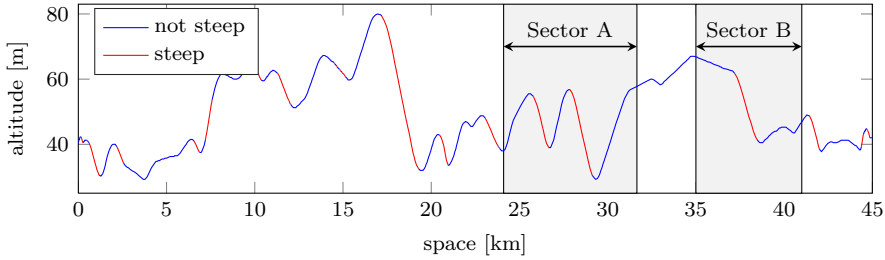


Figure 5.6: Road topography of the 45 km highway stretch between the Swedish cities of Mariefred and Eskilstuna. The red color highlights the uphill and downhill sections for which the slope is too steep for a vehicle of 40 tonnes with a 400 hp engine to maintain a constant speed of 21.5 m/s without exceeding the maximum engine power and without braking.

platoon under multiple control strategies. To make the analysis independent from the low-level tracking strategy, in this section we assume that the vehicles follow exactly the speed trajectories and spacing policies defined by the high-level controllers.

5.4.1 Experiment setup

The comparison is done by using as a benchmark the same road scenario introduced in Section 4.1. We therefore consider a platoon of two heavy-duty vehicles driving over the 45 km road stretch between the Swedish cities of Mariefred and Eskilstuna. In Figure 5.6 we reproduce the road topography for this road stretch, where the red color highlights the uphill and downhill sections for which the slope is too large for a heavy-duty vehicle of 40 tonnes and engine power of 400 hp, as used in the simulation, to maintain a constant speed of 22 m/s without exceeding the engine power limit and without braking. Due to the reduced engine power of the vehicles used in the simulation compared to the experimental ones, some uphill sections that do not allow the vehicles to maintain the constant reference speed have been identified. For the considered road, the steep sections represent 23% of the total length. The controller performance is investigated for both homogeneous and heterogeneous platoons. The performance metrics chosen to compare the different control configurations are the energy and the fuel consumed by the vehicles. In some comparisons, the consumed energy is preferred over the consumed fuel because it can be directly related to the energies dissipated by the various forces, i.e., gravitational, rolling, drag and braking forces. Similarly to what has been done in the motivational experiment analysis of Section 4.1, the simulated braking, gravitational, rolling and aerodynamic forces have been integrated over space according to

$$E_{\square,i} = \int_0^{S_{\text{sim}}} F_{\square,i}^{\text{s}}(s) ds \quad (5.50)$$

to obtain the energy consumption associated with each force. Here, $S_{\text{sim}} = 45$ km denotes the simulation space horizon, while the placeholder \square represents the subindexes b, g, r and d. The total energy consumption E_i is defined according to equation (4.2). The total Ψ_i fuel consumption of vehicle i , instead, is computed according to

$$\Psi_i = \int_0^{S_{\text{sim}}} q_i(F_{t,i}^s(s)v_i(d)) / v_i^s(s) ds, \quad (5.51)$$

where $q_i(\cdot)$ represents the simplified fuel model defined in equation (5.11).

The control configurations considered in the comparisons include three control strategies and three gap policies. In detail, the following control strategies for the first vehicle are considered:

- Cruise control (CC). The first vehicle keeps the constant reference speed v_{CC} on low-grade slopes. If the uphill slope is too large to maintain constant speed, the engine generates the maximum power $P_{\text{max},1}$ until the speed reaches v_{CC} again. If the downhill slope is too large to maintain constant speed without braking, the engine coasts (i.e., does not inject any fuel, generating therefore the minimum power $P_{\text{min},1}$) until the speed reaches v_{CC} again. However, if the vehicle reaches the speed limit v_{max} , the brakes are activated in order not to overcome it.
- Look-ahead control (LAC). The first vehicle exploits the slope information of the road ahead in order to minimize its own fuel consumption. This is implemented using a similar framework of the platoon coordinator where the presence of following vehicle is ignored, i.e., $N_v = 1$.
- Cooperative look-ahead control (CLAC). The first vehicle follows the speed profile generated by the proposed platoon coordinator.

The following gap policies are considered:

- Space-gap policy. The second vehicle keeps a constant distance d_{SG} from the first vehicle.
- Headway-gap policy. The second vehicle keeps a constant headway time τ_{HG} from the first vehicle, i.e., it keeps a distance proportional to its speed ($d_{\text{HG}}(t) = \tau_{\text{HG}}v_i(t)$).
- Time-gap policy. The second vehicle keeps a constant time gap τ_{TG} from the first vehicle according to (5.1).

The combination of CLAC and the time-gap policy represents the proposed platoon coordinator. In order to be able to maintain exactly the desired gap policies as previously assumed, the second vehicle is allowed to overcome the theoretical maximum engine power $P_{\text{max},2}$ and to brake if necessary. In addition, in order

Table 5.1: Vehicle parameters.

m_i	vehicle masses	t	40
l_i	vehicle length	m	18
$c_{r,i}$	rolling coefficient	-	0.003
A_v	cross-sectional vehicle area	m ²	10
$C_{d,0}$	nominal drag coefficient	-	0.6
$C_{d,1}$	first drag reduction coefficient	m ⁻¹	12.8
$C_{d,2}$	second drag reduction coefficient	m	19.7
$P_{\min,i}$	minimum engine power	kW	-9
$P_{\max,i}$	maximum engine power	kW	298

to obtain a fair comparison it is ensured, by tuning the trade-off parameter β of the LAC and CLAC formulations (see definition (5.16)), that the different control strategies have the same average speed \bar{v} and the parameters d_{SG} , τ_{HG} and τ_{TG} are chosen such that the vehicles in the different gap policies have the same distance when driving at constant speed \bar{v} (i.e., $d_{SG} = \bar{v}\tau_{HG} = \bar{v}\tau_{TG} - l_1$). Furthermore, in order to remove the influence of the residual kinematic energy, the initial and final speeds are constrained to be the same in all the controller configurations.

5.4.2 Control strategies comparison

In this section, we present the results of the platoon behavior for the three different control strategies, while keeping a time-gap policy (with $\tau_{TG} = 1.4$ s). In the first part, as in the motivational experiment of Section 4.1, we focus on the homogeneous platoon scenario, while in the second part we consider two heterogeneous platoons (i.e., platoons where the second vehicle is respectively heavier and lighter than the leading one).

We now consider a platoon of two identical vehicles, whose parameters values are displayed in Table 5.1. We start the comparison by analyzing the comprehensive bar diagram displayed in Figure 5.7 representing the energy consumed by each vehicle of the platoon for the three control strategies (the corresponding fuel consumption is displayed in the middle column of Table 5.2). These energies are normalized with respect to the energy consumed by a single vehicle driving alone using CC. The consumed energy is additionally split into the components representing the energies dissipated by the braking, gravitational, rolling and aerodynamic forces. We can first notice how the second vehicle, for all the control strategies, consumes less energy compared to the first one, due to the significant reduction of the energy associated with the drag force. Second, comparing the three control strategies, we can observe how the use of the LAC allows both vehicles to save energy, respectively 3.5% and 6.4% compared to the use of the CC. Instead, by switching from the LAC to the

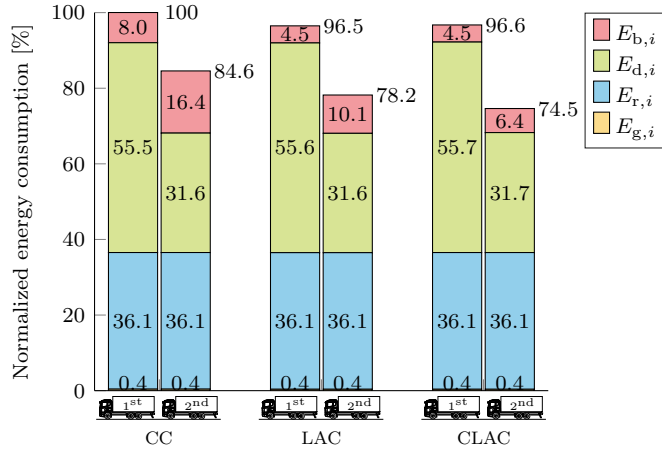


Figure 5.7: Normalized energy consumption of the platooning vehicles divided into the different components, i.e., energies associated with the gravitational, rolling, aerodynamic and braking forces. Both vehicles have a mass of 40 tonnes. In the three simulated scenarios the first vehicle relies on CC, LAC and CLAC, respectively. The second vehicle tracks a constant time-gap.

CLAC, the first vehicle consumes 0.1% more energy, while the second one saves 3.7% of energy; therefore the platoon, given by the combination of the two vehicles, overall saves 3.6% of energy with respect to the use of LAC. This result is in line with our expectation, since the LAC optimizes the fuel consumption of the first vehicle, while the CLAC targets the reduction of the fuel consumption of the entire platoon. Consequently, the savings of the CLAC strategy with respect to the LAC strategy are expected to increase for platoons of more than two vehicles. Going into the details of the various consumed energy components, first, we notice that the gravitational and rolling energy components are the same for both vehicles for all the considered control strategies. This is due to the fact that the energy associated with the gravitational force depends only on the difference of altitude between the initial and final points, while the rolling energy only depends on the driven distance, that is the same by experiment design specification. The drag energy, instead, is significantly different for the two vehicles because of its dependence on the distance to the preceding vehicle, while it is approximately the same for the different control strategies. What significantly changes between the different control strategies is the energy dissipated by braking, denoted by $E_{b,i}$ in Figure 5.7.

In order to understand the role of the control strategies in the braking usage in Figure 5.8 we show part of the simulation results corresponding to the road highlighted as Sector B in Figure 5.6. In this study, we have chosen to focus on a downhill section because this is where the braking action for the CLAC case is taking place. The comparison of the platoon behaviors follows:

- CC: during the downhill, starting from speed v_{CC} , the first vehicle accelerates while coasting due to the large road grade. In the meantime the second vehicle has to brake slightly in order to maintain the time gap and compensate the reduced drag force compared to the first vehicle. At 38.1 km, in order not to overcome the speed limit, both vehicles need to brake significantly.
- LAC: by exploiting the topography information of the road ahead, the first vehicle reduces its speed before the downhill by anticipating the coasting phase such that the speed limit is reached only when the slope grade is small enough to stop accelerating while coasting and therefore it avoids braking. The second vehicle, as in the CC case, has to brake slightly while the first vehicle is coasting but it also avoids the significant braking phase at the end of the downhill.
- CLAC: since in this case the optimization is done considering the fuel consumption of both vehicles, with respect to the LAC case the first vehicle starts to lose speed earlier before the downhill. This allows it to slightly throttle during the downhill, allowing the second vehicle to coast meanwhile and, as in the LAC case, to reach the speed limit only when the slope grade is small enough to stop accelerating while coasting. In this case both vehicles, do not need to brake.

Note that, in the case of longer downhill segments, the lower speed bound does not allow the vehicle to decrease the speed enough before the downhill in order not to hit the upper speed limit during the downhill. This is why in some sections of the 45km benchmark road, in the LAC case, the first vehicle and, in the CLAC case, both vehicles still need to brake.

So far we have considered the case of a homogeneous platoon. What we will investigate in the remainder of the subsection is the role of the different control strategies in the case of heterogeneous platoons. In Table 5.2 we have reported the normalized fuel consumption for the cases of two heterogeneous platoons and the same homogeneous platoon previously considered. More in detail, the vehicles have the same powertrain, but their masses vary between 35, 40 and 45 tonnes. Analyzing the table we can notice how in the case of a heavier second vehicle the CLAC allows to save 10.8% of fuel compared to the CC, while, in the case of a lighter second vehicle, it allows to save 5.4%. However if we only analyze the last row we can note how, with the use of the CLAC, the order of the vehicles does not significantly change the normalized fuel consumption. Note that this is not the case in the LAC strategy.

Concluding, the proposed controller (CLAC combined with the time-gap policy) has a significant impact on the reduction of the energy and fuel consumption. In detail, the majority of the fuel saving is related to the reduction of energy dissipated

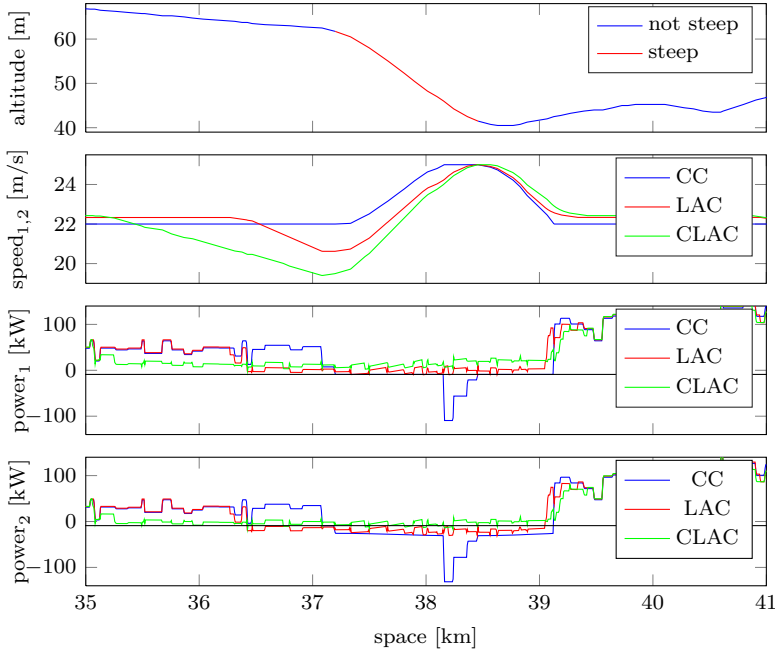





Figure 5.8: Comparison of the behavior of a homogeneous platoon (i.e., $m_1 = m_2 = 40$ t) for three different control strategies, namely CC, LAC and CLAC, while keeping a time-gap policy and driving over the Sector B displayed in Figure 5.6. The first plot shows the road altitude; the second plot shows the speed profiles for the three control strategies followed by both vehicles (because of the time-gap policy, the platooning vehicles follow the same speed profile in the spatial domain); finally the third and fourth plots show the summation between the generated power by the engine and the braking systems for the two vehicles and three control strategies; the black lines in such plots define the theoretical minimum and maximum engine power, respectively $P_{\min,i}$ and $P_{\max,i}$ (hence if the power crosses the lower power limit $P_{\min,i}$, the corresponding vehicle is braking).

Table 5.2: Normalized fuel consumption (in %) of the vehicles in the platoon for different control strategies and scenarios (vehicle weights). The fuel is normalized with respect to the fuel consumed by the corresponding vehicle driving alone using CC.

						
mass	35 t	45 t	40 t	40 t	45 t	35 t
CC	100.0	90.2	100.0	86.3	100.0	82.1
LAC	97.6	84.9	96.9	80.6	96.3	77.2
CLAC	97.8	78.0	97.0	77.4	96.4	76.7

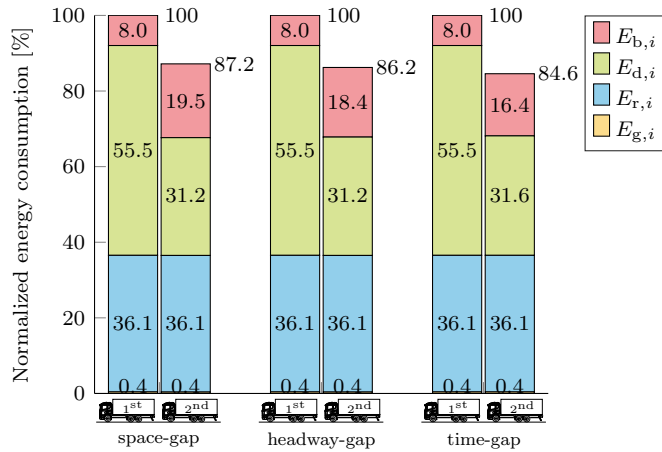


Figure 5.9: Normalized energy consumption of the platooning vehicles divided into the different components, i.e., energies associated with the gravitational, rolling, aerodynamic and braking forces. Both vehicles have a mass of 40 tonnes. In the three simulated scenarios the first vehicle relies on CLAC. The second vehicle tracks a space-gap, a headway-gap and a time-gap, respectively.

by braking during the downhill sections. The impact of such a controller grows in the case of a heavier following vehicle.

5.4.3 Gap policies comparison

In this subsection, we compare the platoon performance for different gap policies, namely a constant space-gap, headway-gap, and time-gap. while the first vehicle keeps the same control strategy (in the analysis we have chosen CC). Note that in order to be able to follow the required gap policy the second vehicle is allowed to

exceed the maximum engine power. In this section, we only focus on the homogeneous platoon, since the results for a heterogeneous platoon are qualitatively the same. In Figure 5.9 we show the comprehensive bar diagram representing the normalized energy consumed by each vehicle in the platoon for the three gap policies, while using CC as a control strategy. Since the first vehicle uses the same control strategy, the energy consumption differs only for the second vehicle. It is interesting to notice that, similar to the comparisons done in the previous section, the main difference between the energy consumption of the second vehicle is related to the energy dissipated by braking. More in detail the headway-gap policy allows the second vehicle to save 1% over the space-gap policy, while the time-gap policy allows to save an additional 1.6% of energy. In order to understand the role of the gap policy on the braking energy, we show the platoon behavior driving over a synthetic hill composed by an uphill section with constant slope grade, a flat section and a downhill section with constant slope grade. The platoon behavior for such a hill is shown in Figure 5.10. Analyzing the second vehicle behavior for each gap policy, the following can be observed:

- time-gap policy: as argued in Section 4.2, the time gap allows the vehicles to follow the same speed profile over space. That means that the generated forces and therefore the generated powers (because of the equal speed result) are equivalent except for a reduction of the air drag component in the second vehicle. Therefore the power generated by the second vehicle, as can be observed in Figure 5.10, is approximately a biased equivalent of the one generated by the first vehicle. As a result, the second vehicle complies with the limitation on maximum engine power.
- space-gap policy: the space gap requires the vehicles to follow the same speed profile over time. An interesting consequence can be observed, for example, at the beginning of the uphill section shown in Figure 5.10; as soon as the first vehicle enters the uphill section and decelerates because of limited engine power, the second vehicle, which is still in the flat section, has to brake in order to respect the space gap requirement. In general, excluding the offset given by the drag power, every time the slope increases (in Figure 5.10, entering the uphill and leaving the downhill sections), the second vehicle has to generate less power than the first vehicle, while every time the slope decreases (in Figure 5.10, leaving the uphill and entering the downhill sections) the second vehicle has to generate more power than the first vehicle. As a consequence, the second vehicle has respectively to brake and to exceed the power limit in order to follow the required space-gap policy.
- headway-gap policy: the headway gap can be considered as a trade-off between a time gap and a space gap. In fact, for example, as soon as the first vehicle enters the uphill section and starts to decelerate, the distance between the two

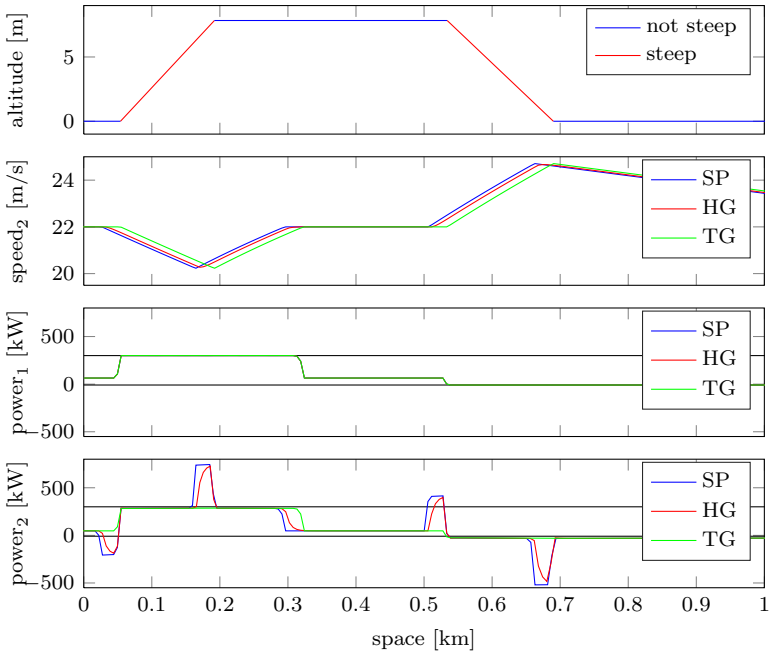


Figure 5.10: Comparison of the behavior of a homogeneous platoon (i.e., $m_1 = m_2 = 40$ t) for three different gap policies, namely space, headway and time-gap policies, while using CC as a control strategy and driving over a synthetic hill. For the plots explanation refer to the caption of Figure 5.8; note that the second plot shows only the speed trajectories of the second vehicle (the speed trajectory of the first vehicle coincides with the one of the second vehicle in the case of time-gap policy).




vehicles is allowed to decrease, but this decrease is not as fast as in the case of the time gap. This has been experienced in the motivational experiment while the platoon was driving along Segment 1 of Figure 4.3.

In conclusion, the time gap allows to save more energy compared to the space and headway gaps. In addition, the time gap allows all the vehicles to follow the same space-defined speed trajectory and, therefore, it scales well with the number of vehicles in the platoon. This is not the case when using a space or headway-gap policy. The complete results for the normalized fuel consumption are reported in Table 5.3.

5.5 Evaluation of the vehicle control layer

In this section, we evaluate the performance of the vehicle control layer presented in Section 5.2. The evaluation is divided into two parts. First, we test the functioning of

Table 5.3: Normalized fuel consumption (in %) of the vehicles in the platoon for different control strategies and gap policies. The fuel is normalized respect to the fuel consumed by the corresponding vehicle driving alone using CC.

	 space-gap		 headway-gap		 time-gap	
CC	100.0	88.6	100.0	87.7	100.0	86.3
LAC	96.9	82.7	96.9	81.9	96.9	80.6
CLAC	97.0	80.4	97.0	79.3	97.0	77.4

the distributed safety constraints by simulating multiple braking actions of the lead vehicle and observing how the platoon reacts. Second, we analyze how disturbances propagate along the platoon for various values of the trade-off parameter $\bar{\zeta}$. The simulated vehicles are identical with parameters' values defined in Table 5.1. The parameter of the MPC formulation are displayed in the second half of Table 5.4.

5.5.1 Safety analysis

The testing of the vehicle controller safety functionality is carried by studying the reaction of a three-vehicle platoon driving on a flat road to multiple braking profiles of the leading vehicle as displayed in Figure 5.11 and Figure 5.12. The braking actions are unplanned and, therefore, are not communicated to the following vehicles in advance.

In Figure 5.11, the leading vehicle brakes with a deceleration of 1, 2 and 3 m/s² for 0.9 s at the time instances 5, 25 and 55 s, respectively. In the second plot of this figure, the effective distances and the ones that would activate the safety constraint (we will refer to it as the safety distance) are shown. First, we can notice how, in line with our expectation, the second and third vehicles are braking (see the third plot) only when the effective distance touches the safety distance. In fact, here we recall that, according to how the vehicle controller is designed (see Section 5.3.5), only the activation of the safety constraint or a braking request from the platoon coordinator can lead to a significant braking action. Consequently, during the first braking instance of 1 m/s², both following vehicles do not brake, despite the deviation of their states from the reference trajectories. During the second braking of 2 m/s², instead, the safety constraint of the second vehicle is activated and therefore it requires a braking action. Finally, during the third braking of 3 m/s², the safety constraints of both following vehicles activate and therefore they both brake. Note that the safety constraint is designed such that fuel-efficiency has priority on driver comfort. In fact, in this case, in order to be fuel-efficient, the braking action is required only when the platoon is in a safety critical situation.

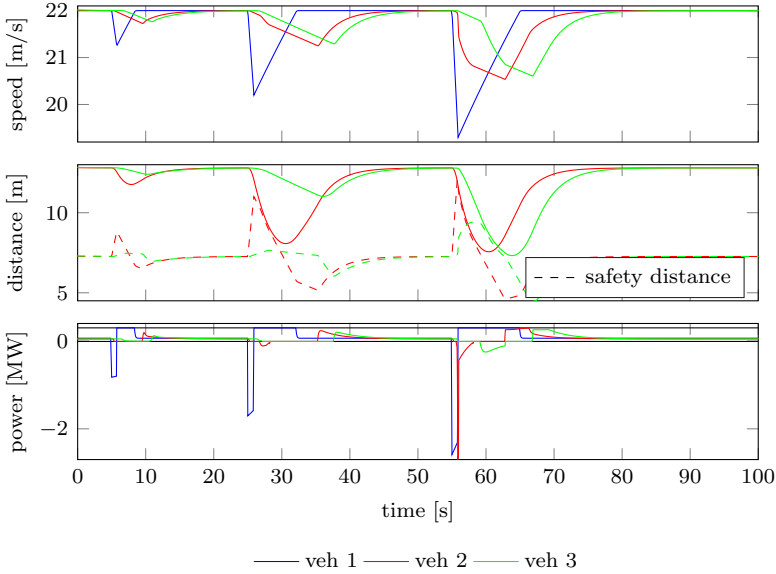


Figure 5.11: Behavior of a three identical vehicles platoon driving on a flat road. The leading vehicle brakes three times at 5, 25 and 55 s, with a braking deceleration of respectively 1, 2 and 3 m/s^2 for 0.9 s. The first plot shows the speed of the three vehicles. The second plot shows the distance between the vehicles and the corresponding safety distance computed using an adaptation of inequality (5.45). The third plot shows the summation between the generated power by the engine and the braking systems of the vehicles.

In Figure 5.12, we consider a more challenging scenario in which the first vehicle brakes with higher intensity, simulating an emergency situation. More precisely, it brakes at 5 s with a deceleration of 7 m/s^2 for 1 s and at 30 s with the same deceleration until it arrives at full-stop. We can notice how, also in this scenario, the safety constraint in each vehicle controller activates the braking action and guarantees that no collision occurs between the vehicles.

5.5.2 Disturbance propagation analysis

Here, we analyze the capability of the vehicle control layer to attenuate disturbances along the platoon. We test the reaction of a four-vehicle platoon driving on a flat road to a small disturbance acting on the lead vehicle. As the model predictive control constraints do not activate, the controller behaves similar to an LQ controller. The platoon behavior is tested for multiple values of $\bar{\zeta}$ that represents the trade-off between the preceding vehicle following and the reference trajectory tracking in the cost function (5.46).

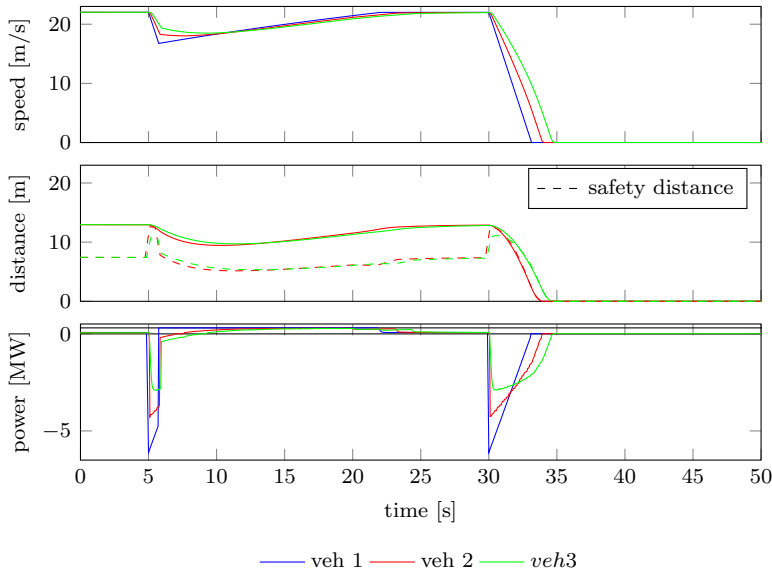


Figure 5.12: Behavior of a three identical vehicles platoon driving on a flat road. The leading vehicle brakes a first time at 5 s for 1 s with a deceleration of 7 m/s^2 and a second time at 25 s with a deceleration of 7 m/s^2 until arriving to full-stop. For the plot explanation refer to the caption of Figure 5.11.

Figure 5.13 shows the reaction of the platoon to a small disturbance acting on the first vehicle. The disturbance is defined as an acceleration for 0.5 s of a tenth of the maximum engine power. Each row in Figure 5.13 represents a different simulation and the value of $\bar{\zeta}$ varies between 0 and 1 between the simulations. The left plot of each simulation represents the vehicle speeds, while the right one represents the control input. The first simulation represents the case where each vehicle is only tracking the time gap, as $\bar{\zeta} = 0$. In this case, we can notice how the disturbance replicates in each vehicle almost unchanged with a time delay equivalent to the time gap. The last simulation represents, instead, the case where each vehicle only tracks the reference trajectories derived by the common reference speed profile, as $\bar{\zeta} = 1$. As the trajectory of preceding vehicles is ignored and the safety constraint do not activate, this is equivalent to the scenario where each vehicle is driving as it was alone. We can notice, in fact, how following vehicles do not react to the fluctuations in the trajectory of the preceding vehicle, resulting in the perturbation immediately dying after the second vehicle. In the intermediate simulations, we can notice how both the speed and engine power fluctuations attenuate along the platoon. This suggests the choice of $\bar{\zeta}$ strictly between 0 and 1.

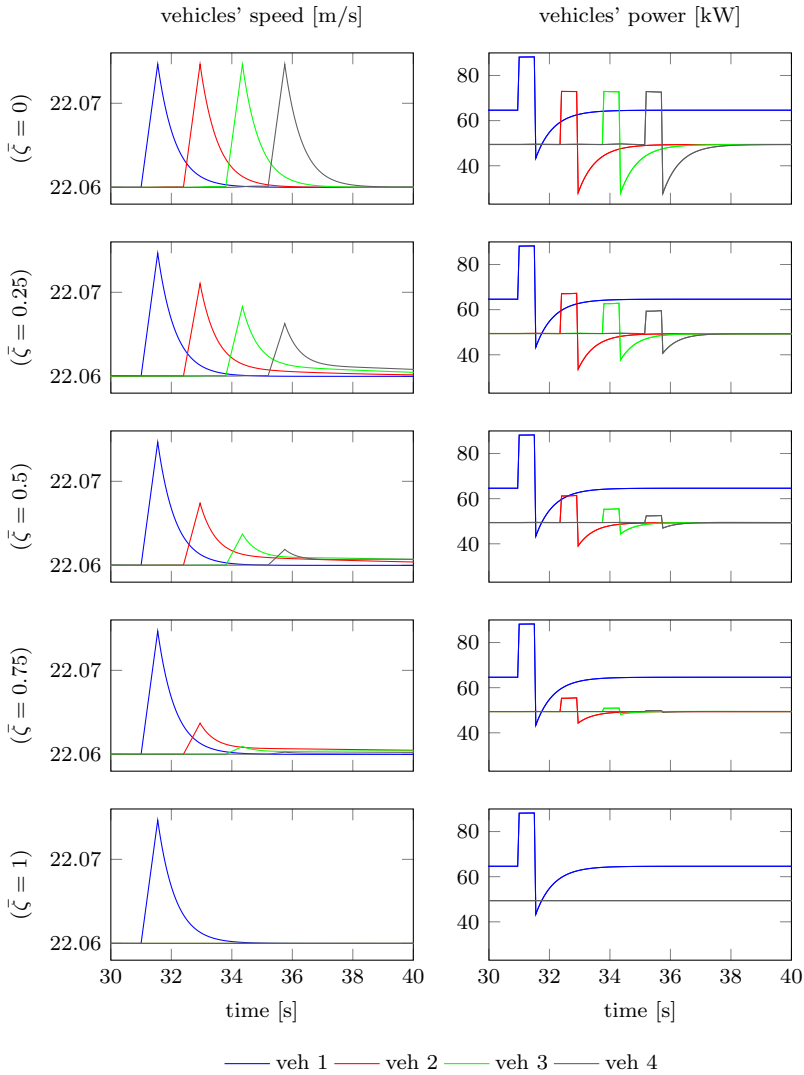


Figure 5.13: Each row of plots represents a different simulation characterized by a certain value of the trade-off term $\tilde{\zeta}$. The simulation results show the reaction of a four-vehicle platoon to a disturbance acting on the lead vehicle. The left and the right plots display the speed and the engine power, respectively.

Table 5.4: Controller parameters.

platoon coordinator			
H_{DP}	DP horizon length	km	2
Δs_{DP}	DP discretization space	m	6
f_{DP}	DP refresh frequency	Hz	0.25
vehicle controller			
H_{MPC}	MPC horizon length	s	8
Δt_{MPC}	MPC discretization time	s	0.05
f_{MPC}	MPC refresh frequency	Hz	20

5.6 Evaluation of the integrated system

In this section, we test the performance of the integrated cooperative control architecture. To this end, we consider a platoon of three homogeneous vehicles driving over the Sector A highlighted in Figure 5.6. This is the same sector for which the experimental results have been analyzed in Section 4.1 and displayed in Figure 4.3. The vehicle and controller parameters are depicted in Tables 5.1 and 5.4, respectively. The vehicle simulation model uses the simplified powertrain model presented in Subsection 5.2.2. We consider first the nominal scenario, where no disturbance acts on the vehicle acceleration. Second, we considered the perturbed scenario, where a drop of the second vehicle traction power takes place during the uphill to emulate the gear shift happening in the motivational experiment presented in Section 4.1.

The simulation results for the nominal scenario are displayed in Figure 5.14. At first glance, as expected from the platoon coordinator formulation, we can notice how all the vehicles approximately follow the same space-defined speed and distance profiles. Additionally, in order to follow such profiles, we can observe in the last plot how the second and third vehicle, thanks to the air drag reduction, need to generate less power than the leading vehicle. We now continue the analysis by focusing on the three critical segments highlighted in Figure 5.14 and corresponding to those analyzed in Section 4.1 for the motivational experiment:

- Segment 1. Due to the steep downhill, all vehicles are not able to maintain the constant speed without braking and, therefore, they accelerate. However, the platoon coordinator requires the leading vehicle to throttle slightly such that the following vehicles can coast. In this case, the coordination role of the platoon coordinator allows to avoid braking action to all vehicles, hereby ensuring a lower overall fuel consumption.

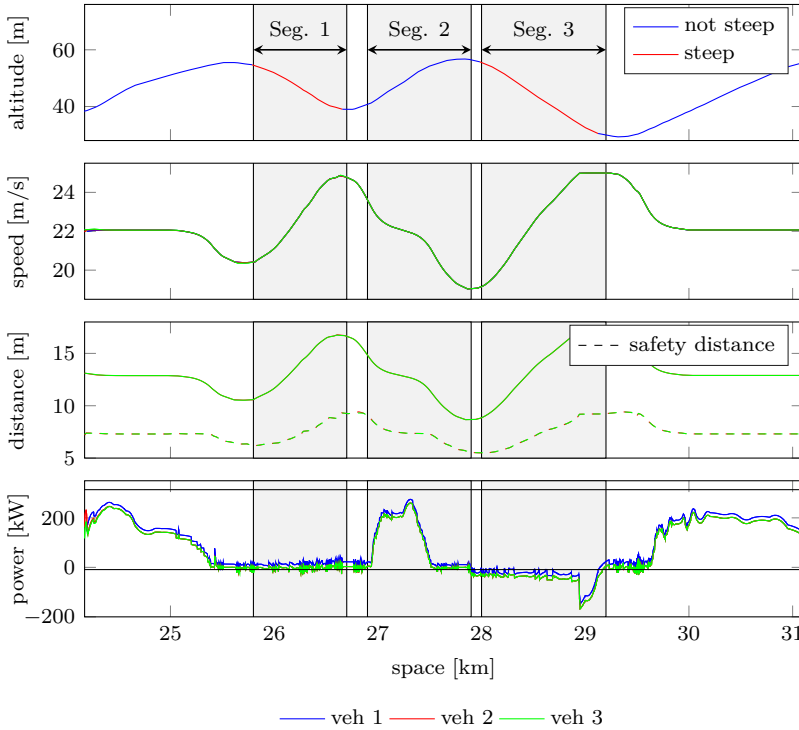


Figure 5.14: Simulation results obtained using the proposed controller for a three-vehicle platoon while driving over the Sector A highlighted in Figure 5.6. The three vehicles are identical with parameters shown in Table 5.1. The first plot shows the road topography. For the explanation of the other plots refer to the caption of Figure 5.11.

- Segment 2. Since no gear shift takes place, the vehicles are able to smoothly follow the reference speed and time gap policy.
- Segment 3. Due to the longer length of the downhill section compared to the the one of Segment 1, the platoon exhibits a different behavior. First, the platoon coordinator requires all vehicles to decrease the speed to the minimum allowed (in this simulation it is set to 19 m/s) in order to hit the maximum speed limit as late as possible. Second, since the speed limit is reached despite the decrease of speed at the beginning of the downhill, the platoon coordinator requires the first vehicle to coast and the following vehicles to brake slightly to maximize the efficiency. In fact, in this case, to require the first vehicle to slightly throttle in the first part of the downhill section and brake at its end would be contradictory and inefficient.

We now discuss the simulation results for the perturbed scenario. Here, we

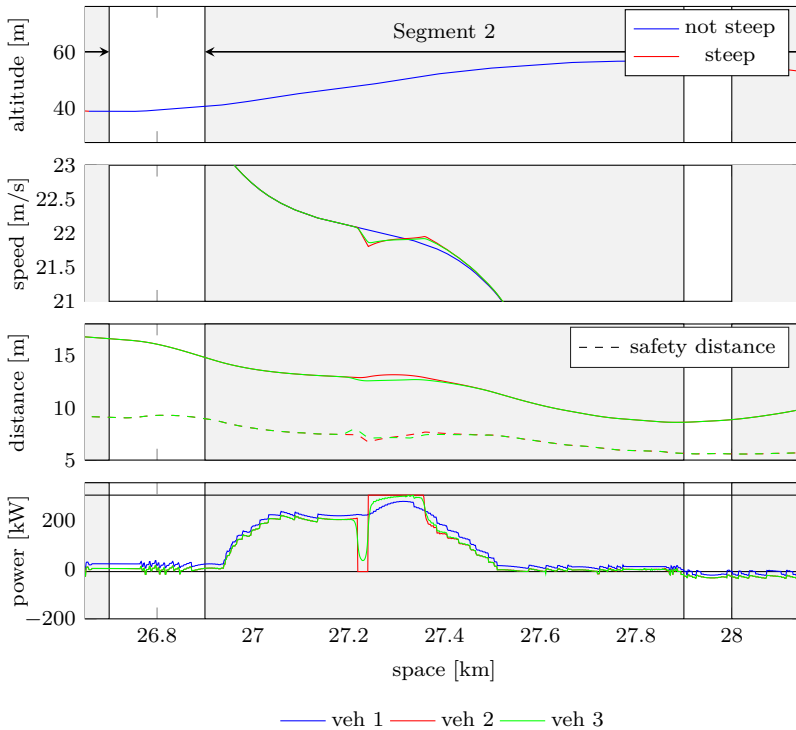


Figure 5.15: Simulation of a similar scenario considered in Figure 5.14, where, instead, a disturbance acts on the input of the second vehicle. In detail, the disturbance is defined as a drop of the engine power to zero for 1 s at space 27.22 km. The figure shows a portion of the simulation corresponding to Segment 2. For the explanation of the plots refer to the caption of Figure 5.14.

emulate a gear shift of the second vehicle during the uphill of Segment 2 as happened in the motivational experiment. The gear shift is simulated as a drop of the traction power to zero at position 27.22 km for a time of one second. In Figure 5.14 we display the simulation results for the platoon driving along Segment 2. The second vehicle, in order to react to the deviation of the state from the reference and the opening of the time gap due to the disturbance, generates the maximum power for 120 m. Thanks to the prediction of the state, the controller stops the full-throttle before reaching the time gap requirement. This gives the time to the second vehicle to reduce its speed while closing the gap. The speed reduction of the second vehicle during the engine power drop is not safety critical as it can be noticed in the distance plot of Figure 5.15 (i.e., the distance between the second and third vehicles does not reach the safety distance correspondent safety distance). The third vehicle, therefore, by fulfilling the time gap requirement, tracks the delayed trajectory of the second

vehicle and starts to reduce its throttling at the same position where the disturbance hits the second vehicle. If the disturbance would have been more intense, the safety constraint could have required the third vehicle to reduce the throttle earlier.

In conclusion, the vehicle controller smoothly handled the emulated second vehicle gear shift. However, if the gear shift would have been longer or would have happened at a close time with respect to other vehicle gear shifts, its repercussions on the platoon behavior could have been more harmful. To address this issue, in the next chapter, we discuss how gear shifts can be directly taken into account in the platooning control architecture.

5.7 Summary

In this chapter, we presented a possible formulation and implementation of a the cooperative control architecture for fuel-efficient and safe platooning.

The control architecture is made up of two layers. The higher layer is referred to as platoon coordinator and is responsible for the overall fuel-efficient operation of the platoon. This is achieved by defining a unique reference speed trajectory for the platoon defined in the spatial domain. The platoon coordinator is implemented by dynamic programming and guarantees that the computed reference trajectory is feasible for all vehicles, minimizes the fuel consumption of the whole platoon and satisfies given average speed requirements. The platoon coordinator is tested in a simulation study where a two-vehicle platoon drives along a hilly road. The trajectories generated by the proposed controller are compared to those generated by alternative platooning control strategies. The comparison show the potential of the proposed platoon coordinator to reduce the fuel consumption of up to 12% for following vehicles with respect to the alternative control strategies.

The lower layer is referred to as vehicle control layer and is responsible for the fuel-efficient and safe tracking of the reference platoon speed trajectory generated by the platoon coordinator. It is implemented by distributed model predictive control where each vehicle controller receives the preceding vehicle predicted trajectory and exploits it to track the reference speed profile and gap policy, while avoiding unnecessary braking. The safety of the platoon is guaranteed by a set of specifically designed constraints distributed in the model predictive controllers. The performance of the vehicle control layer has been evaluated by means of simulations. The simulation study shows the capability of the distributed layer to safely react to unexpected braking of the first vehicle and to attenuate disturbances along the platoon.

The chapter ended with the evaluation of the whole control architecture. The simulations confirm the good behavior of the platoon while driving along a realistic road profile. However, gear shifts can produce large deviations in the platoon trajectory if they take place in unfavorable moments. This issue is addressed in the next chapter.

Gear management in cooperative platooning

In this chapter we study the problem of how to efficiently manage gear shifts in heavy-duty vehicle platoons. The importance of the work is motivated by the analysis of the experiment of Section 4.1 and of the perturbed scenario presented in Section 5.6 and displayed in Figure 5.15.

Gears have a strong impact on the vehicle fuel consumption and on the reference speed and inter-vehicular distance tracking. The wrong gear can lead the engine to operate in an inefficient region, while a gear shift taking place at the wrong moment, e.g., during an uphill stretch, can lead to a large deviation from the references that can be hard to compensate for. This was described in the experiment of Section 4.1, where the following vehicle was changing gear in the middle of the uphill while the controller was requiring maximum torque. As a consequence of the large deviation from the tracked reference, the following vehicle reaches the leading one at a relatively large speed and therefore harshly brakes. The look-ahead capability of the vehicle control layer of the cooperative control architecture presented in the previous chapter allows to alleviate this problem as shown in the simulation results of Section 5.6. However, gear shifts might still generate large perturbations in the platoon reference tracking.

Here, we discuss a variation of the control architecture presented in the previous chapter that takes gear shifts into account. A gear management layer that optimizes the gear selection and the gear shift timing is introduced. The underlying optimal control problem aims at minimizing the vehicle fuel consumption and the speed and inter-vehicular reference tracking deviations. The gear management layer performance is tested in a simulation study that compares it to alternative solutions. The study shows how the proposed solution properly manages the gear shifting task guaranteeing fuel-efficiency and the smooth behavior of the platoon.

The chapter is organized as follows. In Section 6.1, we analyze the gear management problem for vehicle platooning and we propose a modified control architecture. Sections 6.2 and 6.3 present the details of the gear management layer and the vehicle

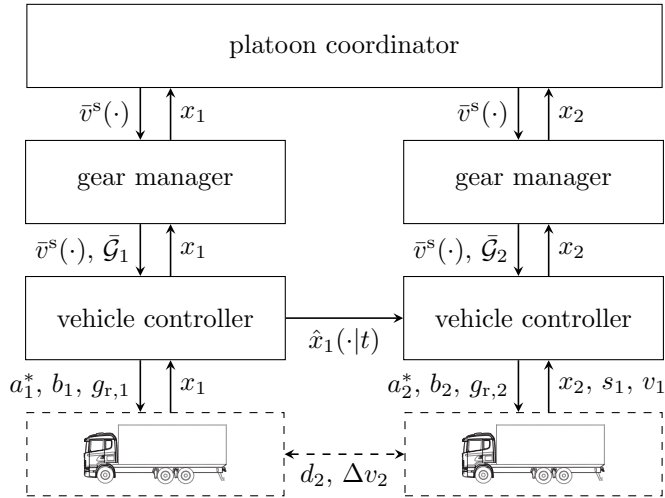


Figure 6.1: Control architecture for cooperative platooning where gear management is taken directly into account.

control layer, respectively. In Section 6.4, we present a simulation study that shows the performance of the proposed method. Finally, Section 6.5 concludes the chapter.

6.1 Control architecture and problem statement

A gear management strategy for platooning should take both vehicle fuel consumption and reference speed and inter-vehicular distance tracking into account. We suggest a three-layer control architecture as depicted in Figure 6.1, which extends the one presented in the previous chapter. This architecture is similar to the one proposed by Johannesson et al. (2015) for the control of a single vehicle driving along a hilly road.

Here, the platoon coordinator, as presented in detail in Section 5.2, computes a reference platoon speed profile defined over space and denoted as $\bar{v}^s(\cdot)$, which is feasible for all vehicles and minimizes the overall platoon fuel consumption.

The gear management layer is responsible for choosing the sequence of gear shifts \bar{G}_i for each vehicle in order to optimally track the reference speed trajectory $\bar{v}^s(\cdot)$. The gear shift sequence is, first of all, optimized according to fuel-efficiency criteria. Furthermore, due to the interruption of the transferred force during gear shifts, the gear managers also penalize the impact of gear shifts on the tracking of the speed and inter-vehicular distance. This is achieved by ensuring that the deviation from the references during gear shifts is small and that it can be compensated for in a limited time. As it will be shown in the simulation study of Section 6.4, these aspects

are crucial for the coordinated behavior of the platoon. The gear management layer is discussed in Section 6.2.

The vehicle control layer, similarly to Section 5.3, tracks the speed reference $\bar{v}^s(\cdot)$ and the chosen spacing policy, while guaranteeing safety. However, the vehicle control layer of this chapter also takes the requested future sequence of gear shifts into account. This allows to compensate for a planned gear shift before it takes place. The vehicle control layer is discussed in Section 6.3.

6.2 Gear management layer

In this section, we present the problem solved by the gear management layer. The gear manager is a controller local to each vehicle that receives the space-defined reference speed profile $\bar{v}^s(\cdot)$ from the platoon coordinator and computes the optimal sequence of gear shifts for the vehicle i :

$$\mathcal{G}_i = \{(g_{l,i}, s_{l,i})\}_{l=1}^{L_i}, \quad (6.1)$$

where $g_{l,i}$ and $s_{l,i}$ denote the l -th required gear and the longitudinal position where it should occur, respectively. The gearbox-clutch dynamics are modeled according to the automaton displayed in Figure 3.5 and presented in Section 3.2. In the work presented in this chapter, freewheeling is not considered as admissible gearbox-clutch state, due to the lack of vehicle controllability when engaged. The required gear $g_{l,i}$ is therefore constrained by

$$g_{l,i} \in \mathcal{G}_{a,i}, \quad (6.2)$$

for $l = 0, \dots, L$, where $\mathcal{G}_{a,i} = \{j \in \mathbb{N} | j \in [g_{\min,i}, g_{\max,i}]\}$ represents the set of the admissible gears. For simplicity, in the remainder of this section index i corresponding to the current vehicle is dropped.

The gear manager is formulated as an optimization problem whose objective is to minimize the vehicle fuel consumption and the impact of the gear shift on the deviation from the reference speed profile and inter-vehicle gap. In detail, the cost that we aim to minimize is

$$J_{\text{fuel}}(\mathcal{G}) + \alpha J_{\text{shift}}(\mathcal{G}), \quad (6.3)$$

where $J_{\text{fuel}}(\mathcal{G})$ denotes the consumed fuel over the gear manager horizon H_{GM} and $J_{\text{shift}}(\mathcal{G})$ quantifies the energy lost during gear shifts (i.e., the energy that the engine would have transferred to the wheels if no gear shift takes place).

The consumed fuel $J_{\text{fuel}}(\mathcal{G})$ is expressed as a function of the sequence of gear shifts \mathcal{G} , the reference speed \bar{v}^s and the reference traction force $\bar{F}_t^s(s)$ needed to track \bar{v}^s . The reference traction force can be approximately computed as

$$\bar{F}_t^s(s) = \max\{0, \bar{F}^s(s)\}, \quad (6.4)$$

where $\bar{F}^s(s)$ is the actuator reference force defined according to the space vehicle model used by the platoon coordinator (5.5b) as

$$\bar{F}^s(s) = m\bar{v}^s(s)\frac{d\bar{v}^s(s)}{ds} + mg_a \sin \alpha(s) + mg_a c_r + \frac{1}{2}\rho A_v C_d(d)(\bar{v}^s(s))^2. \quad (6.5)$$

The definition of the vehicle parameters is introduced in Chapter 3 and synthesized in Table 6.1. Given $\bar{F}_t^s(\cdot)$, the consumed fuel J_{fuel} can be formulated as

$$J_{\text{fuel}}(\mathcal{G}) = \int_{s_0}^{s_0+H_{\text{GM}}} \varphi(\bar{\omega}(\bar{v}^s(s), g_r^s(s)), \bar{T}(\bar{F}_t^s(s), g_r^s(s))) ds, \quad (6.6)$$

where the required gear $g_r^s(s)$ is defined as a function of the gear shift sequence \mathcal{G} as

$$g_r^s(s) = \begin{cases} g_l, & \text{if } s_l \leq s < s_{l+1}, \\ g_L, & \text{if } s_L \leq s < s_0 + H_{\text{GM}}, \end{cases} \quad (6.7)$$

where (g_0, s_0) is a parameter of the optimization and represents the initial engaged gear and position pair. The variables $\bar{\omega}(v, g)$ and $\bar{T}(v, g)$ represent the engine speed and torque needed to track the reference speed profile, respectively, and are defined as

$$\bar{\omega}(v, g) = \frac{v\gamma_g(g)\gamma_f}{r} \quad \text{and} \quad \bar{T}(F_t, g) = \frac{F_t r}{\gamma_g(g)\gamma_f}. \quad (6.8)$$

Here we recall that $\varphi(\cdot, \cdot)$ represents the fuel model defined in (3.10), while the parameters $\gamma_g(\cdot)$, γ_f and r denote the gear ratio, the final drive ratio and the wheel radius, respectively. s_0 is the initial vehicle position.

The energy lost during gear shifts $J_{\text{shift}}(\mathcal{G})$ is expressed as a function of the required traction force $\bar{F}_t^s(s)$ as

$$J_{\text{shift}}(\mathcal{G}) = \sum_{l=1}^L \int_{s_l}^{s_l+2\delta s} \bar{F}_t^s(s) ds, \quad (6.9)$$

where $2\delta s$ represents an upper bound on the space that a gear shift takes. A small energy lost during the gear shift results in a small deviation from the speed and distance references and therefore in the smooth behavior of the platoon.

The minimization of the presented cost function should take place while certain constraints are fulfilled. First, we require that the gear shift sequence \mathcal{G} ensures that the engine operates in the admissible speed range by enforcing the following constraint:

$$v_{\min}(g_l) \leq \bar{v}^s(s) \leq v_{\max}(g_l), \quad (6.10)$$

for all $s \in [s_l, s_{l+1})$. Here,

$$v_{\min}(g) = \frac{r\omega_{\min}}{\gamma_g(g)\gamma_f} \quad \text{and} \quad v_{\max}(g) = \frac{r\omega_{\max}}{\gamma_g(g)\gamma_f}$$

denote the minimum and maximum speeds, respectively, that the vehicle can drive, while gear g is engaged. Second, we ask that the required force \bar{F}_t^s , while driving at the reference speed \bar{v}^s , fulfills the upper bound on engine torque. This is ensured by:

$$\bar{F}_t^s(s) \leq F_{t,\max}(g_l, \bar{v}^s) \quad (6.11)$$

for all $s \in [s_l, s_{l+1})$. Here,

$$F_{t,\max}(g, v) = \frac{T_{\max}(v\gamma_g(g)\gamma_f/r)\gamma_g(g)\gamma_f}{r}$$

denotes the maximum engine force (at the wheel) that can be generated by the engine while gear g is engaged. Third, we require that the gear shifts are not happening too often. By assuming that the vehicle is not allowed to drive faster than a certain speed, the latter requirement is relaxed by requiring that consecutive gear shifts are spaced by a minimum interval Δs_{shift} , i.e.,

$$s_{l+1} \geq s_l + \Delta s_{\text{shift}}. \quad (6.12)$$

Finally we wish to guarantee that deviations from the reference speed profile and desired inter-vehicle gap, caused by the interruption of traction force during the gear shifts, can be compensated in a bounded space span. By choosing this span such that it is always shorter than the time prediction horizon of the vehicle control layer, we provide the basis for a good reference tracking of the vehicle control layer. This requirement is enforced by demanding that the energy lost during the gear shift (that is assumed to take place on a space interval shorter than $2\delta s$) can be compensated in the space intervals Δs before and after the gear shift. Let first introduce the energy quantities $E_{\delta_1}(l)$, $E_{\delta_2}(l)$, $E_{\Delta_1}(l)$ and $E_{\Delta_2}(l)$ displayed in Figure 6.2 and representing the energies lost during the first and second half of the l -th gear shift and the extra energies available in the space intervals Δs before and

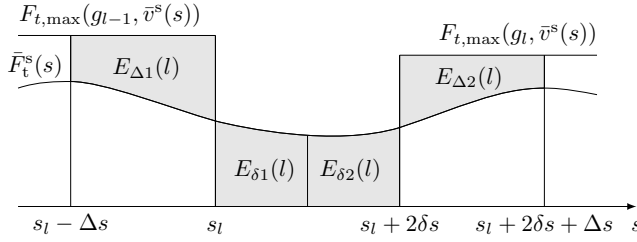


Figure 6.2: Illustration representing the small deviation constraint in the formulation of the gear manager as expressed in (6.14).

after the gear shift, i.e.,

$$\begin{aligned}
 E_{\delta 1}(l) &= \int_{s_l}^{s_l + \delta s} \bar{F}_t^s(s) ds, \\
 E_{\delta 2}(l) &= \int_{s_l + \delta s}^{s_l + 2\delta s} \bar{F}_t^s(s) ds, \\
 E_{\Delta 1}(l) &= \int_{s_l - \Delta s}^{s_l} F_{t, \max}(g_{l-1}, \bar{v}^s(s)) - \bar{F}_t^s(s) ds, \\
 E_{\Delta 2}(l) &= \int_{s_l + 2\delta s}^{s_l + 2\delta s + \Delta s} F_{t, \max}(g_l, \bar{v}^s(s)) - \bar{F}_t^s(s) ds.
 \end{aligned} \tag{6.13}$$

The discussed requirement can be now formalized by the inequalities

$$\begin{aligned}
 E_{\delta 1}(l) &\leq E_{\Delta 1}(l), \\
 E_{\delta 2}(l) &\leq E_{\Delta 2}(l).
 \end{aligned} \tag{6.14}$$

To summarize, the task of each gear manager is to solve the following optimal control problem:

$$\text{minimize}_{\mathcal{G}} J_{\text{fuel}}(\mathcal{G}) + \alpha J_{\text{shift}}(\mathcal{G}) \tag{6.15a}$$

$$\text{subj. to } \bar{F}_t^s(s) \leq F_{t, \max}(g_l, \bar{v}^s(s)), \forall s \in [s_l, s_{l+1}), \tag{6.15b}$$

$$v_{\min}(g_l) \leq \bar{v}^s(s) \leq v_{\max}(g_l), \forall s \in [s_l, s_{l+1}), \tag{6.15c}$$

$$s_{l+1} \geq s_l + \Delta s_{\text{shift}}, \tag{6.15d}$$

$$E_{\delta 1}(l) \leq E_{\Delta 1}(l), \tag{6.15e}$$

$$E_{\delta 2}(l) \leq E_{\Delta 2}(l), \tag{6.15f}$$

$$g_l \in \mathcal{G}_{a,i}, \tag{6.15g}$$

$$s_0 = s_i(t), \tag{6.15h}$$

$$g_0 = g_i(t), \tag{6.15i}$$

for $l = 0, \dots, L$, where equations (6.15h)–(6.15i) represent the initial conditions. Thanks to the discrete nature of gears, the optimization problem can be efficiently solved by using dynamic programming presented in Section 2.5 in a receding horizon fashion. This is achieved by discretizing the spatial domain s with discretization length Δs_{GM} and repeatedly solving the optimization problem with frequency f_{GM} . The optimized gear shift sequence $\bar{\mathcal{G}}_i$ is then communicated to the corresponding vehicle controller.

6.3 Vehicle control layer

In this section, we discuss the problem formulation for the vehicle control layer. Each vehicle controller receives the reference speed $\bar{v}^s(\cdot)$ and the requested sequence of gear shifts $\bar{\mathcal{G}}_i$ from the higher layers, and the optimal state trajectory $\hat{x}_{i-1}(\cdot|t)$ from the preceding vehicle. By solving a model predictive control (MPC) problem aimed at safely tracking the reference speed and the time gap, it computes the required acceleration a_i^* and triggers the gear shifts. For ease of presentation, the optimal control problem solved by MPC is presented in the continuous time.

The state prediction of the MPC problem is based on the vehicle model

$$\begin{aligned}\dot{v}_i(\tau|t) &= a_i(\tau|t), \\ \dot{s}_i(\tau|t) &= v_i(\tau|t),\end{aligned}\tag{6.16}$$

where $v_i(\tau|t)$ and $s_i(\tau|t)$ denote the predicted speed and position of vehicle i at time $\tau \geq t$ computed at time t , respectively (collected in the state vector $x_i = [v_i, s_i]^T$). The control input $a_i(\tau|t)$ denotes the predicted vehicle acceleration. The tracking of the speed reference and the time gap τ_i is guaranteed by the cost function

$$\begin{aligned}J_{\text{MPC}}(a_i(\cdot|t), \varepsilon_i(t)) &= \int_t^{t+H_{\text{MPC}}} \|x_i(\tau|t) - \hat{x}_{i-1}(\tau - \tau_i|t)\|_{(\zeta_{i-1})Q}^2 \\ &\quad + \|a_i(\tau|t) - \hat{a}_{i-1}(\tau - \tau_i|t)\|_{(\zeta_{i-1})R}^2 \\ &\quad + \|x_i(\tau|t) - \bar{x}_i(t)\|_{\zeta_i Q}^2 \\ &\quad + \|a_i(\tau|t) - \bar{a}_i(t)\|_{\zeta_i R}^2 \\ &\quad + \|\varepsilon_i(t)\|_P^2 d\tau.\end{aligned}$$

Here, the first and second terms penalize the deviations from the time gap, the third and fourth terms penalize the deviations from the speed reference, and the last term penalizes the slack variable related to the no-braking constraints that will be later discussed. In order to account for the vehicle model presented in Section 3.1 and the bounds on braking force and engine torque, we introduce the minimum and maximum allowed accelerations, $a_{\min,i}$ and $a_{\max,i}$, respectively, and the coasting acceleration $a_{\text{coast},i}$, i.e., the vehicle acceleration when no fuel is injected in the

engine, defined as follows:

$$a_{\min,i}(\tau|t) = \frac{1}{m_i} (F_{b,\min,i} + F_{\text{ext},i}(\tau|t)), \quad (6.17a)$$

$$a_{\max,i}(\tau|t) = \begin{cases} \frac{1}{m_i} \left(\frac{T_{\max,i} \gamma_{g,i}(g_i(\tau|t)) \gamma_{f,i}}{r} + F_{\text{ext},i}(\tau|t) \right), & \text{if } g_i(\tau|t) \in \mathcal{G}_{a,i} \\ \frac{F_{\text{ext},i}(\tau|t)}{m_i}, & \text{if } g_i(\tau|t) = 0, \end{cases} \quad (6.17b)$$

$$a_{\text{coast},i}(\tau|t) = \begin{cases} \frac{1}{m_i} \left(\frac{T_{\min,i} \gamma_{g,i}(g_i(\tau|t)) \gamma_{f,i}}{r} + F_{\text{ext},i}(\tau|t) \right), & \text{if } g_i(\tau|t) \in \mathcal{G}_{a,i} \\ \frac{F_{\text{ext},i}(\tau|t)}{m_i}, & \text{if } g_i(\tau|t) = 0, \end{cases} \quad (6.17c)$$

where $F_{b,\min,i}$ represents the minimum braking force, $T_{\min,i}$ and $T_{\max,i}$ an approximation of minimum and maximum engine torques, respectively, and $F_{\text{ext},i}(x_i)$ the summation of the external forces acting on the vehicle defined as

$$F_{\text{ext},i}(\tau|t) = -m_i g_a \sin \alpha(s_i(\tau|t)) - c_{r,i} m_i g_a - \frac{1}{2} \rho A_v C_d (\hat{s}_{i-1}(\tau|t) - s_i(\tau|t) - l_{i-1}) v_i^2(\tau|t). \quad (6.18)$$

Note that the predicted engaged gear $g_i(\tau|t)$ is a known parameter in the optimization problem that is computed according to the automaton describing the gearbox-clutch dynamics displayed in Figure 3.5, where the input variable $g_{r,i}$ is driven according to gear shift sequence \mathcal{G}_i . Furthermore, during gear shifts, i.e., $g_i = 0$, the maximum acceleration $a_{\max,i}$ and the coasting acceleration $a_{\text{coast},i}$ coincide. The vehicle acceleration a_i can be now bounded by the hard constraint

$$a_{\min,i}(\tau|t) \leq a_i(\tau|t) \leq a_{\max,i}(\tau|t) \quad (6.19)$$

and the soft constraint

$$a_i(\tau|t) + \varepsilon_i(t) \geq \min(a_{\text{coast},i}(\tau|t), \bar{a}_i(\tau|t)), \quad \varepsilon_i(t) \geq 0. \quad (6.20)$$

By strongly penalizing the slack variable ε_i in the cost function, we are guaranteeing that the braking is taking place only if one of the hard constraints is activated. Furthermore, the prediction horizon H_{MPC} is chosen such that, by assuming a minimum speed allowed, always covers a space longer than $2(\delta s + \Delta s)$, i.e., the space that a gear shift and its compensation take in the gear management layer. This condition, combined with the inclusion of the engaged gear in the acceleration bounds in (6.19), guarantees the good tracking of the reference speed and time gap.

Finally, in order to guarantee the safety operation of the platoon, as argued in

Section 5.3, we introduce the following safety constraints:

$$s_i(\tau + \Delta t_{\text{MPC}}|t) - \frac{v_i^2(\tau + \Delta t_{\text{MPC}}|t)}{2\bar{a}_{\min,i}} \leq \hat{s}_{i-1}(\tau - \Delta t_{\text{MPC}}) - \frac{\hat{v}_{i-1}^2(\tau + \Delta t_{\text{MPC}})}{2\bar{a}_{\min,i-1}} - l_{i-1},$$

$$s_i(\tau + \Delta t_{\text{MPC}}|t) \leq \hat{s}_{i-1}(\tau - \Delta t_{\text{MPC}}) - l_{i-1}. \quad (6.21)$$

Here, Δt_{MPC} denotes the discretization time of the MPC implementation, and $\underline{a}_{\min,i}$ and $\bar{a}_{\min,i}$ denote the conservative lower and upper bounds on $a_{\min,i}$, respectively. The safety constraint is valid under the assumption of maximum delay in sensor measurement of Δt_{MPC} .

To summarize, the optimal control problem solved in each vehicle controller can be formulated as follows:

$$\underset{a_i(\cdot|t), \varepsilon_i(t)}{\text{minimize}} \quad J_{\text{MPC}}(a_i(\cdot|t), \varepsilon_i(t)) \quad (6.22a)$$

$$\text{subj. to} \quad \dot{v}_i(\tau|t) = a_i(\tau|t), \quad (6.22b)$$

$$\dot{s}_i(\tau|t) = v_i(\tau|t), \quad (6.22c)$$

$$a_{\min,i}(\tau|t) \leq a_i(\tau|t) \leq a_{\max,i}(\tau|t), \quad (6.22d)$$

$$a_i(\tau|t) + \varepsilon_i(t) \geq \min(a_{\text{coast},i}(\tau|t), \bar{a}_i(\tau|t)), \quad (6.22e)$$

$$f_{\text{safe}}(x_i(\tau + \Delta t_{\text{MPC}}|t), \hat{x}_{i-1}(\tau - \Delta t_{\text{MPC}}|t)) \leq 0, \text{ if } i \geq 2, \quad (6.22f)$$

$$\varepsilon_i(t) \geq 0, \quad (6.22g)$$

$$v_i(t|t) = v_i(t), \quad (6.22h)$$

$$s_i(t|t) = s_i(t), \quad (6.22i)$$

for $\tau \in [t, t + H_{\text{MPC}}]$, where $f_{\text{safe}}(x_i(\tau + \Delta t_{\text{MPC}}|t), \hat{x}_{i-1}(\tau - \Delta t_{\text{MPC}}|t)) \leq 0$ denotes the safety constraints (6.21). The optimal control problem has been discretized with discretization time Δt_{MPC} and convexified similarly to steps taken in Section 5.3. This allowed to recast the problem in a quadratic constrained quadratic programming (QCQP) and solve it efficiently.

6.4 Performance evaluation

In this section we study the performance of the proposed approach by means of simulations. The simulation setup and results follow.

6.4.1 Simulation setup

We consider a heterogeneous platoon of four vehicles with masses of 25, 40, 25 and 40 tonnes, respectively, and with the same powertrain characteristics. In detail, each vehicle is equipped with the 400 hp engine whose BSFC map is shown in

Table 6.1: Vehicle parameters.

m_1, m_3	first and third vehicles' mass	t	25
m_2, m_4	second and fourth vehicles' mass	t	40
l_i	vehicle length	m	18
$c_{r,i}$	rolling coefficient	-	0.003
A_v	cross-sectional vehicle area	m ²	10
$C_{d,0}$	nominal drag coefficient	-	0.6
$C_{d,1}$	first drag reduction coefficient	m ⁻¹	12.8
$C_{d,2}$	second drag reduction coefficient	m	19.7
τ_{shift}	gearshift time	s	2
$P_{\text{min},i}$	minimum engine power	kW	-9
$P_{\text{max},i}$	maximum engine power	kW	298
$\omega_{\text{min},i}$	minimum engine speed	rpm	800
$\omega_{\text{max},i}$	maximum engine speed	rpm	2200
$T_{\text{min},i}$	approximated minimum torque	Nm	-150
$T_{\text{max},i}$	approximated maximum torque	Nm	1800

Figure 3.4 and a 14-gear gearbox. The vehicle model used in the simulation includes the longitudinal vehicle dynamics and the complete powertrain model presented in Section 3.2. The vehicle and controller parameters are displayed in Tables 6.1 and 6.2, respectively. The altitude profile has been artificially constructed and is composed by an uphill stretch followed by a downhill stretch, as depicted in gray color in the first plot of Figure 6.3. The proposed controller is compared to two alternative solutions:

- Reference gear management: this is the standard gear management common in commercial heavy-duty vehicles. The gear shift takes place when the engine speed reaches certain thresholds. These thresholds are increased when the required normalized torque is higher than 80% for more than 1 s. This allows the engine to operate in a higher power range when this is needed;
- Fuel-based gear management: this is an alternative formulation of the proposed gear manager where only the consumed fuel and the number of gear shifts are minimized, while the constraints on the lost energy during the gear shift (i.e., inequalities in (6.14)) are not included. The number of gear shifts has been included in the cost function in order to avoid that it becomes unnecessarily too large.

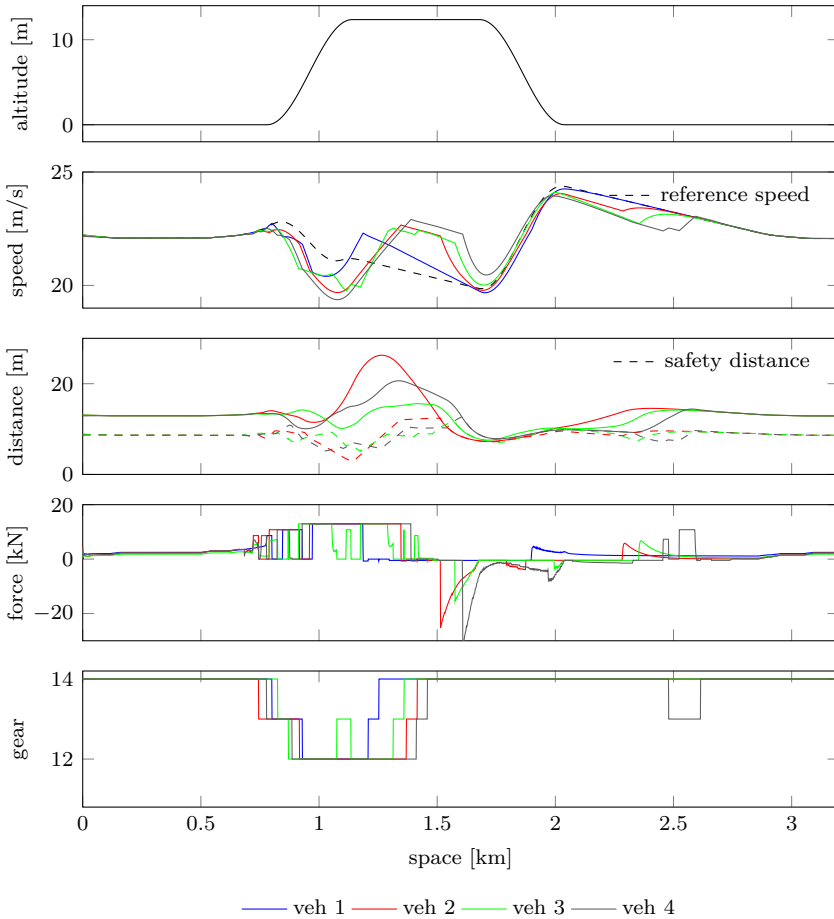


Figure 6.3: Simulation of a four-vehicle platoon driving over a hill, when the reference gear management is deployed. The first plot displays the road altitude in gray color and the speed of the vehicles. The second plot shows the inter-vehicular distance with solid lines and the safe distance computed according to an adaptation of constraint (5.45) with dashed line. The third plot shows the control force, defined as the summation of the traction and braking forces. Finally, the fourth plot displays the gear selected by the gear management. Note that all the variables are plotted as a function of the longitudinal position along the road.

Table 6.2: Controller parameters.

platoon coordinator			
H_{DP}	DP horizon length	km	2
Δs_{DP}	DP discretization space	m	6
f_{DP}	DP refresh frequency	Hz	0.25
gear manager			
H_{GM}	GM horizon length	km	2
Δs_{GM}	GM discretization space	m	6
f_{GM}	GM refresh frequency	Hz	0.25
vehicle controller			
H_{MPC}	MPC horizon length	s	8
Δt_{MPC}	MPC discretization time	s	0.05
f_{MPC}	MPC refresh frequency	Hz	20

Table 6.3: Normalized fuel consumption and reference tracking deviation of the platoon for three gear management strategies, namely the reference, the fuel-based and the proposed gear managements.

Control strategy	Consumed fuel [%]	Tracking deviation [%]
Reference	100	100
Fuel-based	90	12
Proposed	89	5

The three controllers have been compared on the basis of the platoon fuel consumption computed as

$$\sum_{i=1}^{N_v} \int_0^{T_{\text{sim}}} \varphi_i(\omega_i(t), T_i(t)) dt \quad (6.23)$$

and the reference tracking deviation computed as

$$\sum_{i=1}^{N_v} \int_0^{T_{\text{sim}}} \|x_i(t) - \hat{x}_{i-1}(t - \tau_i)\|_{\zeta_i, Q}^2 + \|x_i(t) - \bar{x}_i(t)\|_{(\zeta_{i-1})_Q}^2 dt, \quad (6.24)$$

where T_{sim} denotes the simulation time. The normalized platoon fuel consumption and the reference tracking deviation for the three gear management strategies are summarized in Table 6.3. Let now proceed to the analysis of the three simulations.

6.4.2 Simulation results

Figure 6.3 displays the platoon behavior when the *reference gear management* is used. The deployed gear management does not exploit any information on the road ahead and requires gear shifts only on the basis of the engine variables. We can notice that all four trucks asynchronously downshift two times at the beginning of the uphill. The delays introduced by the gear shifts and the fact that the vehicle control layer cannot take them into account (because with such gear management formulation future gear shifts are unknown) result in a large deviation from the reference speed and time gap for all following vehicles. To compensate for such deviation the vehicle controllers require the engines to generate the maximum torque after the gear shifts take place. Due to the limited prediction horizon, the vehicle control layer does not see far enough to understand that it is counter-productive to require such a large amount of energy from the engine. This behavior leads to fact to the vehicles coasting and finally braking in order to avoid collision with the preceding vehicles. Since the reference speed trajectory computed by the platoon coordinator requires the heaviest trucks to coast after the uphill, only an extremely long prediction horizon would have avoided the braking of the vehicles. A similar behavior has been also experienced in the motivational experiment presented in Section 4.1.

Figure 6.4 shows the platoon behavior when the *fuel-based gear management* is used. Here, topography information of the road ahead is exploited in the computation of the gear shift sequence. The optimization is based only on the fuel consumption and the number of gear shifts, while the impact of the gear shift on reference tracking is ignored. As a result, even if the number of gear shifts during the uphill stretch is reduced to one, the vehicle control layer has trouble to compensate for the generated deviation from the reference. This is due to the fact that the gear shifts take place in sections where the required force $\bar{F}_{t,i}$ necessary to track the reference speed is close to the maximum. Consequently, the third and fourth vehicles full-throttle for a certain amount of time and, in order not to collide with the preceding vehicle, they finally brake.

Figure 6.5 displays the platoon behavior when the *proposed gear management* is used. With respect to the previous case, the gear shift optimization also targets the impact of the gear shifts on the deviation from the reference. In particular, by choosing the parameter Δs equal to 30 m and assuming that the vehicle speed is bounded in a certain interval, we can guarantee that the deviation from the references due to the gear shift can be compensated for over the prediction horizon $H_{\text{MPC}} = 8 \text{ s}$ of the vehicle control layer. By analyzing the simulation results, we can notice that the gear management requires the gear shifts to take place before the start and the end of the uphill section. In such regions, in fact, the energy lost during the gear shifts is small enough to be compensated for in a sufficiently short horizon. As a result, the deviations generated by the gear shifts are promptly

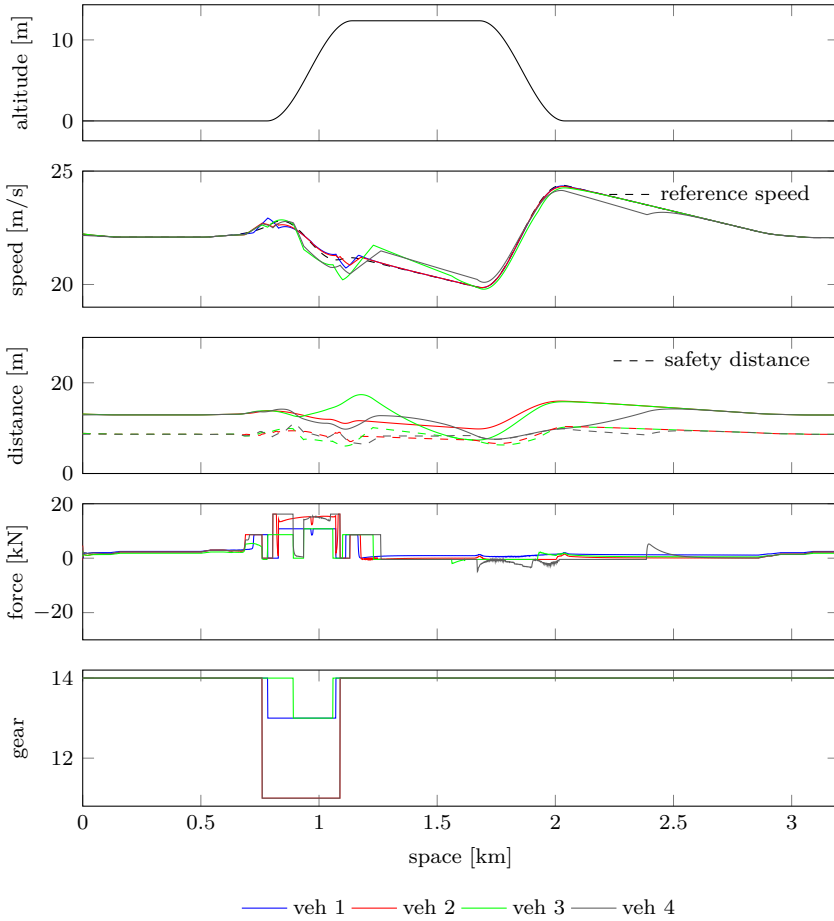


Figure 6.4: Simulation of a four-vehicle platoon driving over a hill, when the fuel-based gear management is deployed. Refer to the caption of Figure 6.3 for the plots explanation.

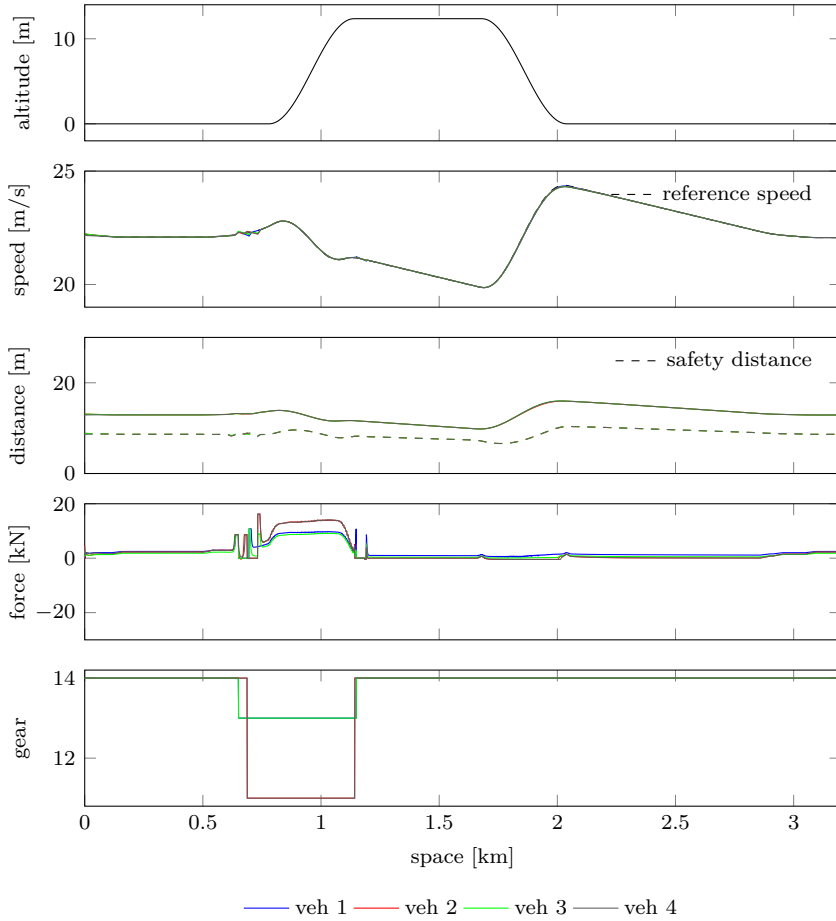


Figure 6.5: Simulation of a four-vehicle platoon driving over a hill, when the proposed gear management is deployed. Refer to the caption of Figure 6.3 for the plots explanation.

compensated and the vehicles smoothly track the reference speed and time gap without engaging the brakes. Besides the good tracking of the reference speed and time gap, the absence of braking leads to an additional fuel saving of the platoon compared to the fuel-based gear management as displayed in Table 6.3.

6.5 Summary

In this chapter we addressed the gear management problem for fuel-efficient heavy-duty vehicle platooning, by proposing a control architecture that extends the one presented in the previous chapter. In particular, we introduced a novel layer referred to as gear management layer that receives the reference platoon speed trajectory from the platoon coordinator and defines the optimal gear shift sequence for each vehicle. The gear sequence is chosen in order to minimize the fuel consumption and the impact of gear shifts over the tracking of the common reference speed trajectory. In order to exploit the information about the future gear shift sequence generated by the gear management layer, we redesign the vehicle control layer accordingly.

The extended control architecture is tested in a simulation study where its performance is compared to alternative solutions. The study shows the capability of the proposed controller to ensure a low fuel consumption and a smooth platoon behavior.

Part II

Non-cooperative platooning

Fuel-optimal vehicle-following control

In this chapter, we study the vehicle-following control problem for heavy-duty vehicles. The problem is formulated as an optimal control problem that exploits road topography information and the predicted trajectory of the preceding vehicle to compute the optimal state and input trajectories for the vehicle under control. The vehicle model includes the longitudinal vehicle dynamics and a powertrain model that captures both the gear shifts and freewheeling (cruising in neutral gear) dynamics. This allows to explore the benefits of combining the fuel savings given by a short inter-vehicular distance with those given by a pulse and glide (PnG) control strategy. Here, we refer to PnG control strategy as the alternation between throttling phases where the engine is working close to the optimal operation point and freewheeling phases where the clutch is disengaged. The control is computed via dynamic programming and is tested in a simulation study where the performance for multiple scenarios and controller setups are compared. In particular, we compare the behavior and fuel savings of a heavy-duty vehicle using the proposed control strategy and using a reference vehicle-following controller that tracks a constant distance. The results show that the proposed control strategy is able to reduce the fuel consumption of up to 18% by keeping a minimum distance of 20 m with respect to the driving alone scenario, and up to 7% with respect to the use of the constant-distance vehicle-following controller.

The chapter is organized as follows. Section 7.1 introduces the non-cooperative control architecture. Section 7.2 details the vehicle and fuel models, while Section 7.3 discusses the optimal control problem formulation and its dynamic programming solution. Section 7.4 presents the simulation study where the performance of the proposed controller is tested and Section 7.5 concludes the chapter.

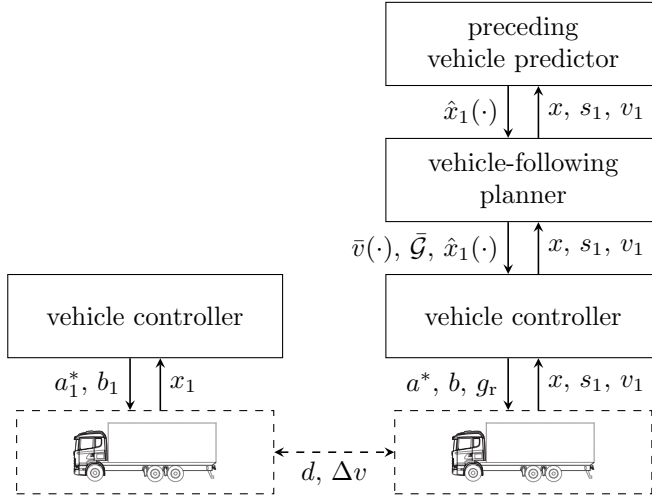


Figure 7.1: Control architecture for non-cooperative platooning.

7.1 Control architecture and problem statement

The control architecture for non-cooperative platooning is shown in Figure 7.1. As in this chapter we focus on the control of the second vehicle, for simplicity of notation index 2, corresponding to the vehicle under control, is dropped. The vehicle-following planner receives the preceding vehicle predicted profile $\hat{x}_1(\cdot) = [\hat{v}_1(\cdot), \hat{s}_1(\cdot)]^T$ and computes the fuel-optimal speed trajectory \bar{v} and the gear sequence $\bar{\mathcal{G}}$. The optimal speed trajectory and gear sequence are then tracked by the vehicle controller presented in the previous chapter in Section 6.3.

The problem of the vehicle-following planner can be synthesized by the optimal control problem formulation displayed in Figure 7.2. The goal is to minimize the fuel consumption of the vehicle exploiting the prediction of the preceding vehicle trajectory, topography information and a vehicle model. As the vehicle-following planner is not handling safety critical aspects and the preceding vehicle predicted trajectory is expected to be slowly varying, the optimization refresh time can be relatively large, of the order of a few seconds.

7.2 Modeling

In this section, we present the vehicle model, the fuel model and the model constraints that will be used in the optimal control formulation.

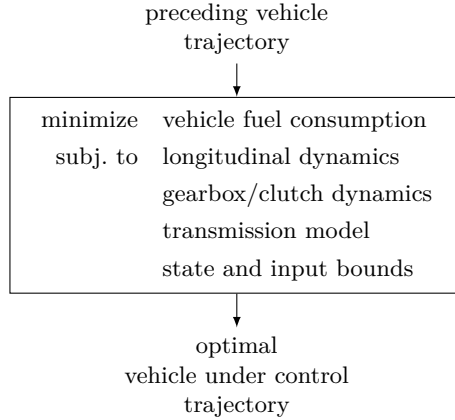


Figure 7.2: Formulation of the vehicle-following optimal control problem.

7.2.1 Vehicle model

The vehicle under control is modeled as a hybrid system. The continuous control inputs are the engine torque T and braking force F_b (collected in the vector $u = [T, F_b]^T$), while the discrete control input is the gear request g_r .

The continuous states characterize the longitudinal dynamics. The state variables are the vehicle under control speed v and the distance to the preceding vehicle d (collected in the state vector $x = [v, d]^T$). The longitudinal vehicle dynamics are described by the differential equations

$$\dot{x} = \begin{bmatrix} \dot{v} \\ \dot{d} \end{bmatrix} = f_1(x, F_t, F_b) = \begin{bmatrix} \frac{1}{m} (F_t + F_b + F_{\text{ext}}(x)) \\ \hat{v}_1 - v \end{bmatrix}. \quad (7.1)$$

The first equation represents the force balance with respect to the longitudinal direction, where the term

$$F_{\text{ext}}(x) = -mg_a \sin \alpha (\hat{s}_1 - d - l_1) - mg_a c_r - \frac{1}{2} \rho A_v C_d(d) v^2$$

collects all the external forces acting on the vehicle, while the second equation defines the distance dynamics. The definition of the vehicle parameters is introduced in Chapter 3 and synthesized in Table ch7:vehicleparameters.

The gearbox-clutch dynamics are characterized by the discrete state g and are described by the automaton presented in Section 3.2 and displayed in Figure 3.5. Here, we recall that such automaton describes both the timing of gear shifts and

freewheeling. In the remainder of the chapter, we refer to this model as

$$g^+ = f_2(g, g_r, \tau_g) \quad (7.2)$$

where τ_g represents the automaton clock.

Finally, the transmission model maps the engine variables (engine speed and torque) to the vehicle variables (vehicle speed and traction force). In order to limit the model complexity, the engine inertia is neglected. This allows to define the engine speed as a state-dependent variable rather than a state, resulting in a significantly reduced complexity of the dynamic programming implementation. The transmission is therefore modeled according to the model presented in Section 3.2 and synthesized by equations (3.11) and (3.12). We will refer to these equations as

$$F_t = F_t(g, T) \quad \text{and} \quad \omega = \omega(v, g). \quad (7.3)$$

7.2.2 Fuel model

The vehicle fuel consumption is computed by integrating over the prediction horizon H_{DP} the fuel flow according to

$$\int_t^{t+H_{DP}} \varphi(\omega, T) d\tau, \quad (7.4)$$

where t denotes the current time. The fuel map $\varphi(\cdot, \cdot)$ refers to a heavy-duty vehicle engine, whose brake specific fuel consumption (BSFC) map is shown in Figure 7.3. The map represents a 450 hp diesel engine that has been obtained by modifying the original BSFC map of a Scania engine.

7.2.3 Model constraints

Here, we present the constraints acting on the vehicle inputs and states:

- The engine speed and torque are bounded by

$$\omega_{\min} \leq \omega \leq \omega_{\max}, \quad (7.5a)$$

$$T_{\min}(\omega) \leq T \leq T_{\max}(\omega). \quad (7.5b)$$

The limitations on the engine speed and the upper bound on the torque are necessary to guarantee the correct functioning of the engine. The lower bound on the torque, instead, represents the braking engine torque when no fuel is injected. These limits are depicted in Figure 7.3 as black lines.

- The vehicle speed is bounded by

$$v_{\min} \leq v \leq v_{\max} \quad (7.6)$$

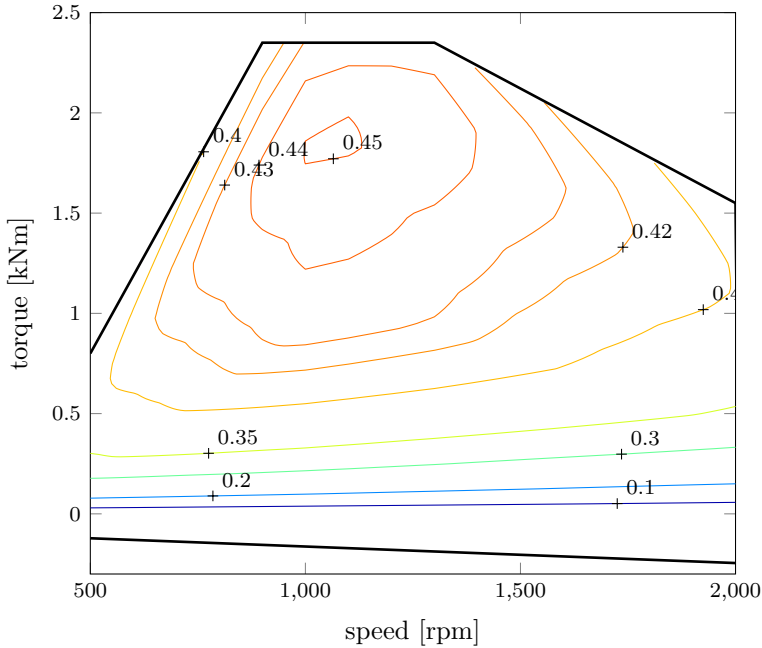


Figure 7.3: Realistic BSFC map of a 450 hp engine used in the simulation. The map has been obtained by modifying the original map of a Scania engine. The contour lines represent operation points with same efficiency.

in order to take speed limits into account. For the sake of simplicity, the speed limits are assumed to be constant, although space-varying speed limits can be handled with no increase of the problem complexity.

- The distance is bounded by

$$d_{\min} \leq d \leq d_{\max}. \quad (7.7)$$

The lower and upper bounds represent the safe and maximum distance allowed for platooning, respectively.

- The braking force is bounded by

$$F_{b,\min} \leq F_b \leq 0. \quad (7.8)$$

- The requested gear g_r is constrained by

$$g_r \in \{0\} \cup \mathcal{G}_a \quad \text{or} \quad g_r \in \mathcal{G}_a, \quad (7.9)$$

depending on whether freewheeling is allowed. Here, we recall that $\mathcal{G}_a = \{i \in \mathbb{N} | i \in [g_{\min}, g_{\max}]\}$ represents the set of admissible gears and $g_r = 0$ indicates that freewheeling is required.

These constraints are summarized by

$$c(x, u, g, g_r) \in \mathcal{C}(\omega). \quad (7.10)$$

7.3 Vehicle-following planner

In this section, we first present the optimal control problem formulation for the vehicle-following planner, obtained by combining the vehicle model, the fuel model and the model constraints. Then, we discuss how the optimal control problem is implemented using dynamic programming and we analyze the complexity of such implementation.

7.3.1 Optimal control problem

The problem solved by the vehicle-following planner can be now formulated by the following optimal control problem:

$$\underset{u(\cdot|t), g_r(\cdot|t)}{\text{minimize}} \quad \int_t^{t+H_{\text{DP}}} \varphi(\omega(v(\tau|t), g(\tau|t)), T(\tau|t)) d\tau \quad (7.11a)$$

$$\text{subj. to} \quad \dot{x}(\tau|t) = f_1(x(\tau|t), F_t(g(\tau|t), T(\tau|t)), F_b(\tau|t)), \quad (7.11b)$$

$$g^+(\tau|t) = f_2(g(\tau|t), g_r(\tau|t), \tau_g(\tau|t)), \quad (7.11c)$$

$$c(x(\tau|t), u(\tau|t), g(\tau|t), g_r(\tau|t)) \in \mathcal{C}(\omega(v(\tau|t), g(\tau|t))), \quad (7.11d)$$

$$v(t|t) = v(t), \quad (7.11e)$$

$$s(t|t) = s(t), \quad (7.11f)$$

$$g(t|t) = g(t), \quad (7.11g)$$

for $\tau \in [t, t + H_{\text{DP}}]$. Here, $x(\tau|t)$, $g(\tau|t)$, $u(\tau|t)$ and $g_r(\tau|t)$ denote the continuous and discrete states and inputs at time τ predicted at time t , while constraints (7.11e)–(7.11g) represent the optimal control problem initial conditions.

7.3.2 Dynamic programming implementation

The optimal control problem (7.11) is solved by dynamic programming. To this end, discretization over time, and over the continuous input and states is carried out. We denote with n_v , n_d , n_T and n_{F_b} the number of discretization points for the speed, the distance, the torque and the braking force, respectively. Δt_{DP} denotes the discretization time, while $N_{\text{DP}} = \lceil H_{\text{DP}}/\Delta t_{\text{DP}} \rceil$ the number of time steps over the

prediction horizon. Here, the operator $\lceil \cdot \rceil$ denotes the upper integer approximation of the argument. The new discretized inputs and states are represented by adding the time step subscript k to the original variables, e.g., $x_k = x(k\Delta t_{\text{DP}})$. Such discretization allows to apply an adaptation (as explained in the next paragraph) of the Bellman equation (2.3) presented in Section 2.5 to the formulated optimal control problem obtaining the following expression:

$$J_k(x_k, g_k) = \min_{u_k, g_{r,k}} \left\{ q_j(x_k, g_k, u_k, g_{r,k}) + \tilde{J}_{k+j}(\xi_j(x_k, g_k, u_k, g_{r,k}), g_{r,k}) \right\}, \quad (7.12)$$

where

- $J_k(x_k, g_{r,k})$ represents the cost-to-go at time $k\Delta t_{\text{DP}}$ (i.e., the optimal fuel consumption from $k\Delta t_{\text{DP}}$ until the end of the horizon H_{DP}) as function of the current state $[x_k, g_k]^T$.
- $\tilde{J}_k(\cdot, \cdot)$ extends the map $J_k(\cdot, \cdot)$ to the points between the discretized states by linear interpolation.
- $q_j(x_k, g_k, u_k, g_{r,k})$ represents the local fuel cost from time $k\Delta t_{\text{DP}}$ to time $(k+j)\Delta t_{\text{DP}}$ by starting from state $[x_k, g_k]^T$ and applying input $[u_k, g_{r,k}]^T$. The fuel cost has been obtained by simulating the vehicle model (7.1–7.3) and integrating (7.4).
- $\xi_j(x_k, g_k, u_k, g_{r,k})$ represents the state x_{k+j} obtained by simulating the vehicle model (7.1–7.3) for time $j\Delta t$ with initial condition $[x_k, g_k]^T$ and input $[u_k, g_{r,k}]^T$.

The aforementioned simulations and integrations between the dynamic programming time steps are carried out using the explicit Euler method with discretization time $\Delta t_{\text{DP}}/n_{\text{sim}}$. By defining the final cost $J_{N_{\text{DP}}}(\cdot, \cdot) = 0$ and proceeding backward, equation (7.12) can be exploited to compute a closed-loop control law for each time step $k \in \{0, \dots, N_{\text{DP}} - 1\}$.

Unlike the conventional Bellman equation, the number of local time steps j is not limited to 1, but is a function of the current state and input, i.e., $j = j(x_k, g_k, u_k, g_{r,k})$. This is exploited, for example, when we compute the argument of $\min\{\cdot\}$ in equation (7.12) for $g_k \in \mathcal{G}_a$ and $g_{r,k} = 0$ (i.e, the cost of requesting freewheeling when a gear is engaged), and $\tau_{\text{fw}} > \Delta t_{\text{DP}}$. Since, after requesting freewheeling, no control input can affect the state for a time span of τ_{fw} , the vehicle model can be simulated for a time of $j\Delta t_{\text{DP}}$, where $j = \lceil \tau_{\text{fw}}/\Delta t_{\text{DP}} \rceil$. In this way, the clock τ_g of the automaton describing the gearbox-clutch dynamics does not need to be treated as a state in the dynamic programming implementation resulting in a reduced complexity of the algorithm.

Table 7.1: Vehicle parameters.

m	vehicle mass	t	30, 40, 50
l_1	first vehicle length	m	18
c_r	rolling coefficient	-	0.005
A_v	cross-sectional vehicle area	m ²	10
$C_{d,0}$	nominal drag coefficient	-	0.6
$C_{d,1}$	first drag reduction coefficient	m ⁻¹	12.8
$C_{d,2}$	second drag reduction coefficient	m	19.7
τ_{fw}	freewheel minimum time	s	8
τ_{shift}	gear-shift time	s	2
ω_{min}	minimum engine speed	rpm	500
ω_{max}	maximum engine speed	rpm	2000

7.3.3 Complexity analysis

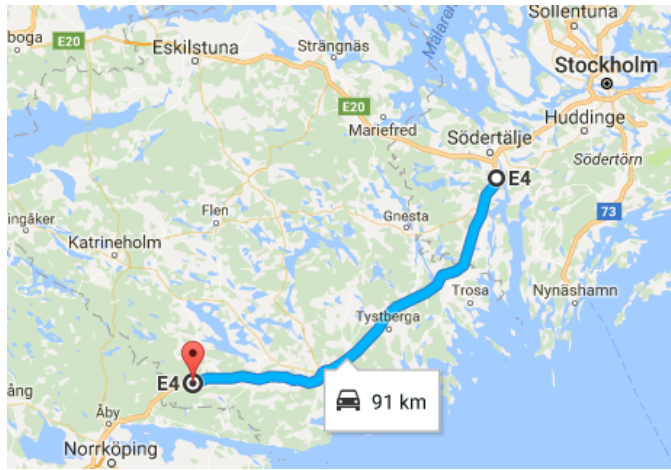
At each time step $k \in \{0, \dots, N_{DP} - 1\}$ and for each pair $(x_k, g_{r,k})$, we solve equation (7.12). Solving each instance of equation (7.12) requires to compare as many cost values as the number of possible input combinations. We note however that the inputs T and F_b are intuitively mutually exclusive, i.e., it is inefficient to throttle and brake at the same time. The complexity of the dynamic programming implementation is therefore

$$\mathcal{O}(N_{DP} n_v n_d (n_T + n_{F_b}) n_{sim} n_g), \quad (7.13)$$

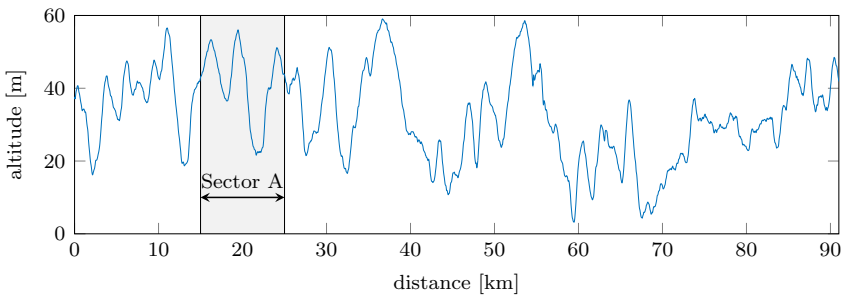
where n_g denotes the number of gears including freewheeling, if exploited. If necessary for real-time implementation, the complexity can be further reduced, for example, by limiting the state space to the robust control invariant set.

7.4 Simulation study

In order to understand the benefits of non-cooperative platooning, in this section we compare the performance of the proposed controller with scenarios where the vehicle under control is driving alone or is following another vehicle using a reference control strategy. The study is conducted considering different masses of the vehicle under control. This allows to analyze how the performance of the various control strategies is affected by the mass distribution in the platoon.



(a) Road map (Map data ©2018 Google).



(b) Road topography.

Figure 7.4: Benchmark highway stretch between the cities of Södertälje and Jönköping, Sweden.

7.4.1 Simulation setup

The vehicle under control is characterized by the parameters' values displayed in Table 7.1. The benchmark road is the highway stretch of 91 km displayed in Figure 7.4 between the cities of Södertälje and Jönköping, Sweden. The topography profile of such road is considered moderately hilly, with a slope grade varying between $\pm 3\%$. The values of the controller parameters are displayed in Table 7.2.

In the simulation study, we assume that the prediction of the preceding vehicle trajectory is exact. Furthermore, the horizon H_{DP} is set long enough such that the whole 91 km road stretch is covered. The vehicle is then controlled using the optimal control feedback law returned by the dynamic programming solution.

We compare the performance of multiple longitudinal control strategies that include scenarios where the vehicle under control is following another one and

Table 7.2: Controller parameters.

all control strategies			
H_{DP}	prediction horizon	s	3800
Δt_{DP}	DP discretization time	s	4
n_{sim}	simulation points per DP step	-	4
n_v	speed discretization points	-	21
n_T	torque discretization points	-	37
n_{F_b}	braking force discretization points	-	51
v_{min}	minimum speed	m/s	19
v_{max}	maximum speed	m/s	25.5
$F_{b,\text{min}}$	minimum braking force	kN	-20
g_{min}	minimum allowed gear	-	13
g_{max}	maximum allowed gear	-	14
driving-alone control strategies			
d_{min}	minimum distance	m	-100
d_{max}	maximum distance	m	100
n_d	distance discretization points	-	157
vehicle-following control strategies			
d_{min}	minimum distance	m	20
d_{max}	maximum distance	m	100
n_d	distance discretization points	-	63

scenarios where it is driving alone. All these scenarios are simulated by adapting the optimal control problem formulation (7.11), as detailed below. The mass of the vehicle under control varies in the different simulation sets between 30, 40 and 50 tonnes. The preceding vehicle, when present, has a mass of 40 tonnes for all the simulations. The control strategies that we compare are divided in the two following categories:

- Driving-alone control strategies:
 - Look-ahead control (LAC) without freewheeling: the vehicle under control optimizes its speed trajectory exploiting road topography information without using freewheeling. This is achieved by redefining $C_d(d) = C_{d,0}$ in the longitudinal dynamics (7.11b) and $g_r \in \mathcal{G}_a$ in constraint (7.11d), and

defining d_{\min} and d_{\max} according to the values displayed in the central part of Table 7.2.

- LAC with freewheeling: similarly to the previous controller, but allowing freewheeling, i.e., $g_r \in \{0\} \cup \mathcal{G}_a$ in constraint (7.11d).
- Vehicle-following control strategies (the preceding vehicle uses the LAC without freewheeling control strategy):
 - Adaptive cruise control (ACC): the vehicle under control keeps a fixed distance from the preceding vehicle, equal to the minimum allowed distance d_{\min} . The engaged gear is the maximum gear that allows to generate the required traction force. For comparison purpose, the gearshift is assumed to be instantaneous.
 - Look-ahead adaptive control (LAAC) without freewheel: the vehicle under control uses the proposed controller with $g_r \in \mathcal{G}_a$ in constraint (7.11d).
 - LAAC with freewheeling: similarly to the previous controller, but allowing freewheeling, i.e., $g_r \in \{0\} \cup \mathcal{G}_a$ in constraint (7.11d).

The simulations run in @MATLAB on a PC with a two-core CPU running at 2.4 GHz and 8 GB of memory RAM. The computation of the optimal closed-loop control law over the whole horizon H_{DP} takes 580 and 165 s for the driving-alone and the vehicle-following cases, respectively (the difference is mainly due to different distance range allowed in the two cases). As the complexity of the dynamic programming algorithm grows linearly with the horizon length H_{DP} , we expect that reducing the horizon length to few minutes can drastically reduce the computation time. Furthermore, implementing the algorithm in a lower-level language as C/C++ and running it on a hardware with parallel architecture as a GPU can additionally reduce this time. These modifications could allow to solve the dynamic programming problem in real-time in the look-ahead planner block displayed in Figure 7.1.

7.4.2 Control strategies comparison

The fuel consumption reduction for all combinations of control strategies and vehicle masses is summarized in Table 7.3. The saved fuel is normalized with respect to the fuel consumption of the LAC without freewheeling controller case. The traveled time and distance are the same in all scenarios.

The left side of Table 7.3 shows the fuel consumption reduction for the driving-alone control strategies. The corresponding behavior of the vehicle driving along a portion of the 91 km stretch highlighted as Sector A in Figure 7.4 is displayed in Figure 7.5. The possibility to freewheel allows the vehicle to save between 2.7 and 4.1 % of fuel. Observing Figure 7.5, we can notice how, in the freewheel case, the vehicle alternates phases of coasting with phases of traction during which the engine

Table 7.3: Fuel consumption reduction [%]

vehicle mass	driving-alone		vehicle-following		
	LAC w/o freewheel	LAC w/ freewheel	ACC	LAAC w/o freewheel	LAAC w/ freewheel
	30 t	0	4.1	12.4	14.5
40 t	0	3.1	8.9	12.5	15.5
50 t	0	2.7	5.1	10.3	12.7

is operating close to the optimal point (this is approximately around 2 kNm as shown in Figure 7.3) and the alternation is adjusted to the road slope. This control strategy is known as PnG.

Remark 7.4.1. The PnG strategy does not exhibit in the case where freewheeling is not allowed as it could be expected by surveying the literature on passenger vehicle optimal control, see, e.g., Lee (2009); Li and Peng (2011). This is probably due to the fact that energy losses at nominal engine speed are relatively higher for trucks respect to cars. However, we expect that the results can variate depending on the used fuel map.

The right side of Table 7.3 shows the fuel consumption reduction for the vehicle-following control strategies. We focus first the attention on the homogeneous platoon case (i.e. preceding and vehicle under control have the same mass) displayed in the middle row of the table for which simulation results are reported in Figure 7.6. In all three cases fuel consumption reduction is registered thanks to the creation of the slipstream effect. The lowest fuel saving is measured in the ACC case. Although maintaining the minimum distance d_{\min} allows to maximize the slipstream effect, it also leads to some phases of braking as evident in the simulation results displayed in Figure 7.6. The braking in the ACC case is attributable to two cases: (i) The reduced aerodynamic drag translates into braking when the preceding vehicle is coasting. (ii) Since the preceding vehicle experiences the changes of slope grade before the vehicle under

apply a larger longitudinal force when the slope grade is decreasing, and a smaller longitudinal force when the slope grade increases. The smaller longitudinal force phases can result in the braking of the vehicle under control when the preceding is exhibiting a close-to-coasting behavior. This phenomenon has been also experienced in the experiment presented in Section 4.1, where a constant headway gap has been used. The optimal control problem solved in the two LAAC controllers allows to fuel-optimally regulate the distance and therefore to avoid the described braking. In particular, in the homogeneous case, LAAC allows to save 3.6 and 6.6 % of fuel when freewheeling is not and it is used, respectively. Note that the additional fuel

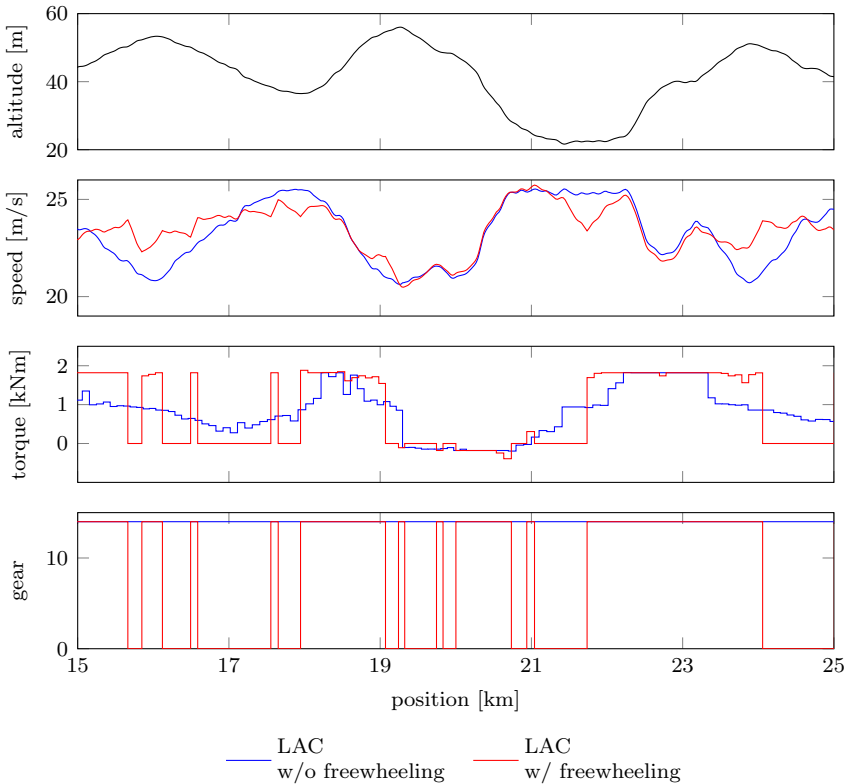


Figure 7.5: Simulation results for a heavy-duty vehicle of 40 tonnes driving alone and using look-ahead control with and without freewheeling. The torque displayed in the third plot includes the engine torque and a scaled version of the braking force.

saving brought by the use of freewheeling is comparable to the one achieved in the driving-alone control case. This result confirms the possibility to combine the benefits of a platooning with those of PnG control.

Finally, we analyze the vehicle-following control strategies for the heterogeneous platoon case, summarized in the first and third row of Table 7.3. The ACC performance deteriorates relatively to the LAACs when the vehicle mass increases. This is due to the increased coasting acceleration during downhills when the vehicle mass is larger that leads to stronger braking action while ACC is used. This is noticeable in the simulation results for the 50 tonnes vehicle case displayed in Figure 7.7, where the vehicle under control needs to apply larger braking torque compared to the 40 tonnes vehicle case displayed in Figure 7.6. This issue is addressed by LAAC controllers by increasing the inter-vehicular distance before downhills, as evident in Figure 7.7. However, due to the large downhill acceleration and the narrow bounds

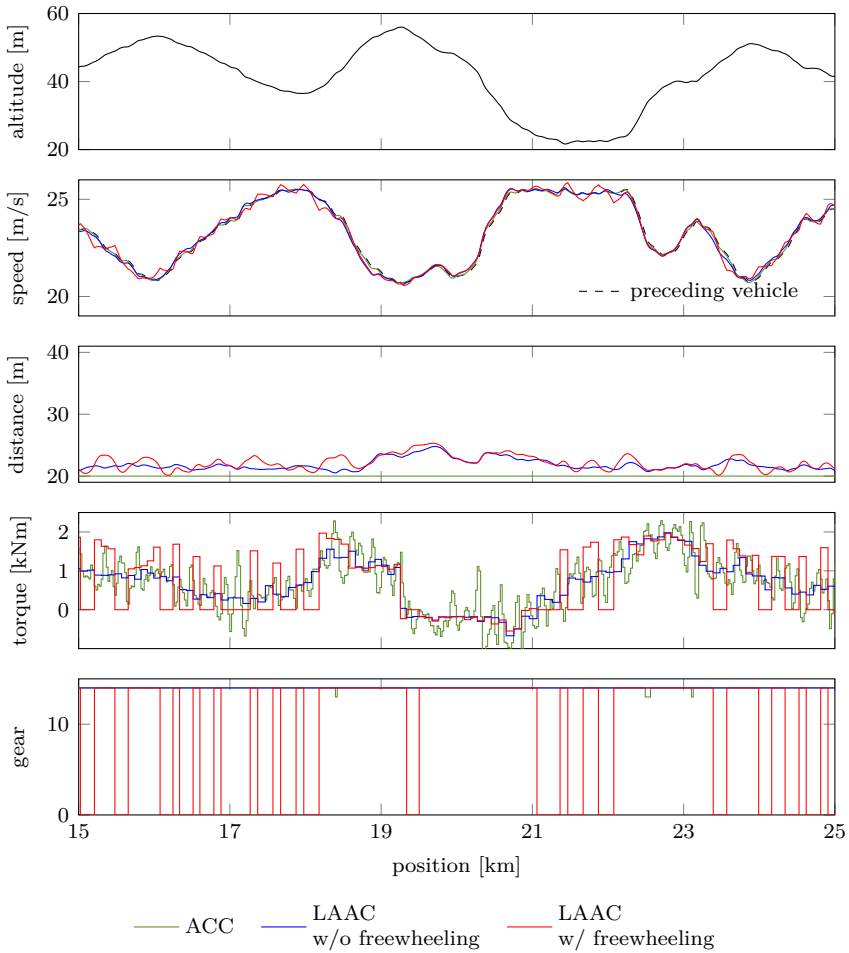


Figure 7.6: Simulation results for a 40 tonnes vehicle using multiple vehicle-following control strategies. The torque plot is explained in the caption of Figure 7.5.

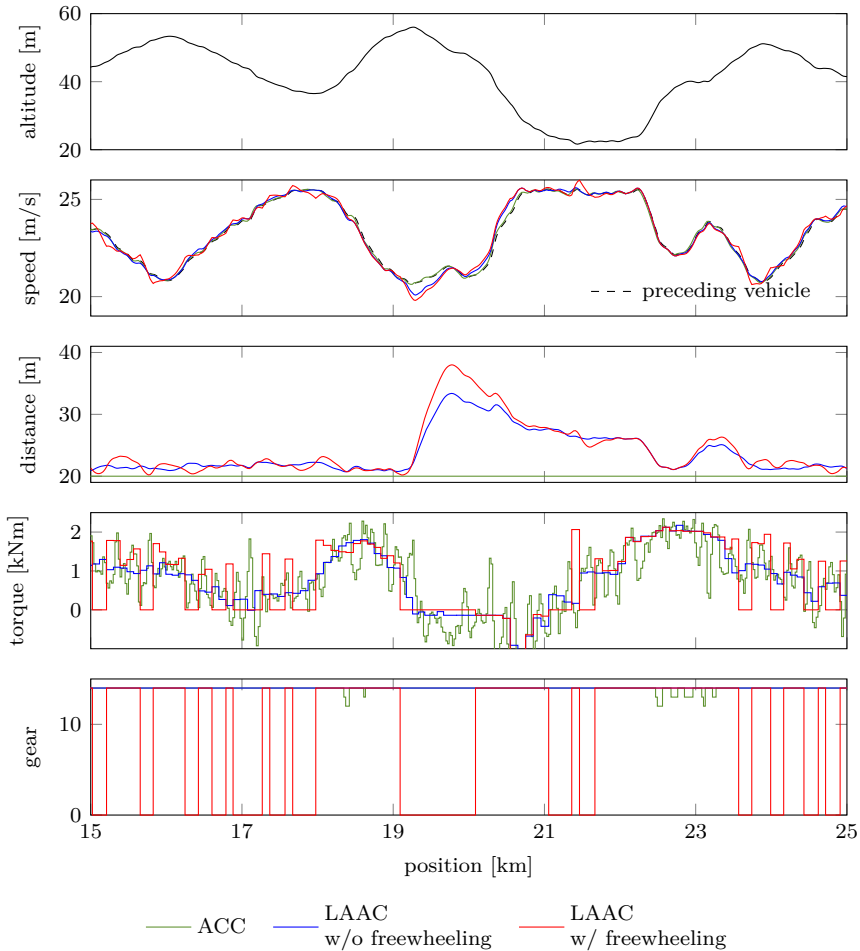


Figure 7.7: Simulation results for a 50 tonnes vehicle using multiple vehicle-following control strategies. The torque plot is explained in the caption of Figure 7.5.

on the vehicle speed, braking cannot be fully avoided.

7.5 Summary

In this chapter, we discussed the fuel-optimal vehicle-following problem for heavy-duty vehicles, where no cooperation between vehicles is possible or desired. We proposed a dynamic programming formulation that exploits topography information and the prediction of the preceding vehicle future trajectory to optimally control the vehicle under control. Since the vehicle model used in the dynamic programming

formulation includes both the longitudinal dynamics and a detailed model of the powertrain, the controller is able to explore the benefits of PnG. We recall that a PnG technique consists in alternating phases of throttling at engine operation points closed to the optimal one with phases of freewheeling, i.e, driving in neutral gear.

The proposed controller has been tested in a simulation study that shows its capability to fuel-efficiently control the vehicle in both homogeneous and heterogeneous platoon scenarios. In particular, the controller is able to adapt the vehicle behavior in order to find the optimal balance between short inter-vehicular distance, no braking action and the exploitation of the PnG technique when freewheeling is allowed. When the constraints corresponding to the speed limits and the distance upper bound are not activated, the controller tries to maintain a small inter-vehicular distance if it does not lead to future braking action. With the availability of freewheeling, the controller also modulates the control inputs according to the PnG technique. These insights will be the base for the design of the lower complexity controller presented in the next chapter.

Low complexity vehicle-following control

In this chapter, we discuss a vehicle-following controller suitable for the fuel-efficient control of passenger cars. The controller receives a prediction of the preceding vehicle trajectory and directly manipulates the inputs of the low-level vehicle controllers. This requires the vehicle-following controller (i) to exploit long previews of the preceding vehicle trajectory for effective fuel-efficiency and (ii) to run fast enough for real-time implementability. These conditions are conflicting as the exploitation of a long preview suggests for a long prediction horizon, while the fast computation calls for a short one. To address this conflict, we propose a model predictive control (MPC) formulation that uses a relatively short horizon and compensates for that by redefining the cost function and introducing a specifically designed terminal state constraint. In particular, the cost function is redefined to include terms that promote the long term fuel-efficient behavior of the vehicle. The terminal state set is designed to include all states that, given the prediction of the preceding vehicle future trajectory, will not require vehicle braking action after the end of the prediction horizon. This choice is driven by the consideration that the main source of fuel-inefficiency, when preview information is not exploited, is in fact braking, as discussed in Section 4.1.

The proposed vehicle-following controller is tested in both real vehicle experiments and simulations. The experiments show that the proposed MPC formulation avoids unnecessary braking and can significantly improve fuel economy and ride comfort. Remarkably, the proposed terminal set can conveniently exploit long previews, while keeping the length of the MPC horizon limited to a few seconds, thus making the real-time implementation realistic. The simulation study shows how the vehicle behavior is comparable when using the proposed controller and when using a similar controller that relies on a significantly longer horizon, representing an approximation of the (acausal) optimum.

The chapter is organized as follows. Section 8.1 presents the control architecture and states the optimal control problem formulation. Section 8.2 illustrates the

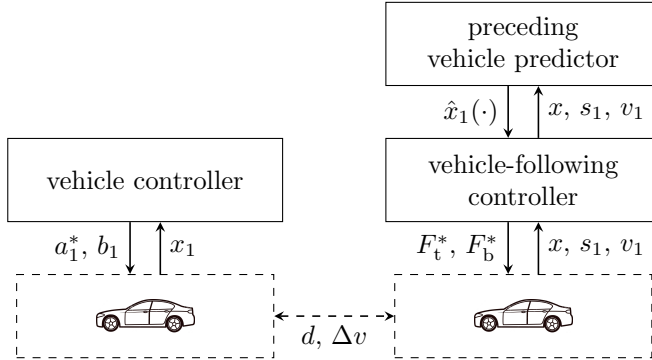


Figure 8.1: Adaptation of the control architecture for non-cooperative platooning.

optimal vehicle-following control formulation, putting a particular emphasis on the terminal state constraint definition. Section 8.3 summarizes the experimental results from the implementation of the proposed controller on a real vehicle. Section 8.4 shows with simulations how the terminal state constraint gives long-sight to the controller. Finally, Section 8.5 concludes the chapter.

8.1 Control architecture and problem statement

In this section, we introduce the control architecture employed in this work and we state the problem formulation for the vehicle-following controller.

The control architecture displayed in Figure 8.1 represents a simplification of the one presented in Section 4.3, as the vehicle-following planner and vehicle controller blocks have been merged in the vehicle-following controller. Here, the preceding vehicle predictor computes a prediction of the preceding vehicle future trajectory over a time H_P , referred to as $\hat{v}_1(\cdot)$. The vehicle-following controller receives such prediction and exploits it to fuel-efficiently control the vehicle by computing the low-level vehicle controller inputs, namely the reference traction and braking forces, F_t^* and F_b^* , respectively.

As the vehicle-following controller is directly interacting with the low-level controllers, it is required to run at a relatively high refresh rate. This is achieved by maintaining a short prediction horizon $H_{MPC} < H_P$ and defining a terminal state set that incorporates the preview information about the preceding vehicle. In particular, the terminal state set is defined as the set of all states that do not require braking action in the time interval $[t + H_{MPC}, t + H_P]$, as braking has been identified as one of the main causes of inefficiency when a short horizon is used. The cost function is defined in order to promote the long term fuel-efficient behavior of the vehicle and ride comfort. In detail, it penalizes deviations from a reference short inter-vehicular

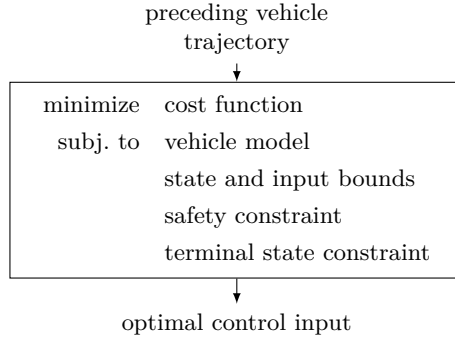


Figure 8.2: Formulation of the vehicle-following optimal control problem.

distance \bar{d} , braking actions and fluctuations of the control input. The cost function minimization is subjected to vehicle dynamics and model constraints, as synthesized in the formulation displayed in Figure 8.2.

8.2 Vehicle-following control

In this section, we present the vehicle model, the model constraints, the cost function and the terminal state constraint that will be employed in the MPC formulation.

8.2.1 Vehicle model

The passenger vehicle model used in the MPC formulation includes the model of the longitudinal dynamics, the distance and the actuator and can be summarized by the following differential equations:

$$\dot{x} = \begin{bmatrix} \dot{v} \\ \dot{d} \\ \dot{F} \end{bmatrix} = f(x, u) = \begin{bmatrix} \frac{1}{m} (F + F_{\text{ext}}(x)) \\ \hat{v}_1 - v \\ \frac{1}{\tau_a} (-F + F_t + F_b) \end{bmatrix}. \quad (8.1)$$

Here, v , d and F denote the speed, the inter-vehicular distance and the longitudinal force, respectively, and they are collected in the state vector $x = [v, d, F]^T$. F_t and F_b denote the traction and braking forces, respectively, and they are collected in the control input vector $u = [F_t, F_b]^T$. Finally, \hat{v}_1 represents the predicted speed of the preceding vehicle and

$$F_{\text{ext}}(x) = -mg_a c_r - \frac{1}{2} \rho A_v C_d (d) v^2$$

collects all the external forces acting on the vehicle. Here, we point out that the gravitational force has been ignored. The parameter definition is provided in Table 8.1 and discussed in detail in Chapter 3.

8.2.2 Model constraints

The model is bounded by the following constraints on inputs and states:

- The vehicle speed is bounded by

$$v_{\min} \leq v \leq v_{\max} \quad (8.2)$$

in order to take speed limits into account.

- The braking and traction forces are bounded by

$$0 \leq F_t \leq F_{t,\max}, \quad (8.3a)$$

$$F_{b,\min} \leq F_b \leq 0, \quad (8.3b)$$

where $F_{t,\max}$ represents a conservative approximation of the maximum traction force.

- Finally, we introduce a simplified version of the safety constraint:

$$d \geq d_{\min}, \quad (8.4)$$

where d_{\min} denotes the minimum allowed distance. This constraint, differently to that one presented in Section 5.3, does not take unexpected emergency braking of the preceding vehicle into account. In the optimal control formulation, we will refer to these constraints as $c(x, u) \in \mathcal{C}$.

8.2.3 Cost function

The objective of the vehicle-following controller is to reach a high level of fuel-efficiency. However, defining the cost function as only the consumed fuel can lead to undesired behaviors due to the limited length of the prediction horizon required for real-time implementation. For example, the controller could not appreciate the benefits of catching-up a preceding vehicle or the drawbacks of braking as those benefits and drawbacks would likely express themselves after the end of the prediction horizon. The cost function of the vehicle-following controller is therefore formulated to promote the long-term fuel-efficiency of the vehicle and to ensure rider comfort. In detail, it encourages short inter-vehicular distances, while it penalizes braking actions and fluctuations of the actuator force, according to the following

formulation:

$$J_{\text{MPC}}(u(\cdot)) = \int_t^{t+H_{\text{MPC}}} \|d(\tau) - \bar{d}\|_Q + \|F_b(\tau|t)\|_P + \|\dot{F}(\tau)\|_D d\tau. \quad (8.5)$$

where the notation $\|\cdot\|_S$ is defined as $\|x\|_S^2 = x^T S x$ and the Q , P and D are properly selected weights. This formulation combined with the terminal state constraint that ensures no braking action after the prediction horizon, aims at the fuel-efficient behavior of the vehicle under control.

8.2.4 Terminal state constraint

The terminal state constraint aims at preventing that the excessive throttling of the vehicle under control leads to braking action and, therefore, power dissipation, after the end of the prediction horizon. This is achieved by exploiting a preview of the preceding vehicle trajectory that at time t is supposed to be known until time $t + H_P$, where $H_P > H_{\text{MPC}}$. To such end, we define the terminal state set \mathcal{T} as the largest invariant set of the approximated coasting dynamics that satisfies the safety constraint (8.4). The approximated coasting dynamics have been derived from the vehicle model (8.1) by setting the longitudinal force $F = 0$ and by substitution $C_d(\cdot)$ with the conservative approximation $C_{d,0}$. They can be summarized by the following differential equations:

$$\dot{v} = g_a c_r - \frac{1}{2m} \rho A C_{d,0} v^2, \quad (8.6a)$$

$$\dot{d} = \hat{v}_1 - v. \quad (8.6b)$$

The set \mathcal{T} is therefore defined as the set of all the pairs distance-speed at time $t + H_{\text{MPC}}$ from which the coasting dynamics (8.6) does not lead to the violation of the safety constraint (8.4) for $\tau \in \{t + H_{\text{MPC}}, t + H_P\}$, i.e.,

$$\mathcal{T} = \left\{ [d(t + H_{\text{MPC}}|t), v(t + H_{\text{MPC}}|t)]^T \mid \text{dynamics in (8.6)}, \right. \\ \left. d(\tau|t) \geq d_{\min}, \forall \tau \in [t + H_{\text{MPC}}, t + H_P] \right\}, \quad (8.7)$$

where $v(\tau|t)$ and $d(\tau|t)$ denote the vehicle speed and inter-vehicular distance at time τ predicted at time t , respectively.

In order to construct the terminal set \mathcal{T} , we first notice that the coasting speed dynamic (8.6a) depends only on speed and can be therefore integrated to compute the speed trajectory $v(\cdot|t)$ between time $t + H_{\text{MPC}}$ and $t + H_P$ with initial condition $v(t + H_{\text{MPC}}|t)$. At this point, the distance trajectory $d(\cdot|t)$ between time $t + H_{\text{MPC}}$ and $t + H_P$ can be computed integrating (8.6b) as function of the predicted speed

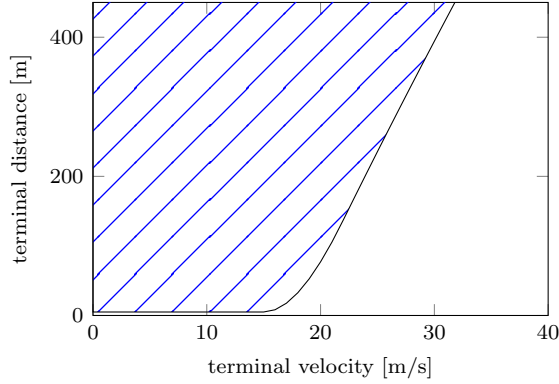


Figure 8.3: Terminal set \mathcal{T} with $\hat{v}_1(\tau) = 25 \text{ m/s}$, $\forall \tau \in [t + H_{\text{MPC}}, t + H_{\text{P}}]$.

trajectory $v(\cdot|t)$, i.e.,

$$d(\tau|t) = d(t + H_{\text{MPC}}|t) + \int_{t+H_{\text{MPC}}}^{\tau} \hat{v}_1(s) - v(s|t) ds, \quad (8.8)$$

for $\tau \in \{t + H_{\text{MPC}}, t + H_{\text{P}}\}$. If we impose the safety constraint (8.4), we obtain

$$d(t + H_{\text{MPC}}|t) \geq d_{\min} - \int_{t+H_{\text{MPC}}}^{\tau} \hat{v}_1(s) - v(s|t) ds, \quad (8.9)$$

that should hold for $\tau \in [t + H_{\text{MPC}}, t + H_{\text{P}}]$. The terminal set \mathcal{T} can be now computed by discretizing the independent-variable time and transforming the integral in inequality (8.9) into summation. By gridding the space of the terminal speed $v(t + H_{\text{MPC}}|t)$ and exploiting (8.9), the pair speed-position of the border of \mathcal{T} can be computed. Figure 8.3 shows the terminal set computed when the preceding vehicle runs at a constant speed of 25 m/s.

8.2.5 Model predictive control formulation

We now have all the elements to state the optimal control problem:

$$\underset{u(\cdot|t)}{\text{minimize}} \quad J_{\text{MPC}}(u(\cdot|t)) \quad (8.10\text{a})$$

$$\text{subj. to} \quad \dot{x} = f(x(\tau|t), u(\tau|t)), \quad (8.10\text{b})$$

$$c(x(\tau|t), u(\tau|t)) \in \mathcal{C}, \quad (8.10\text{c})$$

$$x(t + H_{\text{MPC}}|t) \in \mathcal{T} \times \mathbb{R}, \quad (8.10\text{d})$$

$$x(t|t) = x(t), \quad (8.10\text{e})$$

for $\tau \in [t, t + H_{\text{MPC}}]$. Here, $x(\tau|t)$ and $u(\tau|t)$ denote state and input at time τ predicted at time t , while constraint (8.10e) represents the initial condition.

Table 8.1: Vehicle parameters.

m	vehicle mass	t	2.2
A_v	cross-sectional vehicle area	m ²	3.15
C_d	nominal drag coefficient	-	0.28
c_r	rolling coefficient	-	0.009
τ_a	actuation time constant	s	0.5
$F_{b,\min}$	conservative minimum braking force	kN	-43
$F_{t,\max}$	conservative maximum traction force	kN	3

Table 8.2: Controller parameters.

H_{MPC}	prediction horizon	s	6
H_P	terminal set horizon	s	66
Δt_{MPC}	MPC discretization time	s	0.2
\bar{d}	reference distance	m	20
d_{\min}	minimum distance	m	5
v_{\min}	minimum speed	m/s	0
v_{\max}	maximum speed	m/s	45

By discretizing the independent variable τ with discretization time Δt_{MPC} and solving the resulting optimization problem every Δt_{MPC} the problem is cast into an MPC framework.

8.3 Experimental study

In this section we present the experimental study that we conducted on a full scale vehicle. The goals of this experimental study are to test the proposed control strategy in a representative set of driving scenarios, to demonstrate its practical implementation, and to compare its performance with other baseline approaches.

8.3.1 Experimental setup

The experiments were conducted at the Hyundai-KIA Motors California Proving Grounds, California City, CA, USA. They were run on a full scale following vehicle, while the lead vehicle was simulated. In detail, the radar readings of the vehicle under control were overwritten to take the simulated preceding vehicle into account.

The vehicle used for the experimental tests is equipped with a 3.8 liter V6 engine and an 8-speed automatic transmission. The precise localization of the vehicle in the inertial frame is guaranteed by an OTS RT2002 system, which includes a differential GPS, an inertial measurement unit (IMU) and a digital signal processor (DSP).

Other signals of interest and the control signals are directly obtained from and sent to the vehicle electronic control units (ECUs) via the CAN bus. These signals include wheel speed, fuel flow rate, traction and braking forces. The measured and estimated parameters of the vehicle are displayed in Table 8.1, while the controller parameters in Table 8.2.

The optimization problem (8.10) is solved by a tailored solver automatically generated using Embotech FORCES Pro (Embotech, 2018). The resulting MPC controller and the necessary data processing were implemented and executed in real-time on a dSpace MicroAutobox (dSpace, 2018), which consists of an IBM PowerPC processor capable of running at 900 MHz. In the experiments presented below, the use of a prediction horizon of $H_{\text{MPC}} = 6$ s resulted in the maximum computation time to solve problem (8.10) of 76.4 ms, reasonable for real-time implementation.

8.3.2 Constant speed catch-up

The first experiment reproduces the catch-up of a preceding vehicle driving at a constant speed of 25 m/s. The vehicle under control starts 40 m behind the preceding vehicle at a speed of 7 m/s.

Figure 8.4 shows the experiment results, in terms of speed, distance from the preceding vehicle, and longitudinal control force, i.e. the summation between braking and traction forces. Initially, the controller applies the maximum traction force, so that the large speed gap between the vehicle under control and the preceding vehicle is compensated. The coasting phase starts when the controller predicts that aerodynamic drag, rolling friction, and inertia will decelerate the vehicle, keeping it behind the safety distance d_{min} without additional braking. Coasting brings the following vehicle to a distance from the preceding vehicle smaller than \bar{d} , and, therefore, a second, short acceleration phase is applied to adjust the relative distance to the desired value. Afterwards, the traction force is kept to the constant value that maintains the vehicle under control at the same speed of the preceding vehicle.

The longitudinal force commanded by the controller assumes almost only non-negative values throughout the experiment. Only small deviations from zero are observed in the coasting phase. These deviations are explained by the unavoidable mismatch between the prediction model and the vehicle response in closed loop. Power dissipation through braking is successfully avoided, exploiting the knowledge of the future speed profile of the preceding vehicle.

8.3.3 Sinusoidal speed catch-up

This experiment also considers a catch-up scenario where, however, the preceding vehicle follows a sinusoidal speed profile. The main objective is to show that the proposed controller can successfully catch-up and track the preceding vehicle also when the latter is not following a constant speed profile. The sinusoid has an average

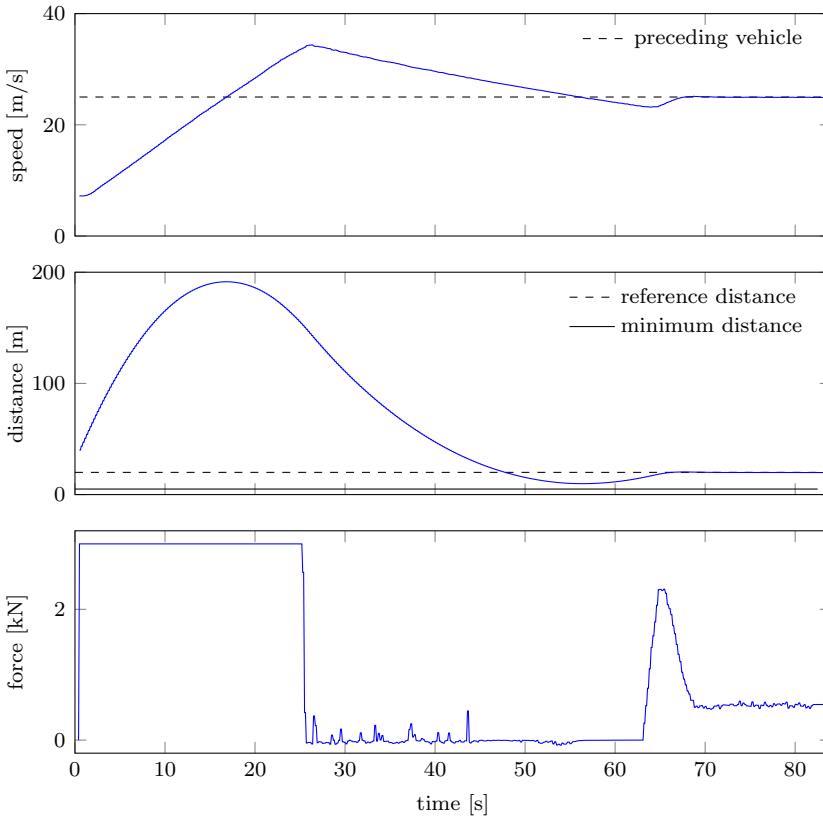


Figure 8.4: Catch-up of a vehicle traveling at constant speed. The plots display the vehicle speeds, inter-vehicular distance, and the longitudinal control force, respectively. In the latter, negatives values denote braking action, while positive values denote traction.

of 22 m/s, an amplitude of 4 m/s and a period of 62.8 s. The vehicle under control is initially 40 m behind the preceding vehicle.

Figure 8.5 shows the closed-loop trajectories of the vehicle under control. During the first 25 s, the controller applies the maximum input to catch-up with the preceding vehicle. Afterwards, the vehicle decelerates by coasting, and starts tracking the sinusoidal speed profile. The behavior during the tracking phase can be observed in the zoomed axes in Figure 8.5 for one period of the sinusoid. A few remarks follow:

- The vehicle under control tracks the sinusoidal speed trajectory of the preceding vehicle without applying any hard braking, nor violating the minimum safety distance. Due to model mismatch, some braking is applied during the coasting phases.

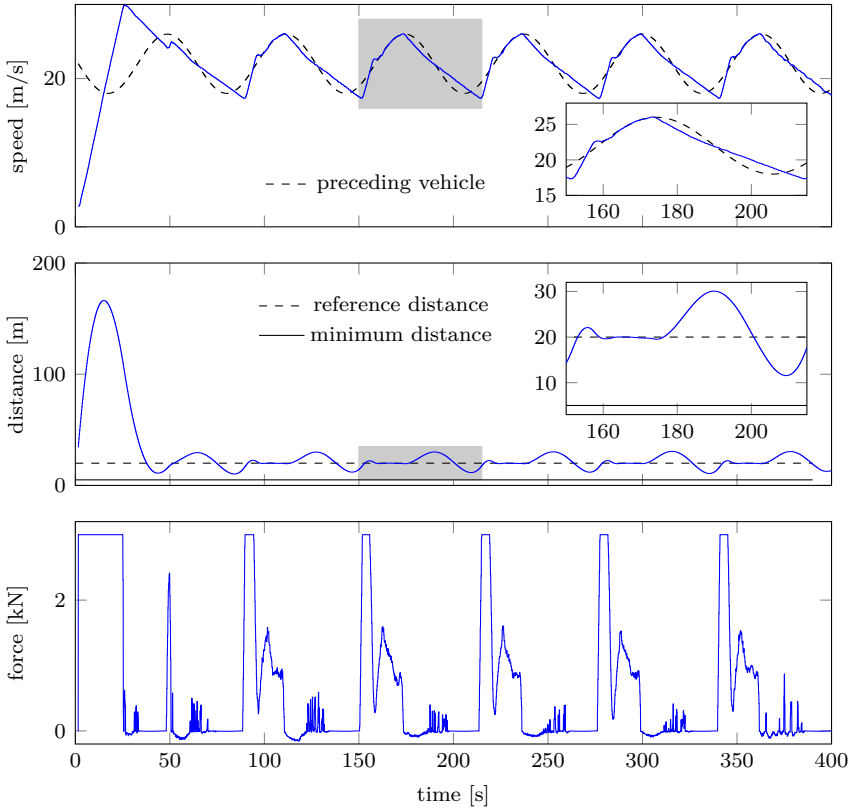


Figure 8.5: Catch-up of a vehicle traveling with sinusoidal speed profile. Zoomed portions show the behavior during one period of the sinusoidal profile.

- During the coasting phases, the relative distance consistently oscillates around the desired value \bar{d} . While the preceding vehicle follows a sinusoidal speed, the vehicle under control aims at coasting. Hence the relative distance first increases over and then decreases below \bar{d} .
- During the accelerating phase, the maximum input force is first applied to match the desired \bar{d} and then the sinusoidal profile is tracked at constant distance until the coasting phase starts.

8.3.4 Performance comparison

Here, we compare the performance of the proposed controller, hereafter referred to as proposed look-ahead adaptive controller (LAAC), with the two following controllers:

- LAAC w/o terminal set. It uses the same formulation of the proposed LAAC expect for the terminal state constraint that is removed.

- LAAC w/o preview. It uses the same formulation of the proposed LAAC, but it does not have access to the preview of the preceding vehicle trajectory. The variable $\hat{v}_1(\cdot)$ is therefore set to the current preceding vehicle speed.

The preceding vehicle follows a sinusoidal speed profile with an average of 14 m/s, an amplitude of 4 m/s and a period of 10.47 s. The vehicle under control starts 40 m behind the preceding vehicle at an initial speed ranging from 6.5 m/s to 9 m/s.

Figure 8.6 compares the trajectories of speed, distance, longitudinal control, and fuel flow rate for the three controllers. The minimum safety distance d_{\min} is maintained throughout the experiments. Every tested controller produces some oscillation in the distance from the preceding vehicle when following the sinusoidal speed reference. The proposed controller and the LAAC w/o terminal set produce smaller distance oscillations, while the LAAC w/o preview shows the biggest oscillation. In particular, the proposed LAAC produces the least fluctuation in speed, resulting in minimum traction force, almost no braking and minimum fuel rate. During the tracking phase (approximately after second 20), the LAAC w/o terminal set behaves similarly to the proposed controller. This is expected because, in this experiment, the prediction horizon is long enough to preview about half period of the sinusoid. Nonetheless, during the catch-up phase (up to second 20), the improvement due to the terminal set is evident, as the LAAC w/o terminal set applies significant braking. Instead, the LAAC w/o preview poorly tracks the profile with large fluctuations in speed, requiring higher traction and braking forces, and fuel rate.

Tables 8.3 and 8.4 summarize the performance of the three controllers, in terms of the fuel consumption and root mean square (RMS) of the vehicle jerk (i.e., the derivative of the vehicle acceleration), during the catch-up and tracking phases, respectively. We define as catch-up phase the segment from 0 to 20 s, and the tracking phase as the segment from 20 to 55 s. Both metrics are normalized with respect to the LAAC w/o preview corresponding metric. During the tracking phase, the LAAC w/o terminal set produces intermediate results, while the proposed controller outperforms both baseline controllers according to both metrics. During the catch-up phase, the controllers have closer performance. The proposed controller is still improving, with about 36 % less fuel and 36 % lower jerk compared to the LAAC w/o preview. Remarkably, the performance of the LAAC w/o terminal set strongly depends on the information contained in the preview $\hat{v}_1(\cdot)$ from time t to time $t + H_{\text{MPC}}$, i.e. during the MPC horizon. Generalizing the performance improvement to some average driving conditions is out of the scope of the present work. Nonetheless, in the representative scenario we selected, performance improvement is consistently attained both during catch-up and during tracking phases.

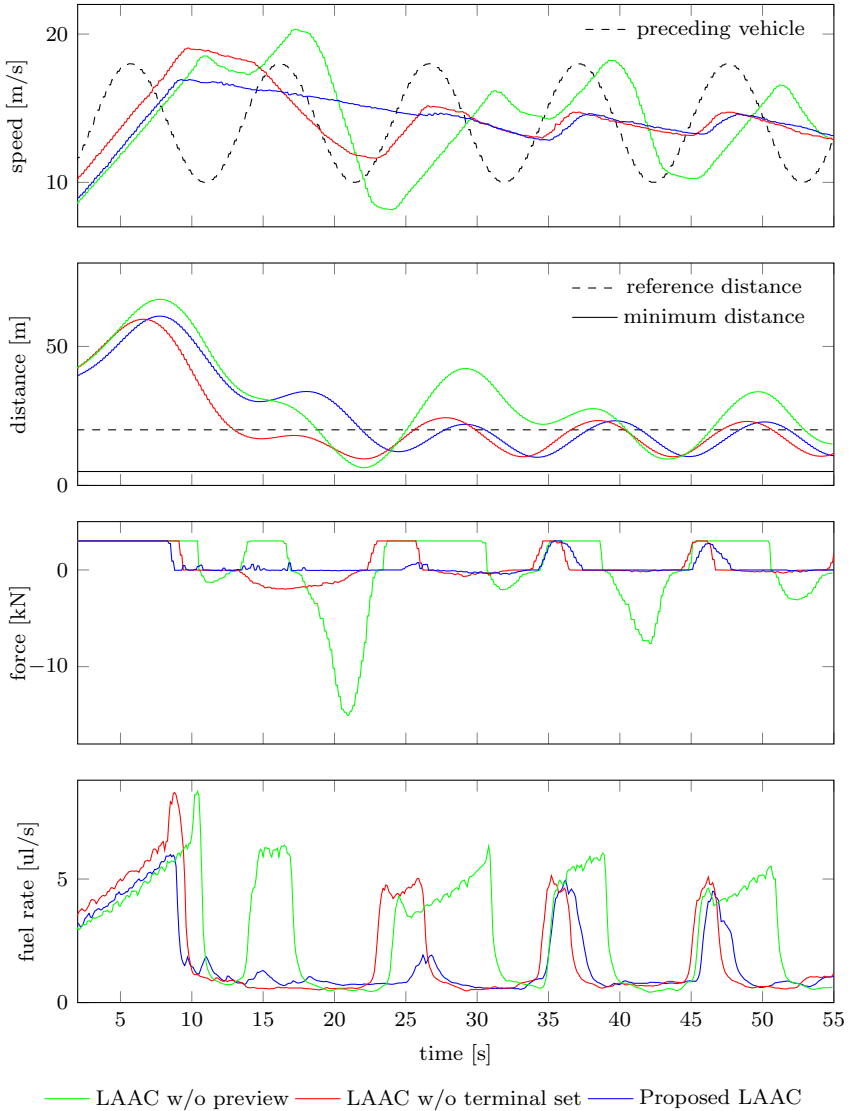


Figure 8.6: Comparison between the proposed controller and two baseline controllers in the catch-up scenario of a vehicle traveling with sinusoidal speed profile.

Table 8.3: Comparison of the controllers in the catch-up phase.

Control strategy	Fuel [%]	Jerk RMS [%]
LAAC w/o preview	100.0	100.0
LAAC w/o terminal set	72.0	83.5
Proposed LAAC	63.8	63.7

Table 8.4: Comparison of the controllers in the tracking phase.

Control strategy	Fuel [%]	Jerk RMS [%]
LAAC w/o preview	100.0	100.0
LAAC w/o terminal set	61.0	37.9
Proposed LAAC	50.0	26.8

8.4 Simulation study

In this section, we present a simulation study conducted in absence of model mismatch. The purpose is to demonstrate how the proposed controller combines a limited prediction horizon with the presented terminal state constraint to approach the performance of a long-sighted controller. We compare the proposed controller with the LAAC w/o terminal set and the LAAC w/ long horizon. The latter uses the same formulation of the proposed controller, but the prediction horizon is set to $H_{\text{MPC}} = 50$ s, and is regarded as an approximation of the acausal optimum. The three controllers follow the realistic speed profile of a preceding vehicle that was recorded in real urban driving. The vehicle under control starts 40 m behind the preceding at a speed of 5 m/s. The optimization problem (8.10) is solved on a laptop with a tailored solver generated by FORCES Pro. The proposed controller and the LAAC w/o terminal set require similar average computational times (8.62 ms and 5.45 ms respectively), while the LAAC w/ long horizon requires significantly higher time (47.12 ms) because of the longer prediction horizon.

Figure 8.7 displays the simulation results. The proposed controller and the LAAC w/ long horizon exhibit very similar behaviors, as both coast whenever possible and avoid excessive throttling and braking. Conversely, the LAAC w/o terminal set is myopic and braking action becomes often inevitable.

8.5 Summary

In this chapter, we discussed a vehicle-following controller suitable for the control of passenger vehicles. The proposed controller aims at reaching high fuel-efficiency, while maintaining a reduced complexity for real-time implementability. This is achieved by defining a model predictive controller that uses a relatively short horizon and

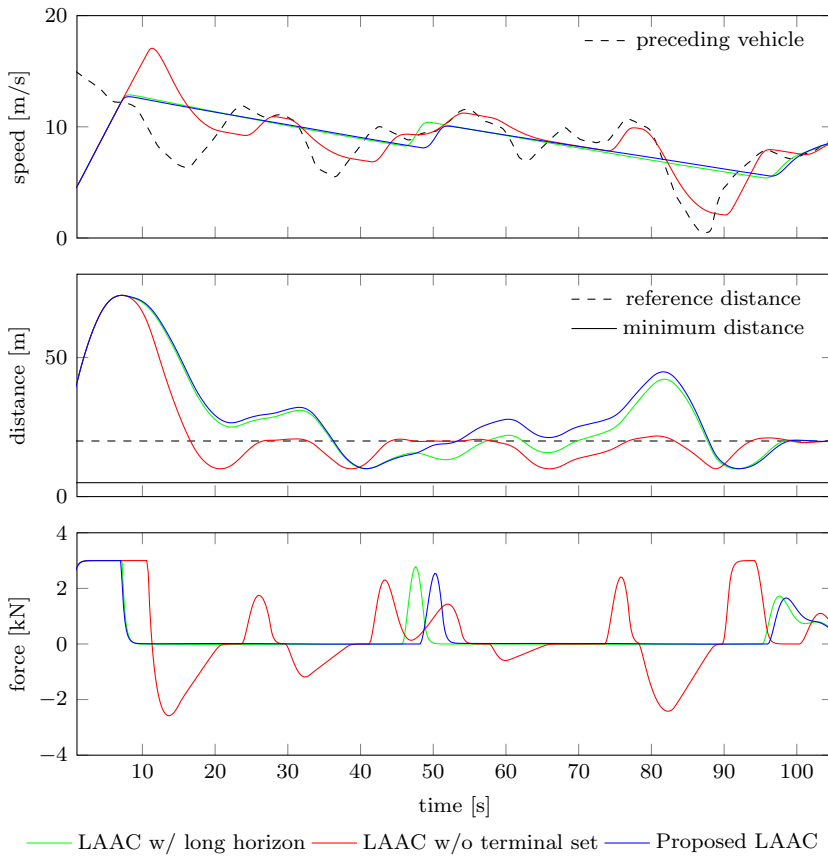


Figure 8.7: Comparison between the proposed controller and two baseline controllers by means of simulation. In the simulated scenario the preceding vehicle is following a realistic speed profile.

compensates for that by redefining the cost function and introducing a specifically designed terminal state constraint. In particular, the cost function is defined to include terms that promote the long term fuel-efficient behavior of the vehicle. The terminal state set is designed to include all states that, given the prediction of the preceding vehicle future trajectory, will not require vehicle braking action after the end of the prediction horizon. The proposed vehicle-following controller was tested in both real vehicle experiments and simulations. The experiments showed that the proposed MPC formulation avoids unnecessary braking and can significantly improve fuel economy and ride comfort. Remarkably, the proposed terminal set can conveniently exploit long previews, while keeping the length of the MPC horizon limited to a few seconds, thus making the real-time implementation possible. The simulation study shows how the vehicle behavior was comparable when using the

proposed controller and when using a similar controller that, however, relies on a significantly longer horizon, representing an approximation of the acausal optimum.

Conclusion and future work

Thanks to their potential in reducing greenhouse gas emissions, improving fuel-efficiency, and increasing safety, vehicle platoons are expected to be soon a reality on our highways. However, altitude variations have a large impact on fuel-efficiency. In this thesis, we addressed the problem of how to fuel-efficiently and safely control heavy-duty vehicle platoons driving along a road with varying topography. This chapter concludes the thesis and outlines possible directions for future research.

9.1 Conclusion

In this section, we first summarize the main contributions, dividing them in those related to cooperative platooning and those to non-cooperative platooning. Second, we provide some conclusive remarks.

Cooperative platooning

In the first part of the thesis we addressed the cooperative platooning control problem where vehicles act together to save fuel.

In Chapter 5, we discussed a two-layer control architecture. The top layer, denoted platoon coordinator, is based on dynamic programming and computes a reference speed profile by minimizing the fuel consumption of the entire platoon. The bottom layer, denoted as vehicle control layer, uses a distributed model predictive control framework that safely tracks the reference speed trajectory. Safety is guaranteed by specifically designed constraints that ensure the recursive feasibility of the model predictive controller. The proposed control architecture was tested in an in-depth simulation study that showed (i) the potential of the platoon coordinator to reduce the fuel consumption of up to 12% for following vehicles with respect to standard platooning controllers, (ii) the capability of the controller to react to harsh braking of the leading vehicle and to attenuate disturbances along the platoon.

In Chapter 6, we studied the problem of how to explicitly manage gear shifts in platoons. We proposed an extension of the cooperative control architecture by introducing a gear management layer. This layer computes a gear shift sequence by minimizing the vehicle fuel consumption at the same time as keeping small speed and inter-vehicular reference tracking deviation. The gear management layer performance was tested in a simulation study and was shown to outperform alternative solutions. The study showed how the proposed solution properly manages the gear shifting task guaranteeing fuel-efficiency and smooth behavior of the platoon.

Non-cooperative platooning

In the second part of the thesis, we addressed non-cooperative platooning control problem. In this framework, the lead vehicle optimizes its fuel consumption ignoring the presence of the following vehicle, while the following vehicle predicts the lead vehicle trajectory to optimize its own fuel consumption.

In Chapter 7, we proposed a vehicle-following controller. The problem was formulated as an optimal control problem that exploits road topography information and the predicted trajectory of the preceding vehicle to compute optimal state and input trajectories. The considered vehicle model included longitudinal vehicle dynamics and a powertrain model that captures both the gear shifts and freewheeling dynamics. The benefits of combining the fuel savings given by a short inter-vehicular distance with those given by a pulse-and-glide strategy we studied. The control was computed via dynamic programming and was tested in a simulation study where the performance for multiple scenarios and controller setups were compared. In particular, we compared the behavior and fuel savings of a heavy-duty vehicle using the proposed control strategy with one using a reference vehicle-following controller that tracks a constant distance. The results showed that the new control strategy is able to reduce the fuel consumption of up to 18% by keeping a minimum distance of 20 m with respect to the driving alone scenario, and up to 7% with respect to the use of the constant-distance vehicle-following controller.

In Chapter 8, we discussed a vehicle-following controller suitable for the fuel-efficient control of passenger cars. The controller relies on a model predictive controller that uses a short horizon to enable real-time implementation. To exploit long previews of the preceding vehicle, it enforces a terminal state constraint that ensures that no braking action should be needed after the end of the prediction horizon. The controller was tested in both real vehicle experiments and simulations. The experiments showed that the proposed controller avoids unnecessary braking and can significantly improve fuel economy and ride comfort. The simulations showed that the vehicle behavior is comparable when using the proposed controller to when using a similar controller that relies on a significant longer horizon, representing an approximation of an (acausal) optimum.

Conclusive remarks

To conclude, the exploitation of topography information in look-ahead control shows a great potential in reducing fuel consumption of heavy-duty vehicle platoon. In both the cooperative and non-cooperative control strategy cases, the proposed look-ahead controllers outperformed reference controllers that do not make use of topography information. Tests showed that the benefits from look-ahead control were larger in the case of heterogeneous vehicles, e.g., when vehicle had different masses. The cooperative control framework was able to reach a high level of fuel-efficiency by coordinating the accelerations of platooning vehicles over uphill and downhill. Herein, the platoon coordinator ensured that such accelerations were feasible for each vehicle and fuel-efficient for the entire platoon. The non-cooperative control framework ensured a high degree of fuel-efficiency of following vehicles by adapting their distance to preceding vehicles mainly based on topography information. Freewheeling in non-cooperative platooning was shown being possible to combine with the benefits given by driving at short inter-vehicular distance.

9.2 Future work

There are several directions to extend the work presented in this thesis. In this section, we discuss some of them.

Robustness to uncertainties in cooperative platooning

In the cooperative platooning discussed in Chapters 5 and 6, we assumed that the control system has access to accurate estimates of vehicle parameters and that vehicles behave according to the model. However, vehicles in a platoon can be manufactured by different companies. The accuracy of the vehicle models, e.g., mass, roll coefficient, and engine parameters, can highly vary between vehicles, while the parameter values themselves can be affected by external factors, such as engine temperature, tire pressure, road friction, fuel tank level, etc. Although these uncertainties are attenuated by the close-loop control formulation, they can still lead to undesired behavior. For example, the incorrect estimate of the maximum engine power can lead to the splitting of the platoon during steep uphill. Meanwhile, the bad estimates of the parameters that define the downhill coasting acceleration can lead to inefficient brakings during downhill. A promising approach to handle these uncertainties is to redefine the vehicle control layer such that each vehicle receives the predicted trajectories of the preceding and following vehicles and exploits them in the gap policy tracking. In such way, the optimal trajectory and input computed by each vehicle controller is the result of “pushing” and “pulling” efforts from the two contiguous vehicles. As a result, during uphill, each vehicle makes sure not to

lose the following vehicle, and, during downhills, it makes sure that the following vehicle will not need to brake.

Preceding vehicle trajectory prediction in non-cooperative platooning

In the non-cooperative platooning controllers discussed in Chapter 7, we assumed that accurately predicted trajectories of the preceding vehicle were available. We argued that they can be computed by the preceding vehicle and communicated to the following one or they can be computed by the following vehicle itself by exploiting past and present measures of the distance and relative speed collected by on-board sensors. The latter problem is not trivial and has not been sufficiently studied. Lang et al. (2014) propose a nonlinear autoregressive model to predict the trajectory of the preceding vehicle in a moderate non-congested traffic scenario. Moser et al. (2018) use a conditional linear Gaussian model to estimate the probability distribution of the preceding vehicle trajectory and exploit it in a stochastic vehicle-following model predictive control framework. However, these methods have been designed by assuming traffic as the main factor for vehicle speed fluctuation, and, therefore, the accuracy of the prediction quickly deteriorates with the length of the prediction horizon. In our work the vehicle speed fluctuation is mainly imputable to varying altitude, so topography information can be exploited to obtain a more accurate prediction of the preceding vehicle future trajectory. Furthermore, since the slipstream effect extends to tens of meters behind vehicles and braking action is highly inefficient, it is interesting to explore the benefits of predicting conservative trajectories of the preceding vehicle, i.e., high-confidence lower bounds on the preceding vehicle trajectory. These conservative trajectories can be computed with limited information about the preceding vehicle, such as the type of used controller (cruise controller or look-ahead controller) and the tracked reference speed.

Interaction between platoons and external traffic

In this thesis, the interference of external vehicles has been mainly accounted for in the safe operation of the platoon. However, as experienced in the tests reported in Lank et al. (2010), when a platoon drives in a moderately-congested traffic scenario, external vehicles can largely affect its fuel-efficiency. An exciting research direction is to study how to explicitly take the presence of other vehicles into account in the fuel-efficient control of platoons. This problem can be separated in (i) how to predict vehicles behavior and (ii) how to exploit such predictions for platoon control.

On the other hand, heavy-duty vehicle platoons can significantly affect the behavior of other vehicles. Due to the length of each vehicle, platoons cover long sections of the road and, due to law restrictions, they drive at a lower speed with respect to surrounding traffic. As discussed in Jin et al. (2018), this can have a large impact on the behavior and fuel-economy of the overall traffic. The automatic

control of the longitudinal dynamics through the platoons provides an opportunity to achieve an improved overall traffic efficiency.

Integrated fuel-efficient road freight transportation

In this thesis, we discussed the platoon control problem and we showed how platooning can significantly affect vehicle fuel consumption. As in Europe there are more than two millions long-haulage trucks transporting goods between countries (European Commission, 2017a), the potential for platooning is large. However, trucks represent only a portion of road traffic and their locations can be sparsely distributed over the road network. In order to fully exploit the benefits of platooning, vehicles need to be coordinated to promote the creation of platoons. This requires the optimization of vehicle route, departure time, and traveling speed for each vehicle by exploiting information about scheduled departure and arrival locations as well as time requirement for each transport mission. The resulting schedules should account for limitations on the maximum number of consecutive hours each driver can operate, disturbances due to traffic, weather conditions and road accidents, inability to platoon in certain road sections, and so on. The overall problem of synthesizing and developing a fuel-efficient road freight transportation system is therefore challenging. Some initial ideas on how to address this problem have appeared in the recent years, e.g. Besselink et al. (2016), as we discussed in Chapter 2. However, this still represents a largely unexplored topic with exciting challenges for future research.

Acronyms

ACC	Adaptive cruise control
BMS	Braking management system
CAN	Controller area network
CC	Cruise control
CACC	Cooperative adaptive cruise control
CLAC	Cooperative look-ahead control
CoG	Center of gravity
DP	Dynamic programming
ECU	Electronic control unit
EMS	Engine management system
GMS	Gear management system
GPS	Global positioning system
INS	Inertial navigation system
ITS	Intelligent transportation systems
LAC	Look-ahead control
LAAC	Look-ahead adaptive control
LQ	Linear–quadratic
LTV	Linear time-variant
MPC	Model predictive control
PATH	Partners for advanced transportation technology
PI	Proportional integrative
PnG	Pulse and glide
RMS	Root mean square
QP	Quadratic program
WSU	Wireless sensor unit

Bibliography

- Ahola. Ahola Transport and Scania into new partnership - Platooning as a next phase. <http://www.aholatransport.com/en/news/general-news/2016/ahola-transport-and-scania-into-new-partnership-%E2%80%93-platooning-as-a-next-phase.html> (2018). Accessed: 2018-04-04.
- A. Alam. *Fuel-efficient heavy-duty vehicle platooning*. Ph.D. thesis, KTH Royal Institute of Technology, Stockholm, Sweden (2014).
- A. Alam, B. Besselink, V. Turri, J. Mårtensson, and K. H. Johansson. Heavy-duty vehicle platooning for sustainable freight transportation: A cooperative method to enhance safety and efficiency. *IEEE Control Systems Magazine*, 35(6): 34–56 (2015).
- A. Alam, A. Gattami, and K. H. Johansson. An experimental study on the fuel reduction potential of heavy duty vehicle platooning. In *13th International IEEE Conference on Intelligent Transportation Systems*, 306–311. Madeira Island, Portugal (2010).
- A. Alam, A. Gattami, K. H. Johansson, and C. J. Tomlin. Guaranteeing safety for heavy duty vehicle platooning : safe set computations and experimental evaluations. *Control Engineering Practice*, 24: 33–41 (2014).
- A. Alam, J. Mårtensson, and K. H. Johansson. Look-ahead cruise control for heavy duty vehicle platooning. In *16th International IEEE Conference on Intelligent Transportation Systems*, 928–935. The Hague, The Netherlands (2013).
- C. J. Almqvist and K. Heinig. European accident research and safety report. Technical report, Volvo Trucks (2013).
- L. Alvarez and R. Horowitz. Safe platooning in automated highway systems. Technical report, California PATH Program (1997).
- J. Axelsson. Safety in vehicle platooning: A systematic literature review. *IEEE Transactions on Intelligent Transportation Systems*, 18(5): 1033–1045 (2017).

- R. Bellman. *Dynamic Programming*. Princeton University Press, Princeton, NJ, USA (1957).
- C. Bergenheim and Q. Huang. Challenges of platooning on public motorways. In *17th ITS World Congress*. Busan, South Korea (2010).
- C. Bergenheim, H. Pettersson, E. Coelingh, C. Englund, S. Shladover, and S. Tsugawa. Overview of platooning system. In *19th ITS World Congress*. Vienna, Austria (2012).
- Berkeley DeepDrive. Berkeley DeepDrive Homepage. <https://deepdrive.berkeley.edu/> (2018). Accessed: 2018-04-04.
- D. P. Bertsekas. *Dynamic programming and optimal control*. Athena Scientific, Belmont, MA, USA (1995).
- B. Besselink and K. H. Johansson. String Stability and a Delay-Based Spacing Policy for Vehicle Platoons Subject to Disturbances. *IEEE Transactions on Automatic Control*, 62(9): 4376–4391 (2017).
- B. Besselink, V. Turri, S. H. van de Hoef, K.-Y. Liang, A. Alam, J. Mårtensson, and K. H. Johansson. Cyber-physical Control of Road Freight Transport. *Proceedings of the IEEE*, 104(5): 1128–1141 (2016).
- K. Bilstrup, E. Uhlemann, E. G. Ström, and U. Bilstrup. Evaluation of the IEEE 802.11p MAC method for vehicle-to-vehicle communication. In *IEEE 68th Vehicular Technology Conference*, 1–5. Calgary, Canada (2008).
- F. Blanchini. Set invariance in control. *Automatica*, 35: 1747–1767 (1999).
- C. Bonnet and H. Fritz. Fuel consumption reduction in a platoon: experimental results with two electronically coupled trucks at close spacing. *SAE Technical Paper* (2000).
- F. Borrelli, A. Bemporad, and M. Morari. *Predictive Control for Linear and Hybrid Systems*. Cambridge University Press, Cambridge, England (2017).
- F. Browand, J. Mc Arthur, and C. Radovich. Fuel saving achieved in the field test of two tandem trucks. Technical Report June, Institute of Transportation Studies, University of California’s Berkeley, Berkeley, CA, USA (2004).
- F. Bu, H.-S. Tan, and J. Huang. Design and field testing of a cooperative adaptive cruise control system. In *Proceedings of IEEE American Control Conference*, 4616–4621. Baltimore, MD, USA (2010).
- C. C. Chien and P. Ioannou. Automatic vehicle-following. In *Proceedings of the IEEE American Control Conference*, 1748–1752. Chicago, IL, USA (1992).

- K.-C. Chu. Decentralized control of high-speed vehicular strings. *Transportation Science*, 8(4): 361–384 (1974).
- M. Čičić, K.-Y. Liang, and K. H. Johansson. Platoon Merging Distance Prediction using a Neural Network Vehicle Speed Model. In *Proceedings of IFAC 20th World Congress 20th World Congress*, 3720–3725. Toulouse, France (2017).
- E. Dagan, O. Mano, and G. P. Stein. Forward Collision Warning with a Single Camera Modeling Acceleration Momentary Time to Contact. In *IEEE Intelligent Vehicles Symposium*, 37–42. Parma, Italy (2004).
- L. Del Re, F. Allgöwer, L. Glielmo, C. Guardiola, and I. Kolmanovsky. *Automotive model predictive control: models, methods and applications*. Springer (2010).
- A. Doi, T. Butsuen, T. Niibe, T. Takagi, Y. Yamamoto, and H. Seni. Development of a rear-end collision avoidance system with automatic brake control. *JSAE Review*, 15(4): 335–340 (1994).
- dSpace. dSpace homepage. <https://www.dspace.com/> (2018). Accessed: 2018-04-04.
- W. B. Dunbar and D. S. Caveney. Distributed receding horizon control of vehicle platoons: stability and string stability. *IEEE Transactions on Automatic Control*, 57(3): 620–633 (2012).
- W. B. Dunbar and R. M. Murray. Distributed receding horizon control for multi-vehicle formation stabilization. *Automatica*, 42(4): 549–558 (2006).
- Embotech. Embotech homepage. <https://www.embotech.com/> (2018). Accessed: 2018-04-04.
- EPA. EPA and NHTSA adopt first-ever program to reduce greenhouse gas emissions and improve fuel efficiency of medium- and heavy-duty vehicles. Technical report, US Environmental Protection Agency (2011).
- ERSO. Traffic Safety Basic Facts – Heavy Goods Vehicles and Buses. Technical report, European Road Safety Observatory (2016).
- ETSI. Intelligent Transport Systems (ITS); Access layer specification for Intelligent Transport Systems operating in the 5 GHz frequency band. Technical report, European Telecommunications Standards Institute, Valbonne, France (2012).
- European Commission. White paper – Roadmap to a single European transport area: towards a competitive and resource efficient transport system. Technical report, European Commission, Brussels, Belgium (2011).

- European Commission. An Overview of the EU Road Transport Market in 2015. Technical report, European Commission, Brussels, Belgium (2017a).
- European Commission. *EU Transport in Figures –Statistical Pocketbook 2017*. Bietlot, Charleroi, Belgium (2017b).
- F. Farokhi and K. H. Johansson. A game-theoretic framework for studying truck platooning incentives. In *16th International IEEE Conference on Intelligent Transportation Systems*, 1253–1260. The Hague, The Netherlands (2013).
- H. C. Frey and P.-Y. Kuo. Assessment of potential reductions in greenhouse gas emissions in freight transportation. *16th Annual International Emission Inventory Conference* (2007).
- General Motors. General Motor - To New Horizons. <https://archive.org/details/ToNewHor1940> (1939). Accessed: 2018-04-04.
- J. Guanetti, J. Kim, and F. Borrelli. Control of Connected and Automated Vehicles: State of the Art and Future Challenges (2018). Submitted for journal publication.
- B. Gutelius. Follow the Leddar – Review of a low-cost detection and ranging device. *LiDAR News Magazin*, 4(5) (2014).
- L. Guzzella and A. Sciarretta. *Vehicle Propulsion Systems*, volume 1. Springer, Berlin, Germany (2007).
- J. Hasch, E. Topak, R. Schnabel, T. Zwick, R. Weigel, and C. Waldschmidt. Millimeter-wave technology for automotive radar sensors in the 77 GHz frequency band. *IEEE Transactions on Microwave Theory and Techniques*, 60(3 PART 2): 845–860 (2012).
- C. R. He, H. Maurer, and G. Orosz. Fuel Consumption Optimization of Heavy-Duty Vehicles With Grade, Wind, and Traffic Information. *Journal of Computational and Nonlinear Dynamics*, 11(6): 061011 (2016).
- J. K. Hedrick, M. Tomizuka, and P. Varaiya. Control issues in automated highway systems. *IEEE Control Systems*, 1(December): 21–32 (1994).
- E. Hellström, J. Aslund, and L. Nielsen. Design of an efficient algorithm for fuel-optimal look-ahead control. *Control Engineering Practice*, 18: 1318–1327 (2010).
- E. Hellström, A. Fröberg, and L. Nielsen. A real-time fuel-optimal cruise controller for heavy trucks using road topography information. *SAE Technical Paper*, 2006-01-0008 (2006).

- E. Hellström, M. Ivarsson, J. Åslund, and L. Nielsen. Look-ahead control for heavy trucks to minimize trip time and fuel consumption. *Control Engineering Practice*, 17(2): 245–254 (2009).
- M. Henriksson, O. Flårdh, and J. Mårtensson. Optimal Speed Trajectories Under Variations in the Driving Corridor. *IFAC-PapersOnLine*, 50(1): 12551–12556 (2017).
- N. Hill, S. Finnegan, J. Norris, C. Brannigan, D. Wynn, H. Baker, and I. Skinner. Reduction and testing of greenhouse gas emissions from heavy duty vehicles. Technical Report 4, AEA Technology (2011).
- J. Hooker. Optimal driving for single-vehicle fuel economy. *Transportation Research Part A: General*, 22(3): 183–201 (1988).
- R. Horowitz and P. Varaiya. Control design of an automated highway system. *Proceedings of the IEEE*, 88(7): 913–925 (2000).
- D. Hrovat, S. Di Cairano, H. Tseng, and I. Kolmanovsky. The development of Model Predictive Control in automotive industry: A survey. In *IEEE International Conference on Control Applications*, 295–302. Dubrovnik, Croatia (2012).
- W.-H. Hucho. *Aerodynamics of road vehicles*. Butterworth-Heinemann (1987).
- ICCT. European Heavy Duty Vehicles – Cost effectiveness of fuel efficiency technologies for long haul tractor trailers in the 2025-2030 time frame. Technical report, International Council on Clean Transportation, Brussels, Belgium (2018).
- IEEE-SA. IEEE Standard for information technology – Amendment 6: wireless access in vehicular environments. Technical report, IEEE Standards Association, New York, NY, USA (2010).
- P. A. Ioannou and C. C. Chien. Autonomous Intelligent Cruise Control. *IEEE Transactions on Vehicular Technology*, 42(4): 657–672 (1993).
- IPCC. Summary for Policymakers. In *Climate Change 2014: Mitigation of Climate Change. Contribution of Working Group III to the Fifth Assessment Report of the Intergovernmental Panel on Climate Change*. [Edenhofer, O., R. Pichs-Madruga, Y. Sokona, E. Farahani, S. Kadner, K. Seyboth, A. Adler, I. Baum, S. Brunner, P. Eickemeier, B. Kriemann, J. Savolainen, S. Schlömer, C. von Stechow, T. Zwickel and J.C. Minx (eds.)]. Cambridge University Press, Cambridge, United Kingdom and New York, NY, USA (2014).
- ITF. ITF Transport Outlook. Technical report, International Transport Forum (2017).

- L. Jin, M. Čičić, S. Amin, and K. H. Johansson. Modeling the Impact of Vehicle Platooning on Highway Congestion : A Fluid Queuing Approach. In *Proceedings of ACM Workshop on Hybrid Systems: Computation and Control*. Porto, Portugal (2018).
- L. Johannesson, N. Murgovski, E. Jonasson, J. Hellgren, and B. Egardt. Predictive energy management of hybrid long-haul trucks. *Control Engineering Practice*, 41: 83–97 (2015).
- A. Kaku, A. S. Kamal, M. Mukai, and T. Kawabe. Model predictive control for ecological vehicle synchronized driving considering varying aerodynamic drag and road shape information. *SICE Journal of Control, Measurement, and System Integration*, 6(5): 299–308 (2013).
- P. Kokotovic and G. Singh. Minimum-energy control of a traction motor. *IEEE Transactions on Automatic Control*, 92–95 (1972).
- M. P. Lammert, A. Duran, J. Diez, K. Burton, and A. Nicholson. Effect of platooning on fuel consumption of Class 8 vehicles over a range of speeds, following distances, and mass. *SAE International Journal of Commercial Vehicles*, 1–14 (2014).
- D. Lang, R. Schmied, and L. Del Re. Prediction of Preceding Driver Behavior for Fuel Efficient Cooperative Adaptive Cruise Control. *SAE International Journal of Engines*, 7(1): 2014–01–0298 (2014).
- C. Lank, S. Deutschle, G. Keßler, and M. Hakenberg. Elektronisch gekoppelte Lkw auf Autobahnen—Ergebnisse des KONVOI-Projektes. In *4th Nutzfahrzeug Workshop*. Graz, Austria (2010).
- J. Larson, K.-Y. Liang, and K. H. Johansson. A distributed framework for coordinated heavy-duty vehicle platooning. *IEEE Transactions on Intelligent Transportation Systems*, 16(1): 419–429 (2015).
- J. Lee. *Vehicle Inertia Impact on Fuel Consumption of Conventional and Hybrid Electric Vehicles Using Acceleration and Coast Driving Strategy*. Phd thesis, Virginia Polytechnic Institute and State University (2009).
- W. S. Levine and M. Athans. On the optimal error regulation of a string of moving vehicles. *IEEE Transactions on Automatic Control*, 11(3): 355–361 (1966).
- P. Li, L. Alvarez, and R. Horowitz. AHS safe control laws for platoon leaders. *IEEE Transactions on Control Systems Technology*, 5(6): 614–628 (1997).
- S. Li, K. Li, R. Rajamani, and J. Wang. Model predictive multi-objective vehicular adaptive cruise control. *IEEE Transactions on Control Systems Technology*, 19(3): 556–566 (2011).

- S. Li, K. Li, and J. Wang. Economy-oriented vehicle adaptive cruise control with coordinating multiple objectives function. *Vehicle System Dynamics*, 51(1): 1–17 (2013).
- S. E. Li and H. Peng. Strategies to minimize the fuel consumption of passenger cars during car-following scenarios. *Proceedings of the Institution of Mechanical Engineers, Part D: Journal of Automobile Engineering*, 226(3): 419–429 (2011).
- S. E. Li, H. Peng, K. Li, and J. Wang. Minimum fuel control strategy in automated car-following scenarios. *IEEE Transactions on Vehicular Technology*, 61(3): 998–1007 (2012).
- K.-Y. Liang, J. Mårtensson, and K. H. Johansson. Heavy-Duty Vehicle Platoon Formation for Fuel Efficiency. *IEEE Transactions on Intelligent Transportation Systems*, 17(4): 1051–1061 (2016a).
- K.-Y. Liang, S. van de Hoef, H. Terelius, V. Turri, B. Besselink, J. Mårtensson, and K. H. Johansson. Networked control challenges in collaborative road freight transport. *European Journal of Control*, 30: 2–14 (2016b).
- D. Liberzon. *Calculus of variations and optimal control theory: a concise introduction*. Princeton University Press, Princeton, NJ, USA (2012).
- R. Liu and I. M. Golovitcher. Energy-efficient operation of rail vehicles. *Transportation Research Part A: Policy and Practice*, 37(10): 917–932 (2003).
- MIT SelfDrivingCars. MIT Self-Driving Cars Homepage. <https://selfdrivingcars.mit.edu/> (2018). Accessed: 2018-04-04.
- V. Monastyrsky and I. Golownykh. Rapid computation of optimal control for vehicles. *Transportation Research Part B: Methodological*, 27(3): 219–227 (1993).
- D. Moser, R. Schmied, H. Waschl, and L. Del Re. Flexible Spacing Adaptive Cruise Control Using Stochastic Model Predictive Control. *IEEE Transactions on Control Systems Technology*, 26(1): 114–127 (2018).
- N. Murgovski, B. Egardt, and M. Nilsson. Cooperative energy management of automated vehicles. *Control Engineering Practice*, 57(December): 84–98 (2016).
- NASEM. *Attribution of Extreme Weather Events in the Context of Climate Change*. The National Academies Press, Washington, DC, USA (2016).
- G. Naus, R. Vugts, J. Ploeg, M. van de Molengraft, and M. Steinbuch. String-Stable CACC Design and Experimental Validation : A Frequency-Domain Approach. *IEEE Transactions on Vehicular Technology*, 59(9): 4268–4279 (2010).

- B. Németh and P. Gáspár. Optimised speed profile design of a vehicle platoon considering road inclinations. *IET Intelligent Transport Systems*, 8: 200–208 (2013).
- D. Nigicser, V. Turri, J. Mårtensson, A. A. Mustafa, and E. S. da Silva. Predictive vehicle motion control for post-crash scenarios. In *Proceedings of 14th International Symposium on Advanced Vehicle Control*. Beijing, China (2018). To appear.
- D. Norrby. *A CFD study of the aerodynamic effects of platooning*. Master thesis, KTH Royal Institute of Technology, Stockholm, Sweden (2014).
- H. Pacejka. *Tire and Vehicle Dynamics*. Elsevier, Amsterdam, The Netherlands (2012).
- Peloton. Peloton homepage. <https://peloton-tech.com/> (2018). Accessed: 2018-04-04.
- L. E. Peppard. String stability of relative-motion PID vehicle control systems. *IEEE Transactions on Automatic Control*, 579–581 (1974).
- L. A. Pipes. An operational analysis of traffic dynamics. *Journal of Applied Physics*, 24(3): 274 (1953).
- J. Ploeg, B. T. M. Scheepers, E. van Nunen, N. van de Wouw, and H. Nijmeijer. Design and Experimental Evaluation of Cooperative Adaptive Cruise Control. In *14th International IEEE Conference on Intelligent Transportation Systems*, 14–19. Washington, DC, USA (2011).
- J. Ploeg, N. van de Wouw, and H. Nijmeijer. Lp string stability of cascaded systems: application to vehicle platooning. *IEEE Transactions on Control Systems Technology*, 22(2): 786–793 (2014).
- R. Rajamani, H.-S. Tan, B. K. Law, and W.-B. Zhang. Demonstration of integrated longitudinal and lateral control for the operation of automated vehicles in platoons. *IEEE Transactions on Control Systems Technology*, 8(4): 695–708 (2000).
- K. Ramachandran, M. Gruteser, R. Onishi, and T. Hikita. Experimental analysis of broadcast reliability in dense vehicular networks. *IEEE Vehicular Technology Magazine*, 2(4): 26–32 (2007).
- M. Raya and J.-P. Hubaux. The security of vehicular ad hoc networks. In *3rd ACM Workshop on Security of Ad Hoc and Sensor Networks*, 11. ACM Press, New York, NY, USA (2005).
- J. Richalet, A. Rault, J. L. Testud, and J. Papon. Model Predictive Heuristic Control : Applications to Industrial Processes. *Automatica*, 14: 413–428 (1978).

- M. Roeth. CR England Peloton Technology Platooning Test Nov 2013. Technical report, North American Council for Freight Efficiency, Fort Wayne, IN, USA (2013).
- Roland B. Automated Trucks – The next big disruptor in the automotive industry? Technical report, Roland Berger, Munich, Germany (2016).
- J. Ryu and J. C. Gerdes. Integrating Inertial Sensors With Global Positioning System (GPS) for Vehicle Dynamics Control. *Journal of Dynamic Systems, Measurement, and Control*, 126(2): 243 (2004).
- SAFE. Heavy-Duty Innovation: Energy , Automation , and Technology in the Trucking Sector. Technical Report November, Securing America’s Future Energy, Washington, DC, USA (2017).
- T. Sandberg. *Heavy truck modeling for fuel consumption simulations and measurements*. Licentiate thesis, Linköping University, Linköping, Sweden (2001).
- Scania. Autonomous truck platoon in Singapore. <https://www.scania.com/global/en/home/experience-scania/features/autonomous-truck-platoon-in-singapore.html> (2018). Accessed: 2018-04-04.
- A. Schwarzkopf and R. Leipnik. Control of highway vehicles for minimum fuel consumption over varying terrain. *Transportation Research*, II: 279–286 (1977).
- P. Seiler, A. Pant, and J. K. Hedrick. Disturbance propagation in vehicle strings. *IEEE Transactions on Automatic Control*, 49(10): 1835–1841 (2004).
- P. Seiler, B. Song, and J. K. Hedrick. Development of a collision avoidance System. In *SAE World Congress*. Detroit, MI, USA (1998a).
- P. Seiler, B. S. Song, and J. K. Hedrick. Application of Nonlinear Control to a Collision Avoidance System. *5th World Congress ITS* (1998b).
- S. Sheikholeslami and C. A. Desoer. Longitudinal control of a platoon of vehicles. In *Proceedings of the IEEE American Control Conference*, 1549–1579 (1990).
- S. Shladover. PATH at 20–history and major milestones. *IEEE Transactions on Intelligent Transportation Systems*, 8(4): 584–592 (2007).
- S. Shladover. Recent international activity in cooperative vehicle-highway automation systems. Technical report, California PATH Program (2012).
- M. L. Sichertiu and M. Kihl. Inter-vehicle communication systems: a survey. *IEEE Communications Surveys Tutorials*, 10(2): 88–105 (2008).
- A. Spulber. Impact of Automated Vehicle Technologies on Driver Skills. Technical report, Center for Automotive Research, Ann Arbor, MI, USA (2016).

- T. Stanger and L. del Re. A model predictive Cooperative Adaptive Cruise Control approach. *American Control Conference (ACC)*, 2013, 1374–1379 (2013).
- D. Swaroop and J. K. Hedrick. String stability of interconnected systems. *IEEE Transactions on Automatic Control*, 41(3): 349–357 (1996).
- D. Swaroop, J. K. Hedrick, C. C. Chien, and P. Ioannou. A Comparison of Spacing and Headway Control Laws for Automatically Controlled Vehicles. *Vehicle System Dynamics*, 23(1): 597–625 (1994).
- S. Thrun, M. Montemerlo, H. Dahlkamp, D. Stavens, A. Aron, J. Diebel, P. Fong, J. Gale, M. Halpenny, G. Hoffmann, K. Lau, C. Oakley, M. Palatucci, V. Pratt, Pascal S., S. Strohband, C. Dupont, L.-E. Jendrossek, C. Koelen, C. Markey, C. Rummel, J. van Niekerk, E. Jensen, P. Alessandrini, G. Bradski, B. Davies, S. Ettinger, A. Kaehler, A. Nefia, and P. Mahoney. Stanley: The Robot that Won the DARPA Grand Challenge. *Journal of Field Robotics*, 23(April): 245–267 (2006).
- S. Tsugawa. An overview on an automated truck platoon within the energy ITS project. In *7th IFAC Symposium on Advances in Automotive Control*, 41–46. Tokyo, Japan (2013).
- V. Turri. *Fuel-efficient and safe heavy-duty vehicle platooning through look-ahead control*. Licentiate thesis, KTH Royal Institute of Technology, Stockholm, Sweden (2015).
- V. Turri, B. Besselink, and K. H. Johansson. Gear management for fuel-efficient heavy-duty vehicle platooning. In *Proceedings of IEEE 55th Conference on Decision and Control*, 1687–1694. Las Vegas, NV, USA (2016).
- V. Turri, B. Besselink, and K. H. Johansson. Cooperative look-ahead control for fuel-efficient and safe heavy-duty vehicle platooning. *IEEE Transactions on Control Systems Technology*, 25(1): 12–28 (2017a).
- V. Turri, B. Besselink, J. Mårtensson, and K. H. Johansson. Fuel-efficient heavy-duty vehicle platooning by look-ahead control. In *Proceedings of IEEE 53rd Conference on Decision and Control*, 654–660. Los Angeles, CA, USA (2014).
- V. Turri, A. Carvalho, H. E. Tseng, K. H. Johansson, and F. Borrelli. Linear model predictive control for lane keeping and obstacle avoidance on low curvature roads. In *Proceedings of IEEE 16th International Annual Conference on Intelligent Transport*, 378–383. The Hague, The Netherlands (2013).
- V. Turri, O. Flärdh, J. Mårtensson, and K. H. Johansson. Fuel-optimal look-ahead adaptive cruise control for heavy-duty vehicles. In *Proceedings of IEEE American Control Conference*. Milwaukee, WI, USA (2018). To appear.

- V. Turri, Y. Kim, J. Guanetti, K. H. Johansson, and F. Borrelli. A model predictive controller for non-cooperative eco-platooning. In *Proceedings of IEEE American Control Conference*, 2309–2314. Seattle, WA, USA (2017b).
- UNFCCC. Adoption of the Paris agreement. Technical report, United Nations Framework Convention on Climate Change, Paris, France (2015).
- A. Vahidi and A. Eskandarian. Research advances in intelligent collision avoidance and adaptive cruise control. *IEEE Transactions on Intelligent Transportation Systems*, 4(3): 143–153 (2003).
- S. van de Hoef, K. H. Johansson, and D. V. Dimarogonas. Fuel-optimal centralized coordination of truck platooning based on shortest paths. In *Proceedings of the IEEE American Control Conference*, 3740–3745. Chicago, IL, USA (2015).
- S. van De Hoef, K. H. Johansson, and D. V. Dimarogonas. Fuel-Efficient en Route Formation of Truck Platoons. *IEEE Transactions on Intelligent Transportation Systems*, 19(1): 102–112 (2018).
- D. van Dooren, S. Schiessl, A. Molin, J. Gross, and K. H. Johansson. Safety Analysis for Controller Handover in Mobile Systems. *IFAC-PapersOnLine*, 50(1): 10090–10095 (2017).
- E. van Nunen, F. Esposto, A. K. Saberi, and J. P. Paardekooper. Evaluation of safety indicators for truck platooning. In *Proceedings of IEEE Intelligent Vehicles Symposium*, 1013–1018 (2017).
- E. van Nunen, D. Tzempetzis, G. Koudijs, H. Nijmeijer, and M. van Den B. Towards a safety mechanism for platooning. *IEEE Intelligent Vehicles Symposium, Proceedings*, 2016-Augus(Iv): 502–507 (2016).
- P. Varaiya. Smart cars on smart roads: problems of control. *IEEE Transactions on Automatic Control*, 38(2): 195–207 (1993).
- J. Wenger. Automotive Radar – Status and Perspectives. *IEEE Compound Semiconductor Integrated Circuit Symposium*, 21–24 (2005).
- M. Whaiduzzaman, M. Sookhak, A. Gani, and R. Buyya. A survey on vehicular cloud computing. *Journal of Network and Computer Applications*, 40: 325–344 (2014).
- WHO. Global Health Risks: Mortality and burden of disease attributable to selected major risks. Technical report, World Health Organization, Geneva, Switzerland (2009).
- WHO. Global Status Report on Road Safety. Technical report, World Health Organization, Geneva, Switzerland (2015).

- M. Wille, M. Röwenstrunk, and G. Debus. KONVOI: Electronically coupled truck convoys. Technical report, Rheinisch-Westfälische Technische Hochschule, Aachen, Germany (2007).
- T. Willke, P. Tientrakool, and N. Maxemchuk. A survey of inter-vehicle communication protocols and their applications. *IEEE Communications Surveys & Tutorials*, 11(2): 3–20 (2009).
- D. Yanakiev and I. Kanellakopoulos. Longitudinal control of heavy-duty vehicles for automated highway systems. In *Proceedings of IEEE American Control Conference*, June (1995).
- F. Yasuhiko, K. Akuzawa, and M. Sato. Radar brake system. *Society of Automotive Engineers of Japan Review*, 16(1): 113 (1995).
- M. Zabat, N. Stabile, S. Farascarioli, and F. Browand. The aerodynamic performance of platoons: final report. Technical report, California Partners for Advanced Transit and Highways (PATH) (1995).
- M. Zhao, A. Mammeri, and A. Boukerche. Distance measurement system for smart vehicles. In *IEEE 7th International Conference on New Technologies, Mobility and Security*. Paris, France (2015).